



Review and verification of marine riser analysis programs:

Global response analysis

Up to demand of deepwater exploration, a variety of techniques and methods have been developed for decades to analyze response of marine riser system in a dynamic sea environment. The state-of-the-art computation programs coupled by increasing computer capacity have provided proficient accuracy of prediction and simulation in spite of existence of uncertainties, such as pipe-soil interaction, sea bed friction, etc.

However, subsea riser technology is still far away from being mature, and back analysis even shows our poor ability to predict actual response. Moreover, robust design relies on experience and knowledge of the designer and the complexity of using programs makes it difficult to feel confident of the result gained in analysis. Hence, it is deemed necessary to find approaches to verify the results. Besides, more sufficient understanding of computation mechanism adopted by the computer programs is required.

This thesis is intended to provide comparison methods for Riflex/DeepC both in static and dynamic analyses, and further complement guidance to usage of Riflex, especially with respect to interpretation of results, limitation of adopted methods, sensitivity study. It is emphasized that the focus of the thesis is global response analysis for flexible riser. The content of work probably includes below,

1. Introduction of typical commercial programs employed in riser analyzes. Describe briefly applicable configurations and methodologies used for static and dynamic calculation. Make comparison of different programs.
2. Reveal limitations of applied methods. Try to provide actual cases for each limitation. Give practical advice to avoid selecting a wrong analysis method.
3. Verification of the analysis results. Carry out case verification for static and dynamic analysis respectively. Analytical solution like classic catenary equation could be one approach for static result (MATLAB can be programming tool. Abaqus is alternative for static analyze). Different dynamic methods from that for RIFLEX, such as finite difference method, other numeric integration than FEM, could be employed. The boundary layer method of ODE (ref. to paper issued by University of São Paulo) is going to be adopted to generate conditional asymptotic reference to compare TDP.
4. Parameter sensitivity study, for instance, convergence of tension force, bending moment, shear force with respect to mesh size, length of time step, effect of damping factor, constant/nonlinear stiffness of soil.



In the thesis the candidate shall present his personal contribution to the resolution of problems within the scope of the thesis work. Theories and conclusions should be based on mathematical derivations and/or logic reasoning identifying the various steps in the deduction. The candidate should utilise the existing possibilities for obtaining relevant literature.

The thesis should be organised in a rational manner to give a clear exposition of results, assessments, and conclusions. The text should be brief and to the point, with a clear language. Telegraphic language should be avoided.

The thesis shall contain the following elements: A text defining the scope, preface, list of contents, summary, main body of thesis, conclusions with recommendations for further work, list of symbols and acronyms, references and (optional) appendices. All figures, tables and equations shall be numerated.

The supervisor may require that the candidate, in an early stage of the work, presents a written plan for the completion of the work. The plan should include a budget for the possible use of computer and laboratory resources which will be charged to the department. Overruns shall be reported to the supervisor.

The original contribution of the candidate and material taken from other sources shall be clearly defined. Work from other sources shall be properly referenced using an acknowledged referencing system.

The thesis shall be submitted in 3 copies:

- Signed by the candidate
- The text defining the scope included
- In bound volume(s)
- Drawings and/or computer prints which cannot be bound should be organised in a separate folder.

Supervisor: Professor Bernt J. Leira

Deadline: June 14th 2010

Trondheim, January 18th, 2010

Bernt J. Leira



Abstract

Availability of diverse computation packages for marine risers eases structural assessment and reduces cost for experiments and design. Successful industrial applications have proven that time domain analysis programs provide effective solution for global response analysis. Nevertheless, good command of methodologies adopted by popular programs and awareness of limitations corresponding to different techniques are imperative, if the analyst intends to make proper use of the computerized tools. Frequently it remains uncertain to know the correctness of analyze results due to lack of comparison approach and proficient understanding of structural behavior, even if the analysis is conducted as instructed by software supplier.

This thesis makes a review of the most popular computation programs. Comparison work is done to indicate their common features and particular characteristics. Further, a careful examination lists limitations and uncertainties of the applied analysis technologies and gives explanation to the source of the problems. General guidance is provided for how to avoid these unsolved imperfections.

The core part of this thesis is to make verification of Riflex accounting for global analysis of catenary risers. Static validation is based on Faltisen's catenary equations. MATLAB is employed to program a simple routine to calculate static configuration of SCR and LWR. Dynamic validation refers to a boundary layer value method proposed by J.A.P. Aranha. A semi-independent comparison is performed to verify dynamic bending moment at TDA.

Last, parametric study is carried out to investigate stability of numeric integration. The effects of time step setting and mesh density are studied. Besides, to better understand structural behavior of catenary risers, effects of water depth, riser wall thickness and arc length are tested on the basis of previous work last semester.



Abbreviations

ALS	Accidental Limit State
API	American Petroleum Industry
DeepC	One Subprogram name of DNV SeaSam
Deeplines	Global analysis program of risers, moorings and flow lines
FEM	Finite Element Method
FD	Frequency Domain
Flexcom	FEM analysis package of compliant and rigid offshore structures
FPSO	Floating platform for production, storage and offloading
GUI	Graphical User Interface
LWR	Lazy Wave Riser
MATLAB	A numerical computing environment and programming language developed by MathWorks
OrcaFlex	Dynamic analysis package of offshore marine systems
QTF	Quadratic Transfer Function
RAO	Response amplitude operator
Riflex	Analysis program of slender structures developed by SINTEF
SCR	Steel Catenary riser
TDA	Touch Down area
TDP	Touch Down point
TLP	Tension Leg Platform
TTR	Top tensioned riser
ULS	Ultimate Limit State
VIV	Vortex induced vibration



Content

Chapter 1	Computation Programs for marine riser analysis.....	1
Section 1.1	Introduction.....	1
Section 1.2	OrcaFlex [1]	2
Section 1.3	Deeplines[2]	4
Section 1.4	Flexcom[3].....	6
Section 1.5	Riflex[4]	8
Section 1.6	Summary	10
Chapter 2	Limitations of riser analysis programs	12
Section 2.1	Introduction.....	12
Section 2.2	Limitation of Catenary method	12
Section 2.3	Limitation of Newton-Raphson Iteration Method.....	13
Section 2.4	High frequency noise induced by FEM model [1]	14
Section 2.5	Restriction of discretisation.....	15
Section 2.6	Stability of Numerical Integration	16
Section 2.7	Limitation of Frequency domain method.....	18
Section 2.8	Bucking problem	20
Section 2.9	Uncertainty of soil-pipe interaction model	22
Section 2.10	Limitation of Hydrodynamic force model.....	26
Chapter 3	Validation of static analysis.....	27
Section 3.1	Introduction of Riflex method	27
Section 3.2	Introduction of verification method.....	30
Section 3.3	Comparison of SCR.....	31
Section 3.4	Comparison of LWR	34
Section 3.5	Conclusion	39
Chapter 4	Validation of Dynamic bending moment.....	40
Section 4.1	Introduction of boundary layer value method.....	40
Section 4.2	Case Study I: Regular wave sea state	43
Section 4.3	Case Study II: Irregular wave sea state.....	45



Section 4.4	Summary	48
Chapter 5	Parametric study.....	49
Section 5.1	Mesh density.....	49
Section 5.2	Time Step.....	55
Section 5.3	Water depth influence on riser design.....	63
Section 5.4	Variation of Wall thickness V.S Arc Length	68
Chapter 6	Summary	72
Reference.....		74
Appendix A Static Validation: MATLAB Code		75
SCR		75
LWR Approach I.....		80
LWR Approach II.....		86
File of Current Profile.....		89
Appendix B Validation of dynamic bending moment at TDA.....		90
Regular wave sea state.....		90
Irregular sea state		92
Appendix C Parametric Study.....		95
“M5TS01_inpmo.d.inp”		95
“M5TS01_stamo.d.inp”		100
“M5TS01_dynmo.d.inp”		102
“semi_RAO.tra”		104

Chapter 1 Computation Programs for marine riser analysis

Section 1.1 Introduction

Given that fixed rigid design is not feasible in deepwater environment, marine riser becomes a more complicated entity due to large displacement induced by nonlinear interaction between riser and fluid, riser and soil, and also time dependent floater motion. The advent of computation and simulation programs provides a low cost and high accuracy platform for simulation of riser response. Since then, lacking of analytical solution and physical restriction of laboratory experiments is not a challenge for analysis any more. At the early stage, computer programs were only able to conduct computation for standard geometrical configurations under particular environmental conditions. The employed methods were limited to linearization of displacement, spectral methods and time integration with assumption of unvarying tension. Supported by rapidly improved computer hardware, the analysis programs nowadays are able to provide more accurate time simulation of riser response with fewer limitations of application and easier user interface for input and post processing.

At present, computer programs are applied in almost all practical concepts of slender structures, including

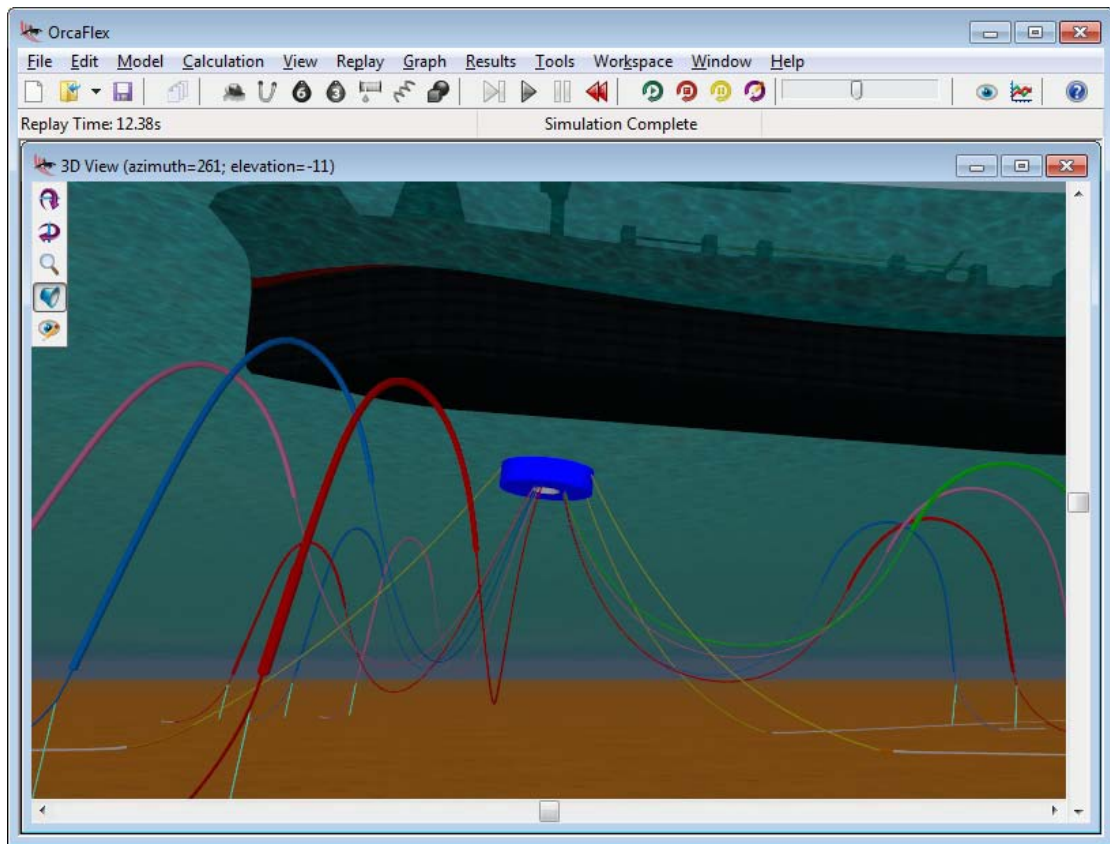
- Flexible risers, umbilical and hose configurations
- Rigid production and drilling risers
- Hybrid riser concepts
- Mooring lines and multi-components offshore systems
- Pipeline and flow-line laying and on-bottom stability
- Subsea equipment installation

Most of these programs provide access to

- Static and quasi-static analyses
- Modal analyses and frequency domain analyses
- Time domain dynamic analyses
- VIV prediction models
- Interference analyses
- Coupled analyses of vessels, risers and moorings
- Code criterion checking against industrial standard
- 3D simulation

This section provides an overview of popular programs in riser analysis by presenting their features and applications.

Section 1.2 OrcaFlex [1]



Inventor

Orcina Ltd, UK

History

First released in 1986, the latest version 9.3c

Application

- ◆ Riser systems: SCRs, TTRs, hybrids, flexibles, umbilicals, hoses.
- ◆ Mooring systems: spread, turret, SPM, jetty, etc.
- ◆ Installation planning with capabilities across the full range of scenarios.
- ◆ Towed systems: bundle dynamics, seismic arrays, towed bodies, etc.
- ◆ Defense, marine renewable, seabed stability and many other types of system.

User

BP, Aker solution, Technip, Subsea7



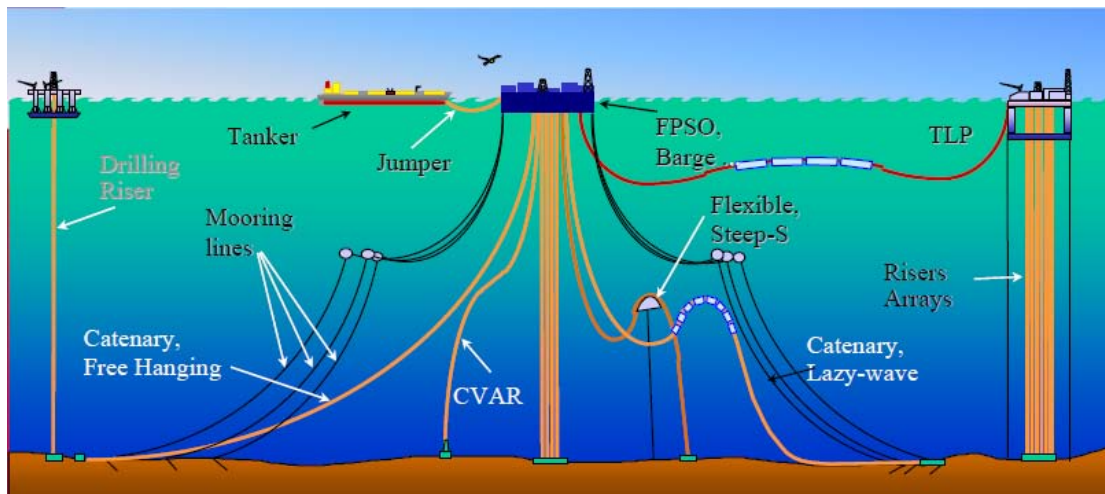
Features

- Fully 3D, non-linear, large displacement analysis.
- Consistent and robust modeling of compression and snatching.
- Fully coupled tension, bending and torsion.
- Bend Stiffener / Tapered Stress Joint model generation.
- Rayleigh damping.
- Highly robust and accurate finite element formulation.
- Choice of implicit or explicit time integration methods.
- Fully coupled vessel/line analysis.
- Flat, 2D profile or 3D seabed surface.
- Linear elastic or non-linear hysteretic soil model.
- Non-isotropic Coulomb friction for a broad range of contact objects.
- Best of class fully interactive GUI.
- System visualization as either wire frame or shaded view with perspective and hidden line removal.
- Modal analysis.
- Contact and clearance analyses.
- Fatigue analysis (regular, rain flow and spectral).
- Full environmental description including wave spreading.
- Vortex induced vibration analysis (VIV).
- Parallel processing to take advantage of multi-core and multi-processor hardware.
- Wake Interference Modeling (Huse, Blevins, User Specified).
- Automation facilities for parametric, sensitivity and load case studies.

Core principles

- Finite element model with 6 degrees of freedom at each segment end.
- Element formulation is extremely robust, accurate and widely applicable.
- Choice of implicit (constant or variable time step) or explicit time integration methods.
- Parallel processing to take advantage of modern multi-core and multi-processor hardware.
- Slow varying water particle loads can be computed at a larger time step than structural displacements.
- Facility for FFT re-construction of wave field from single point elevation time history.
- Fluid forces based on industry-standard Morison and cross-flow assumptions.
- 1st and 2nd order wave loads on floaters calculated from wave load RAOs and QTFs.

Section 1.3 Deeplines[2]



Inventor

Principia and IFP, France

History

The latest version 4.4, 2009

Industrial applications

- ◆ All flexible risers, umbilical, and floating hoses configurations,
- ◆ Rigid production (SCR) and drilling risers,
- ◆ Hybrid riser concepts,
- ◆ Mooring lines (catenary, taut, synthetic, etc) and multi-bodies offshore systems,
- ◆ Pipeline and flow line laying and stability,
- ◆ Towing systems,
- ◆ Subsea equipments installation.

User

Technip, Saipem, Total, Acergy

Key features

- Powerful and robust finite element method including bending/torsion coupled effects, nonlinear beam laws (elastic-plastic, hysteresis), and thermal loads.



- Quasi-static analyses
- Full 3D time domain dynamic analyses
- Modal analysis including multi-bodies systems
- Graphical user interface (GUI) for pre- and post-processing including animation,
- Output for risers, moorings and floating supports: tension, stress, curvature, built-in angles, tensioner strokes, deformed shape, compatible with Excel
- Batch command for launching analysis and output requests.

Special features

■ Coupled analysis

Multi-bodies fully coupled analyses with risers, mooring, and any other connections

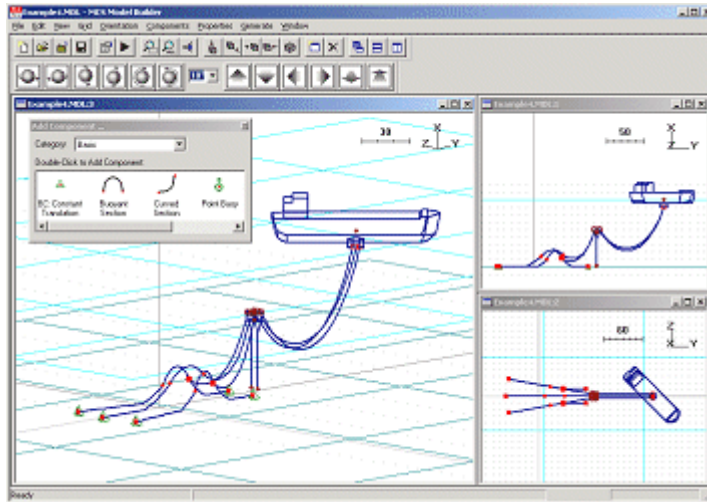
- Wind, current and wave loads on a floating body,
- Low frequency analysis (with Newman's approximation for waves loads),
- Wave frequency coupled analysis with regular or irregular waves.

■ Contact

Full range of contact features

- Sliding contact with a beam inside another beam (pipe-in-pipe, keel-joint),
- External contact between beams, e.g. clash
- Contact with any surface defined by triangular elements, fixed or moving , e.g. soil, moon pool
- Anisotropic friction law
- Non-linear contact stiffness, suction effect with soil shape change
- Automatic detection of proximity and generation of contact elements.

Section 1.4 Flexcom[3]



Inventor

MCS Kenny Ltd., Ireland

History

First released in 1983, the latest version is Flexcom 7

Application

- ◆ All flexible riser configurations
- ◆ Top-tensioned risers: drilling, production and completion
- ◆ Steel catenary risers
- ◆ Pipe-in-Pipe analyses
- ◆ Hybrid/rigid flexible systems
- ◆ Multiple/bundled risers
- ◆ Umbilical & jumper hoses
- ◆ Transfer lines & offloading systems
- ◆ Catenary mooring systems
- ◆ Integrated riser/mooring systems
- ◆ Tanker mooring and loading systems (CALM, SALM etc.)
- ◆ Towed array systems and floating bodies
- ◆ TLP tethers (towing, upending and operating)
- ◆ Pipelines and pipe lay operations
- ◆ CALM/TALM buoy coupled analyses



User

JP Kenny, successful applications on projects for Kerr McGee, Total, Shell

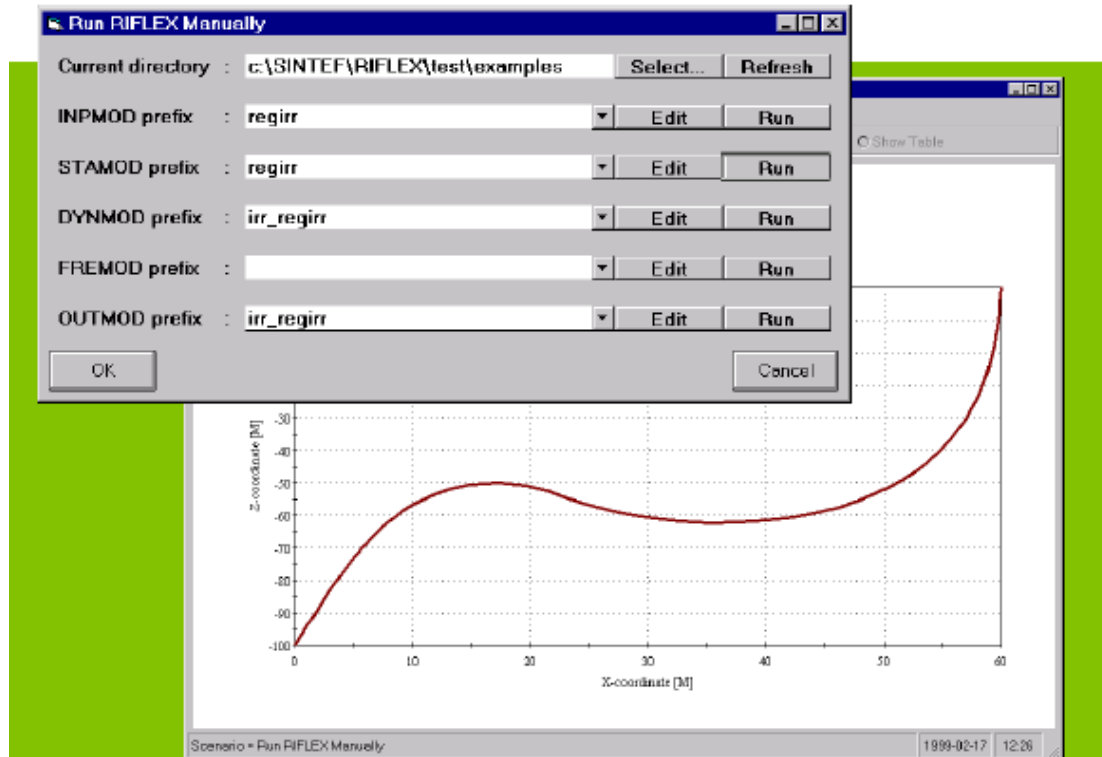
Key features

- Time and frequency domain analysis capabilities
- Wealth of practical modeling facilities including hinges, flex joints, guide surfaces, damper elements, winch elements, point masses, point buoys, bend stiffeners, and tapered stress joints
- Many productivity-enhancing options such as cable pre-static step for instantaneous static analysis of flexible risers and SCRs, and a highly efficient automatic time-stepping algorithm
- Range of non-linear material models, including non-linear bending with hysteresis
- Pipe-in-pipe configurations
- Soil-structure interaction
- Wake interference
- Line clashing
- Coupled analysis
- Robust seabed contact algorithm, for flat, sloping and arbitrary rigid and elastic seabed, all with anisotropic Coulomb friction
- Range of sea state modeling options': Regular Airy, Stokes V, Dean's Stream, Pierson-Moskowitz, Jonswap, Ochi-Hubble, Torsethaugen, User-defined

Optional modules:

- Modes - Calculates natural frequencies and corresponding mode shapes of offshore structures
- Clear - Clearance/interference postprocessor for calculating clearance between adjacent structures
- Lifetime - Time domain fatigue analysis and general cycle counting
- Life Frequency - Frequency domain fatigue life prediction
- Histogram - Frequency domain general cycle counting tool

Section 1.5 Reflex[4]



Inventor

Marintek and NTNU, Norway

History

The latest Version 3.6.7

Application

- ◆ Flexible risers
- ◆ Top tensioned risers
- ◆ Metallic catenary risers
- ◆ Mooring lines
- ◆ TLP tendons
- ◆ Loading hoses
- ◆ Umbilical
- ◆ Towing Lines
- ◆ Pipe laying
- ◆ Seismic cables
- ◆ Fish farming systems



User

MARINTEK, DNV, Subsea7, BP Petroleum Development, Conoco Norway, Esso Norge, Norsk Hydro, Saga Petroleum, Statoil

Key features

- Flexible modeling of simple as well as complex riser systems including connected systems and riser bundles.
- Finite element formulation allowing for unlimited displacements and rotations in 3-D space.
- Beam and bar elements
- Nonlinear material properties including a hysteretic material description
- Nonlinear static finite element analysis
- Nonlinear time domain dynamic analysis

Special features

- Efficient static finite element analysis of the standard systems utilizing the catenary start configuration.
- Connector element for modeling of swivels and hinges
- Arbitrary boundary conditions at supports
- Identification of contact problems
- Special options available: Restart, release/rupture
- Loading due to internal slug flow

DNV develops a new analysis package called "DeepC" with a combination of several modules: Simo, Mimosa, Riflex and Xtract. This tool performs calculation of risers based on Riflex module. The input and output environment is improved by provision of graphical and dialogue interfaces. The functions are extended to conduct code checking (DNV OSF201, ISO 13628-7, Von- Mises Stress) and statistical post processing. One more feature is that, animation is also available for easier inspection.



Section 1.6 Summary

All the programs introduced above have demonstrated their robustness in industrial application. The environment for modeling and post-processing (GUI) differs from one program to another, nevertheless the core solutions for analysis do not vary much. The comparison of the features of these programs reveals the common characteristics below, and also indicates some differences.

1 The subjected structure

All the programs are subjected to analyzing response of slender structures. Never mind whether the object is riser or umbilical or mooring line in arbitrary geometrical configuration, or whether the scenario is transient installation operation or permanent production states. The structures are characterized by the following common features:

- Small bending stiffness
- Large deflection
- Large upper end motion excitation
- Nonlinear cross section properties
- Complex cross section structure

2 The load mode

2.1 Wave potential

Regular wave is described by Airy linear wave theory or Stokes' 5th order wave theory. Irregular wave is expressed by multidirectional sea states with contribution from Wind Sea, or swell, or combination. Wave spectrum options are available for ISSC, JONSWAP, Ochi-Hubble, Torsethaugen, etc.

2.2 Current

Current speed and direction is given by 3D constant or piecewise linear current profile. Normally, time constant current with speed variation along depth is enough for analysis.

NB! Orcaflex permits time variation and horizontal variation of current.

2.3 Hydrodynamic loading

The hydrodynamic forces are calculated from Morison's equation. The drag coefficients and added mass coefficients will in general depend on structural form, Reynolds number, roughness ratio, Keulegan-Carpenter number, current velocity relative to wave induced velocity, etc.

NB! Riflex gives an optional addition of a linear drag force term

2.4 Contact mode

Rigid and elastic seabed contact model is formulated with anisotropic Coulomb friction, arbitrary seabed profile, seabed suction, trenching and lateral seabed stiffness. The soil model could be linear elastic or non-linear hysteretic.



2.5 Vessel motion

Forced vessel motion model is generated via vessel RAOs, or imported from arbitrary motions history files. Vessel motion normally consists of high- frequency and low- frequency motion.

3 Static analysis

Two main approaches are commonly used, catenary static analysis and FEM analysis.

The former method is recommended to gain a fast result but ignore the effect of bending and torsion stiffness, and also interaction with solids.

The FEM method will take all load effects into account, but is more computation demanding. FEM analyze is allowed to start from different configurations, e.g. stress free shape, catenary shape, and user defined shape.

NB! Orcaflex provides Bezier spline shape for start configuration.

4 Dynamic analysis

The dynamic analysis is a time simulation of the motions of the model over a specified period of time, starting from the position derived by the static analysis.

Based on dynamic force equilibrium equation, one specifies a constant time step for numeric integration scheme. Force equilibrium is achieved in each time step by iteration. Typical numerical integration methods include Newmark- β , Wilson method, etc. Newton-Raphson method is frequently used for iteration.

NB! Orcaflex also employs Generalised- α implicit integration scheme, which is designed with controllable numeric damping to minimize low frequency damping. This method is introduced more stable for longer time step integration.

5 Scope of analysis

All the programs concentrate on evaluation of global response and local strains and stresses in different cross section layers and material are not considered. Regardless complexity of cross section for risers, global model only requires input of key cross section parameters like axial, bending and torsion stiffness. However, most of these programs except Riflex, are accessible to fatigue assessment, even though calculation of fatigue damage gets local analysis involved. To overcome the disadvantage of user interface and incompleteness of functions, DNV DeepC is developed with extensive functions on the basis of Riflex and able to do quick fatigue assessment.

Chapter 2 Limitations of riser analysis programs

Section 2.1 Introduction

Robustness of computer software is verified by experimental results. Nevertheless, numerical methods have their shortages. The engineer using the software should be responsible for analyze results. Therefore, good understand of limitations of the methods involved in computation, and further avoidance of misuse of methods is necessary. Moreover, when varieties of methods are available, one shall choose the most effective solution. In order to give guidance for more effective use of riser programs, typical problems of riser analysis are introduced in this chapter.

Section 2.2 Limitation of Catenary method

It is noted by all the analysis packages that, catenary method is far more effective than FEM analysis regarding computation demand. However, one has to keep in awareness that catenary analysis often presents only approximate results, and therefore is preferred to be start configuration for full static analyze rather than replacement of FEM.

The catenary method calculates the equilibrium position of the line, but it ignores the effects of bending and torsional stiffness of the line or its end terminations. In addition, the catenary method also ignores contact forces between the line and any solid shapes in the model, although it does include all other effects, including weight, buoyancy, axial elasticity, current drag and seabed touchdown and friction.

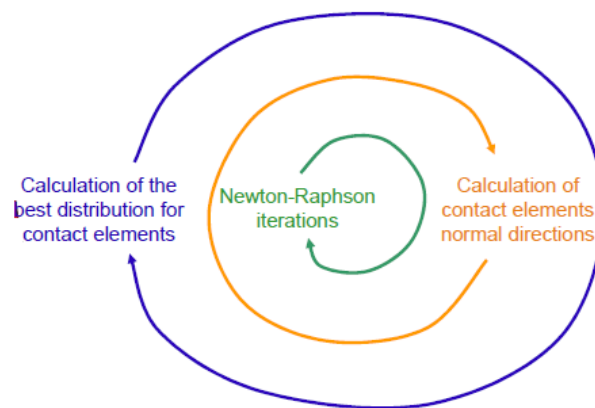
Because bend stiffness (and other) effects are not included, the position found by the Catenary method is not, in general, an equilibrium position. Therefore full statics should normally be included unless it is known that the omitted effects are unimportant. Nevertheless, the Catenary position is often quite close to the true equilibrium position, especially when bend stiffness is not a major influence. The next chapter will make comparison between a pure catenary method and FEM.

Moreover, the catenary method cannot handle the case where the line is in compression. This is because, when bending stiffness is ignored, compression means the line is slack and there is no unique solution.[1]

Section 2.3 Limitation of Newton-Raphson Iteration Method

Newton-Raphson method is frequently used due to its effectiveness to capture equilibrium position for nonlinear structure problem. Load increment method combined with full or modified Newton-Raphson method is the common solution technique for riser analysis programs. Most of nonlinear problems can be solved, but non-convergence is encountered when load increment method is used to pass a limit point. That is why more advanced technique like Riks method is employed to solve unstable structure behavior by the popular FEM software, such as Abaqus, ANSYS, etc. Typical difficulties occur with riser clashes and the wake effect.

In order to solve detection of contact and wake flow evaluation, Deeplines employs specially “the fixed point method” to iterate in addition to the Newton-Raphson algorithm. Typical iteration loop is shown in the following figure.



For instance, in case of riser clashes, the area of neighborhood is first determined. According to them, contact elements are created with their own normal vector. At that stage, the virtual work principle is solved taking into account contact reactions. Their modulus is adjusted but the contact elements are fixed as well as the contact directions, even if the structures move. That's why getting out of the Newton-Raphson algorithm, the location of contact elements is up-dated and the system of equations is solved again.

Finally, only one iteration step is enough to find the equilibrium. For practical reasons, the number of loops for the fixed point method is limited with the keyword *CONTACT. The final convergence state is supposed to be acceptable.[2]

Section 4.6 “Guidance to Static Analysis” in “Riflex Theory Manual” instructs cautious selection when sequence of load steps is ordered. Two classical examples are given: [9]

- Application of volume force as 1st load condition for vertical tensioned riser
- Application of current force to current sensitive systems

Both cases are intrinsic instability problem which cannot be solved by load increment technique combined with New-Raphason iteration.

Section 2.4 High frequency noise induced by FEM model [1]

Finite element models may contain spurious high frequency response, a feature inherent in the finite element method. Minimization of high frequency noise is introduced explicitly by Orcina. Two solutions are available in the latest version of OrcaFlex.

Line Target Damping

Line Target Damping specifies damping whose effect is usually only to damp down this high frequency noise. The data specifies damping ratio in the % critical damping level that will be achieved for oscillations at the shortest natural period of each node. These oscillation periods are typically very short and depend on the segment length and stiffness values of the line section involved.

The % critical damping generated for longer oscillation periods is inversely proportional to the period, and for typical response periods (usually much longer) the damping level is usually insignificant. To achieve a significant level of damping at wave period usually requires that a very high Line Target Damping data value to be calculated and specified. This often also requires shorter time steps and so longer simulations. Hence, it is recommended to use Rayleigh Damping to model the effects of structural damping.

The target damping can be specified independently for tension, bending and torsion. Within broad limits, this damping has little influence on the results of a simulation unless the system is subject to very rapid variations in tension or bending, for example when snatch loads occur. A value between 5% and 50% of target damping is usually assumed.

Numeric damping of implicit integration scheme

The Generalized- α integration scheme has controllable numerical damping which is desirable since it removes this spurious, non-physical high frequency response. This numerical damping also leads to much more stable convergence and hence allows for longer time steps and much faster simulations.

Any integration scheme which includes numerical damping of high frequency response must be careful to avoid damping response at lower frequencies. The Generalized- α integration scheme is designed to minimize the low frequency damping.

The numerical damping is determined by specifying the level of high frequency dissipation, ρ_∞ . OrcaFlex uses a built-in value of 0.4 which has been chosen to give fast simulation run times without compromising accuracy.

Section 2.5 Restriction of discretisation

Finite element or finite difference techniques are typically employed to reduce the differential equilibrium equations to a set of coupled algebraic equations that can be solved numerically. The riser must be discretized carefully to avoid numerical errors from too coarse a mesh while producing a model that can be analyzed with a reasonable amount of computational effort. The level of discretization that is ultimately acceptable depends on the numerical representation of tension variation, the spatial variation in physical properties of the riser and in the magnitude of applied load, frequency content of the applied load and the accuracy of the desired results. In general, coarser meshes are acceptable for determining approximate displacement solutions to problems dominated by vessel motions, while finer meshes are essential for accurately determining stresses in the splash zone or at a stress joint for fatigue analysis.

An optimum discretization model should not only satisfy representative of response variation and but also demand computation time as little as possible. The balance could be achieved based on good understanding of response behavior for the specified riser. Therefore, the analyst has to make a clear view of where a finer mesh is necessary according to parametric study. Further discussion about optimization of discretization model is given in the latter chapter.

As a general guideline, API 2RD establishes basic criteria for upper limit of finite element length listed below:

- a) Near a boundary, element length should not exceed: $C = \sqrt{\frac{EI}{T}}$
- b) Away from boundaries, element length should not exceed: $C = \frac{\pi}{\omega} \sqrt{\frac{EI}{T}}$,
where ω is the highest lateral frequency to be included in the analysis.
- c) The ratio of lengths of successive elements should not exceed about 1:2.

Although finer mesh is preferred for the sake of more accurate results, sometimes however, for example riser clash, contact stiffness is rarely known with any precision, and it may not be practicable to discrete the line sufficiently to represent the deformation. The measure of contact strain energy shows that, longer segments give higher values of contact strain energy. This means that the reported strain energy for a coarsely segmented model is generally conservative. In practical cases, it may be possible to reduce segment length sufficiently to show that contact strain energy is below damaging levels, without applying finer discretisation.[10]

Section 2.6 Stability of Numerical Integration

Stability and accuracy of the time integration should be carefully considered when setting up the time-domain analysis run. Most popular methods are conditionally stable, meaning that the time step size must be below a certain threshold for the analysis to yield meaningful results. The most popular and unconditional stable method is the Newmark- β Constant Average Acceleration method. However, all methods require that the time step be small enough to accurately reflect important frequencies in the load or response. This is analogous to proper spatial discretization of the model and careful selection of frequencies in the frequency-domain method. Large time steps may result in a quicker analysis that is accurate for the frequencies represented but may miss important higher frequency contributions. All methods have some degree of integration error that is associated with frequency and amplitude of the integrated response. In certain situations, slight errors in frequency alone can accumulate and lead to numerical “beating” of the response. It is important to recognize and understand these errors when performing time-domain analysis, particularly for the purpose of simulating long time histories and developing statistics for extremes.[10]

Despite that time step size achieving stable integration is strongly system and excitation dependent, a summary of guidance given by OrcaFlex, Deeplines and Riflex, along with time step study in latter chapter presents the following suggestion for setting time step.

1. Definitions

Inner time step- fraction of the shortest natural period

For most cases the inner time step can safely be set to 1/10th of the shortest natural nodal period.

Outer time step- three options (Only applicable to OrcaFlex)

1) Multiple of inner time step

The recommended outer time step will be no greater than this value times the inner time step.

2) Fraction of wave period or up crossing period T_z

The recommended outer time step will be no greater than T divided by this value, where T is either the wave period (for regular waves) or T_z (for random waves).

3) Fraction of Wake Oscillator Strouhal period

This value is only available for a Wake Oscillator VIV model. The recommended outer time step will be no greater than the minimum Wake Oscillator Strouhal Period divided by this value.



2. Recommendation for time step

Most calculations during the simulation are done every inner time step, but some parameters like the more slowly-varying motion are only recalculated every outer time step. This reduces the calculations needed and so increases the speed of simulation.

The usual effect of setting one of the time steps too large is that the simulation becomes unstable, in the sense that very large and rapidly increasing oscillations develop, usually very near the start of the simulation. It is generally worth repeating important simulations with smaller step sizes to ensure that no significant loss of accuracy has occurred.

Examples of more numerically sensitive analyze requiring a rather small time step and narrow convergence criterion are:

- Systems undergoing large transverse seabed excursion
- Low tension problems including snapping and compression
- Nonlinear cross sectional modeling using bending moment hysteresis
- Transient release or rupture analysis
- High value of seabed stiffness

Both time steps must be short enough to give stable and accurate simulation. Experience indicates that the inner step should not exceed 1/10th to 1/20th of the shortest natural nodal period of motion for any degree of freedom in the model. The shortest natural nodal period is available in results of Eigen mode analyze.

The outer time step can usually be set to 10 times the inner time step; this gives a good saving in computing time without risking instability. In addition, the outer time step should generally not be more than 1/40th of the wave period. If a Wake Oscillator VIV model is used, then the outer time step is no more than 1/200th of the minimum Wake Oscillator Strouhal Period.

In some programs an option “Automatic subdivision of time step if required accuracy is not obtained with original time step or if incremental rotations are too large” is available.

In other programs such as OrcaFlex, there are 2 modes of operation: “Always use recommended time steps” and “specify by user”. The former mode is recommended because automatic modification of time step can avoid risk of instability and specifying too short time step. This mode is quite useful during design phase when parameter is frequently modified or there are a large number of similar simulations using batch script methods.

If one uses OrcaFlex, even time step is specified by user himself and the program still will calculate the recommended time step and give warning information if the given time step is larger. This seems to be an advantage feature specially given by Orcaflex compared with other software.[1]

Section 2.7 Limitation of Frequency domain method

Riser dynamic finite element equations of motions are typically expressed in matrix form as

$$M\ddot{x}(t) + C\dot{x}(t) + Kx(t) = f(t) \quad 2.7.1$$

Eq. (2.7.1) has no closed form solution for the dynamic response $x(t)$, and so the solution must be found numerically in either the time or the frequency domain.

Time domain analysis involves using a temporal operator to rewrite Eq. (2.7.1) at discrete times in terms of the (unknown) displacements at that time, and the (known) displacements, velocities and accelerations at a previous step or steps. The analysis inputs are time histories of wave and vessel motions; the outputs are response time histories on which a riser design is based. One advantage of time domain analysis is that all nonlinear effects can be retained in full for a high level of accuracy. The disadvantage is that the method is expensive in terms of computer time, and the level of output generated for subsequent post processing, for example in a fatigue load case random sea analysis, can be significant.

Frequency domain analysis is fast; the level of output generated is minimal; and there is no “statistical uncertainty” associated with the results of random sea analyses, since the input and output are respectively wave and response spectra. In the time domain, the inputs are time histories of wave elevation and vessel motion, and the outputs are time histories of response, all of which represent single realizations only of the respective random processes.

However, frequency domain analysis assumes M , C and K do not vary with time. This assumption is not valid where geometric nonlinearities are important or where intermittent effects like seabed interaction occur. So the frequency domain is generally used for linear system, typically top tension riser (TTR). TTRs are simply vertical structures, consisting of tensioned beams in which rotations normally are less than 6° , to avoid large bending at ends. Because of the relatively moderate riser rotations, all stages of the riser response determination, including the prediction of the mean offset position and the dynamic displacements about this mean, are linear or nearly linear, and can be based on a small angle assumption.

Frequency domain analysis of SCRs on the other hand poses a number of challenges not normally addressed in TTR analysis.

First, 2D linearization approach has been demonstrated conservative and sufficient for TTR analysis. But 3D Drag linearization is deemed to be necessary for compliant risers, like SCRs. Choice of linearization technique is crucial to success of frequency domain method.

Second, the effects such as intermittent contact between riser and seabed in the plane normal to the seabed, and friction forces in the plane of the seabed, cannot be included in full in a methodology based on frequency domain analysis.

Third, 2nd order vessel motion shall be taken into account for SCRs due to significant contribution to fatigue damage induced by interaction between riser and seabed.

In spite of lack of mature application on flexible riser analysis, frequency domain method is

proven making some sense by the paper [5]. The author makes comparison between 3 hours time domain realizations and improved frequency domain solution gained by Freecom- 3D.

Bending moment comparison is illustrated in Figure 2.7-1 and 2.

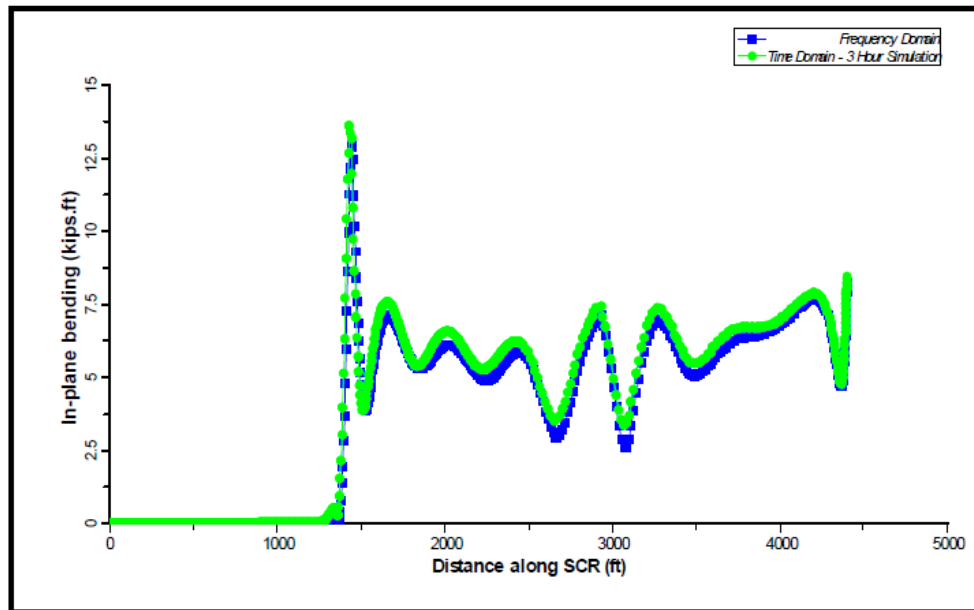


Figure 2.7-1 standard deviation of bending moment, in plane

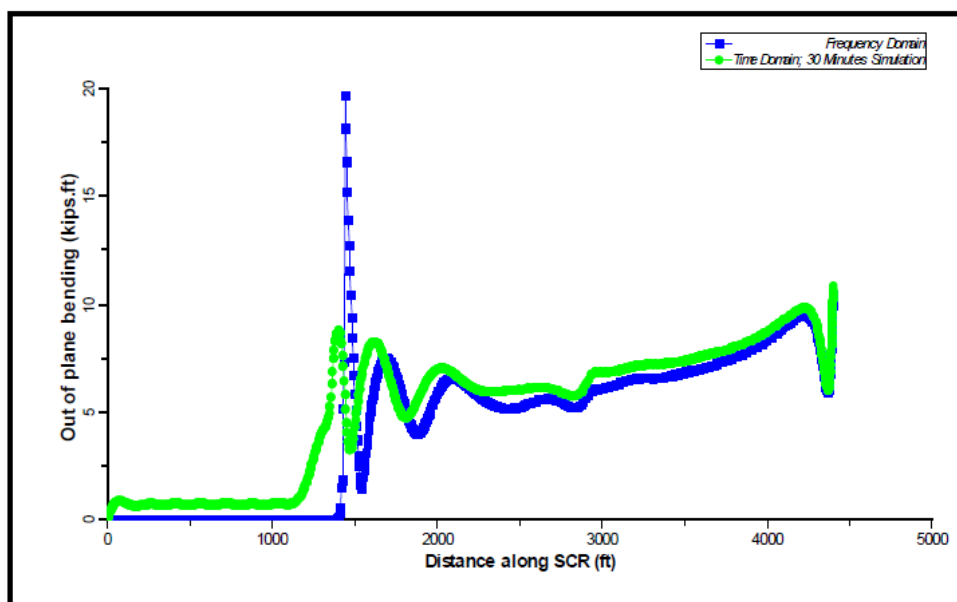


Figure 2.7-2 bending moment, out of plane, 2nd order motion

The examination shows, frequency domain method could be used as screening tool in initial SCR design phase to filter unfeasible options, and used for sensitivity study during detailed design phase. Above all, frequency domain method is not reliable for a complex and demand area of SCR design, even though it can provide similar trend of load variations as time domain method.

Section 2.8 Bucking problem

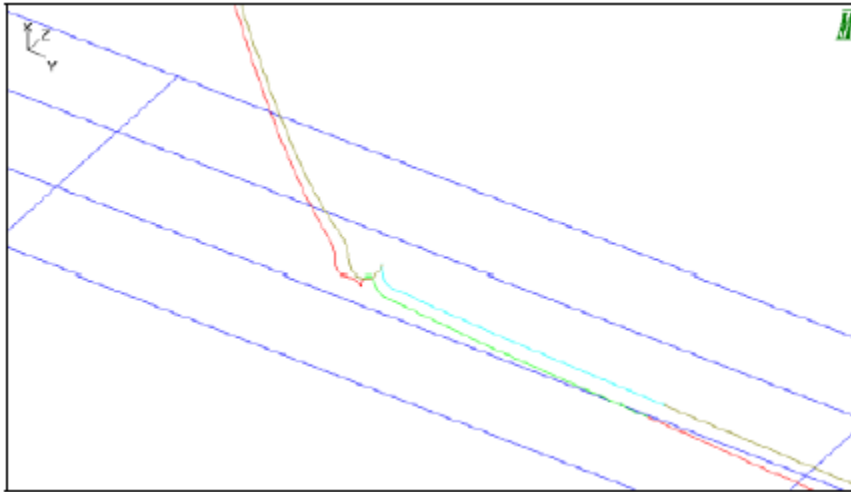


Figure 2.8-1 Snapshot of global buckling at touchdown area acquired from Flexcom

Normally global buckling is not a problem for risers applied in TLP or Spar concept where vertical motion of hang off point is restricted. Whereas, when vertical motion of the floater is significant, compression forces may arise at TDP. If amplitude of vessel heave motion is very large under extreme states, or hang off point is distant from vessel's center of gravity so that pitch motion amplifies the motion of top end, global buckling of the pipe section will reduce the dynamic pipe minimum bend radius. Thus, if compressive response arises, global buckling of the pipe cross section must be verified. Typical case is catenary risers for FPSO design.[6]

The current guidelines like DNV OS-F201 do not address analysis technique of global buckling. One of the difficulties here is that a large variation in post buckling behavior can arise depending on how the problem is numerically modeled and these can lead to difficulties in comparing against a fixed MBR criterion. In other words, there is no single "true" answer.

Buckling is an instability problem intrinsic to motion equations. It is characterized by no determinant for stiffness matrix when FEM is concerned. When buckling occurs, the structure exhibits large displacements.

To account for unstable post buckling behavior, stiffness matrix should have geometrical stiffness included in addition to small displacement stiffness. Besides, proper push over technique should be used to achieve convergence of solution for snap through behavior.

In general, most of analysis packages such as OrcaFlex, Deeplines and Flexcom have been tested and validated by other FEM tools for post buckling analysis. However, it is noted that accurate prediction of onset of buckling and post buckling behavior is based on the following conditions:



1. Sensible values of element length and time step are used
2. The Euler buckling load within each individual element is not exceeded.

Many of these analysis packages use finite element solution schemes and are based on beam bending equations that have force equilibrium equation for beam-column as a cornerstone.

$$EIw'' = -Pw \qquad 2.8.1$$

As a result, deflection in the element will increase with increasing compressive load until the theoretical buckling load is reached. At the buckling load, the deflection tends towards infinity and the solution crashes. In reality, although the structure deforms at the buckling load, under post buckling behavior, the structure can accommodate increasing level of load as it become increasingly distorted. Therefore, when the effective compression in an element achieves the theoretical element compression limit, the solution becomes numerically unstable and will terminate. The principle is to reduce the element lengths sufficiently to ensure that each element can withstand the maximum compressive load expected.

Under static loading conditions, load increment method with stepwise iteration by Newton-Raphson is adopted by Deeplines and Riflex. Hence, snap-through behavior has to be avoided during all load steps due to non- convergence.

Under dynamic loading conditions, the transverse deflection is resisted by a combination of inertia force and bending. It is fully capable of achieving convergence and modeling snap-through behavior provided the two conditions mentioned above are satisfied.

Referring to theory manual of OrcaFlex, OrcaFlex provides a convenient way for automatic comparison for all segments and report to any infringements of the segment Euler load.

What are we going to do if Euler load is exceeded by compression force?

If the segment Euler load is infringed during a simulation, then we have to decide what to do about it. If infringement occurs only during the build-up period, perhaps as a result of a starting transient, then we can safely ignore it. If it occurs during the main part of the simulation, then we should examine the time histories of tension in the affected areas. Where infringements are severe and repeated or of long duration the analysis should be repeated with shorter segments in the affected area. However it may be acceptable to disregard occasional minor infringements of short duration on the following grounds:

1. Transverse deflection caused by compression takes some time to occur because of inertia.
2. The segment Euler load used in OrcaFlex as a basis for comparison is the lowest of the various alternatives, and assumes pinned joints with no bend stiffness at each end of the segment. This is a conservative assumption.

Section 2.9 Uncertainty of soil-pipe interaction model

Traditionally sea floor is modeled as linear springs in both horizontal and vertical directions. This model describes seabed stiffness very simple and effective in the viewpoint for global analysis. However, when fatigue stresses is to be estimated, special care should be given to the interaction between the seafloor and the riser because of the high non-linearity of soil response. This issue is especially crucial for touchdown area where it is proved to be the critical location of fatigue analysis due to high level of bending moment range. Although linear elastic seafloor model provides very useful insights about seafloor-riser interactions, it is noted linear model cannot fully describe the complex interaction problem including trench formation, non-linear soil stiffness, limited soil suction, detachment of the riser from the seabed, and cyclic degradation of soil stiffness, as shown by full-scale experimental testing. Previous studies have shown that fatigue damage is sensitive to seabed stiffness. Therefore a nonlinear pipe-soil interaction model giving more accurate description of real soil behavior is essential to evaluate fatigue damage of compliant risers.[8]

Two types of seafloor model: “Linear” and “Non-linear” Soil model will be introduced in the following:

1. Linear Model

The Linear model treats the seabed as a simple linear spring in both the seabed normal direction and the seabed shear directions (i.e. the axial and lateral directions in the seabed tangent plane). This gives a seabed normal resistance that is proportional to the penetration, and a seabed lateral resistance that is proportional to the lateral displacement of the contact point (e.g. a node on a line) from its undisturbed position. The linear spring stiffness in the normal and lateral directions can be specified independent from each other.

When explicit integration is used, the linear model also includes linear dampers in the normal and lateral directions, which give an extra damping resistance that is proportional to the rate of penetration (for the normal direction) or the rate of lateral movement (for the lateral directions). The linear damper in the normal direction only acts when penetration is increasing, not when penetration is reducing, so the model does not model any suction effect. Also, note that there is no seabed damping contribution when implicit integration is used.

Linear Model Parameters

1) Normal Seabed Stiffness

The constant of proportionality of the spring force in the seabed outward normal direction. The stiffness equals the spring reaction force, per unit area of contact, per unit depth of penetration. A high value models a surface such as rock; a low value models a soft surface such as mud.

2) Tangential Seabed Stiffness

This value is used by the friction calculation.

3) Seabed Damping

The constant of proportionality of the damping force, and is a percentage of critical damping. Seabed damping is always zero when using the implicit integration scheme.

Beware that, if you use the explicit integration scheme, high seabed stiffness will shorten the natural periods of parts of the system lying on it, and this may require the use of a smaller simulation time step.

2. Non-linear Soil Model

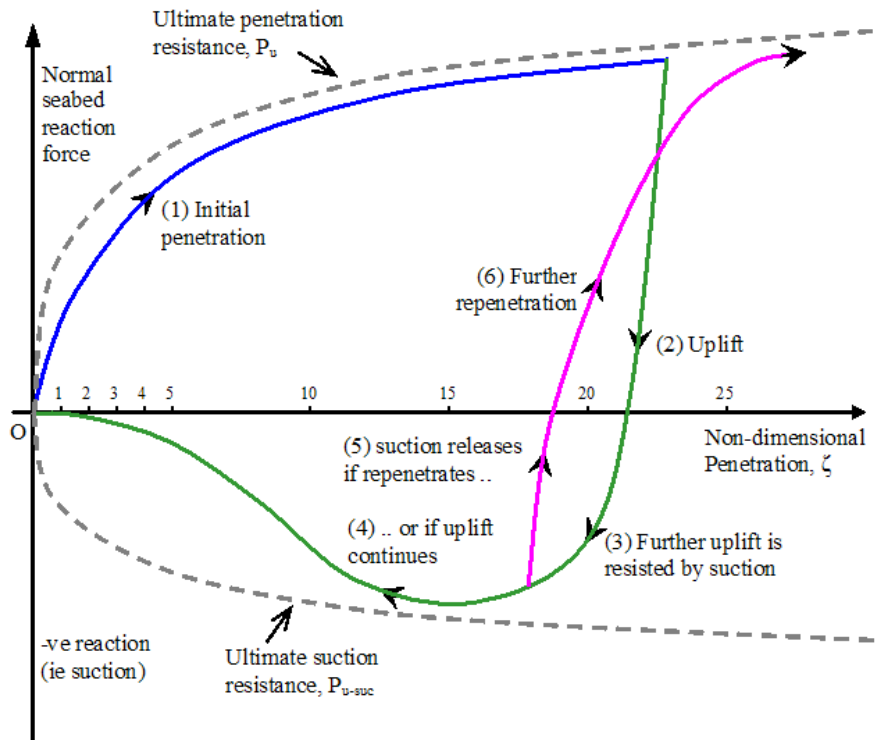


Figure 2.9-1 Nonlinear Pipe- Soil Interaction model

The non-linear soil model is more sophisticated than the linear model. It models the non-linear and hysteretic behavior of seabed soil in the normal direction, including modeling of suction effects when a penetrating object rises up sufficiently. The typical non-linear characteristics of soil are illustrated in the figure above. The non-linear modeling only applies to the seabed normal direction. In the seabed lateral directions the seabed is modeled in the same way as described above for the linear model.

The non-linear soil model is suited to modeling soft clays and silt clays, and it is particularly relevant for cases (such as deepwater seabed) where the mud line undrained shear strength is only a few kPa or less and the seabed stiffness response to catenary line contact is dominated by plastic penetration rather than elastic response. Note that the non-linear model is not suitable for cap rock conditions, and is not suitable for modeling sand without very careful choice of soil data and model parameters to reflect sand response.

Beware that, implicit integration is used for dynamic analysis. A shorter time step with the non-linear soil model is to be used than with the Linear model.

Non-linear Soil Model Parameters

Several non-dimensional constants control how to model the soil response.

- 1) Penetration Resistance Parameters
- 2) Soil Buoyancy Factor

This factor controls the modeling of the extra buoyancy effect that occurs when a penetrating object displaces soil.

- 3) Normalized Maximum Stiffness

This factor determines the reference penetration.

- 4) Suction Resistance Ratio

This factor controls the ultimate suction resistance.

- 5) Normalized Suction Decay Distance

The factor controls the suction decay limit term in Uplift mode.

- 6) Re-penetration Offset after Uplift

This parameter controls the penetration at which the re-penetration resistance limit in re-penetration mode merges with the bounding curve for initial penetration resistance.

Former Case Study [7]

The paper issued by Luca De Amicis in ISOPE 2008 performed comparison between linear and non-linear soil model. Flexcom is employed to investigate effect of pipe-soil model for the entrenched touchdown region for SCRs.

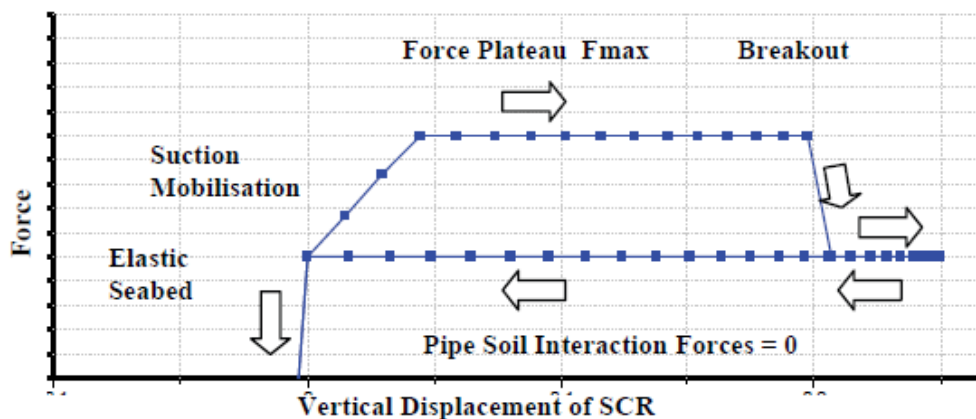


Figure 2.9-2 Non-linear pipe soil interaction modeling load path

Two advanced methodologies are presented for the nonlinear modeling of pipe soil interaction. In total, four models were built as follows;

- a) Single element model (Simple verification model);
- b) Base case model of the SCR on a flat seabed with no pipe-soil interaction other than elastic seabed (Traditional model);



- c) Model of entrenched SCR with pipe-soil interaction modeled using nodal springs acting without hysteretic type load path "Advanced Model A";
- d) Model of entrenched SCR with pipe-soil interaction modeled using implicit nodal springs acting with hysteretic type load path "Advanced Model B";

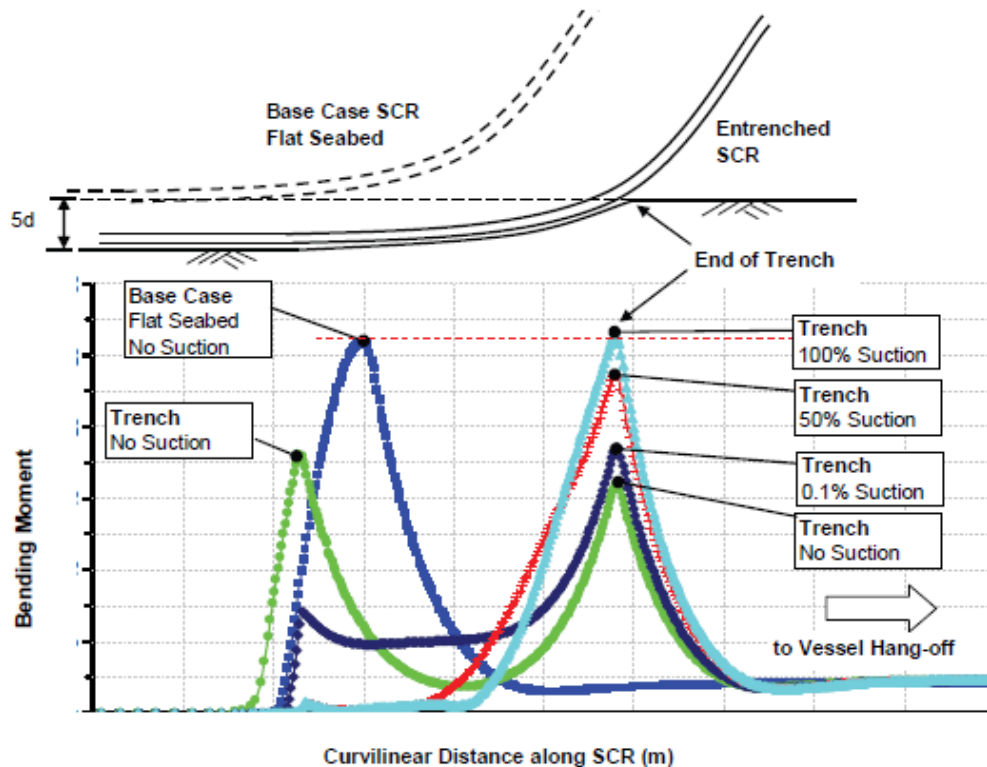


Figure 2.9-3 Effect of soil pipe interaction mode, regular wave study

The regular wave study illustrated in Figure 2.9-3 shows that a general trend - the standard deviation of bending moment increases with severity of sea state and depth of entrenchment, i.e. level of pipe soil interaction. The results also suggest that the traditional approach of ignoring soil pipe interaction in the assessment of fatigue is inconclusive with respect to level of conservatism. Besides, it is indicated that, implicit definition of the springs considering the hysteretic effect yields lower moment amplitudes in general.

Modeling the full range of expected trench conditions has indicated an overall beneficial effect on predicted fatigue life due to reduced bending stresses in the touchdown area. However, the benefit of modeling the trench profile at the mean position is reduced by soil pipe interaction as the vertical loads tend to hold the SCR in the trench and increase extreme bending stresses at the departure point of the trench.

Section 2.10 Limitation of Hydrodynamic force model

Study of four popular riser analysis programs in last chapter suggests that, hydrodynamic force is modeled with the same theory-“Morison equation”.

A careful examination reveals the following notes to give special care:

1. Hydrodynamic force coefficient

The hydrodynamic forces are calculated according to a generalized Morison's equation formulation. The specified coefficients are constant referring to experimental results. But in fact, it is impossible to measure the real force by a constant coefficient. The dependency on Reynold's number, Keulegan-Carpenter number and roughness should be taken into account when specifying the constant drag coefficients as input.

Typical cases are given here:

- 1) Vortex shedding inducing additional oscillatory force which is neglected by most of programs.
- 2) Variation of drag coefficient and added mass coefficient when the structure is close to boundary, for example, pipe floating on free surface.

2. Position for calculation of wave kinematics

Wave kinematics is usually calculated at mean position. Even though comparison between mean position and instantaneous position shows there is not crucial difference for analysis results, it is specially instructed in Riflex Theory Manual:

The external load is in nonlinear analysis always applied at instantaneous structural position. Nonlinear analysis should therefore also be considered when using wave kinematics computed at instantaneous structural position to obtain full consistency in the numerical model.

3. Axial drag force

In most of cases, drag force is dominated by normal force and axial force is almost negligible due to very little effect from riser or buoy skin friction. Nevertheless, it is highlighted in some paper; omission of axial drag has been shown to lead to non-conservative results in some case. [11]

OrcaFlex indeed provides 6D buoy mode which is able to specify axial drag for SPAR buoy. But this is not applicable to other programs. For instance, Riflex models axial drag force in the same way as normal drag force. That means axial drag force only takes skin friction into account, so that it is impractical to specify a varying axial drag force depending on the moving buoy.

Chapter 3 Validation of static analysis

Section 3.1 Introduction of Riflex method

Riflex provides different solutions for static analysis. As introduced in Theory manual [9], the main approaches are:

1. 2D catenary method, applicable for standard systems
2. FEM, based on different options of start configuration, such as catenary, user defined stress free shape, etc.

3.1.1 Principles for Static Catenary Analysis

Shooting method is used to compute the static equilibrium configuration of a composite single line with boundary conditions specified at both ends. Mathematically the problem is a two point boundary value problem. If all boundary conditions are specified at one end, the configuration is uniquely determined. This reduces the problem to an initial value problem and the static configuration can be found by catenary computations, element by element, starting at the end with all boundary conditions specified.

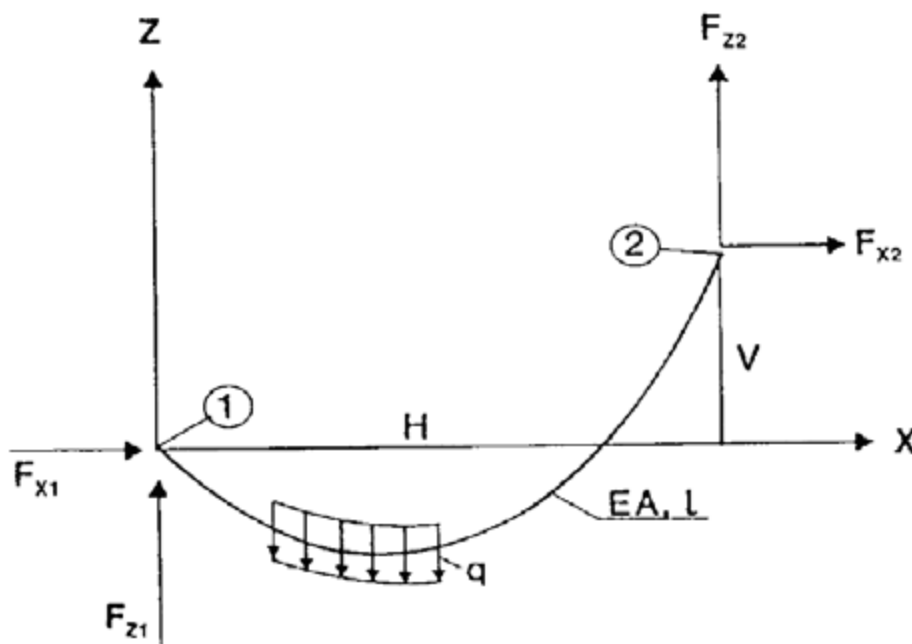


Figure 4.1-1 Definition of terms in classic catenary equations

The classic catenary equations are applied to compute the coordinates and force components at 2nd element end in the local element system (see for instance Peyrot and Goulois, 1979) [13]:



$$F_{x2} = -F_{x1} \quad (3.1.1)$$

$$F_{z2} = -F_{z1} + ql \quad (3.1.2)$$

$$H = -F_{x1} \left[\frac{l}{EA} + \frac{1}{q} \ln \left(\frac{F_{z2} + T_2}{T_1 - F_{z1}} \right) \right] \quad (3.1.3)$$

$$V = \frac{l}{2EAq} (T_2^2 - T_1^2) + \frac{1}{q} (T_2 - T_1) \quad (3.1.4)$$

$$I_d = l + \frac{l}{2EAq} \left[F_{z2}T_2 + F_{z1}T_1 + F_{x1}^2 \ln \left(\frac{F_{z2} + T_2}{T_1 - F_{z1}} \right) \right] \quad (3.1.5)$$

$$\text{Where } T_1 = \sqrt{F_{x1}^2 + F_{z1}^2}; \quad T_2 = \sqrt{F_{x2}^2 + F_{z2}^2}$$

3.1.2 Static FEM analysis

The purpose of the static analysis is to determine the nodal displacement vector so that the complete system is in static equilibrium. The static equilibrium is found by the equation:

$$R^S(r) = R^E(r) \quad (3.1.6)$$

r : nodal displacement vector

$R^S(r)$: internal structural reaction force vector

$R^E(r)$: external force vector

The static equilibrium is found by application of an incremental loading procedure with equilibrium iteration at each load step (i.e. a so-called incremental-iterative procedure with Euler-Cauchy increment).

The basic principle in this approach is to accumulate the external loading in a number of small load increments. The static configuration at each load step is then found by iterative solution of Eq. (3.1.6) for the accumulated external load vector using the displacement vector from previous load increment as start solution.

Incremental equilibrium iterations

The force imbalance vector at incremental load step is introduced as:

$$R_k(r) = R_k^S(r) - R_k^E(r) \quad (3.1.7)$$

The static equilibrium configuration at load step is governed by zero imbalance force, which can be found according to the following iteration procedure:

Computation of start values

Start values for the equilibrium iteration are based on the static equilibrium configuration computed at previous load step:

$$\Delta r_k^0 = - \frac{R_k^S(r) - R_k^E(r)}{\frac{\partial R_{k-1}}{\partial r}} \quad (3.1.8)$$

$$r_k^0 = r_{k-1} - \Delta r_k^0 \quad (3.1.9)$$



Newton-Raphson iteration procedure

Several iteration cycles can be performed to improve the start solution given by Eq. (3.1.3) and (3.1.4). A Newton-Raphson approach is adopted due to the quadratic convergence rate offered by this procedure j . $j = 0$ corresponds to the start values described above while $j = M$ is the maximum number of iteration cycles allowed.

The expressions for correction of the displacement vector at interaction cycle are given by:

$$\Delta r_k^j = \frac{R_k^{j-1}(r)}{\frac{\partial R_{k-1}}{\partial r}} \quad (3.1.10)$$

$$r_k^j = r_k^{j-1} - \Delta r_k^j \quad (3.1.11)$$

Section 3.2 Introduction of verification method

This paper is going to employ basic catenary cable equations presented in “Sea loads” [12] to compute static configuration. Above all, this method neglects the effect of bending stiffness and cable elasticity.

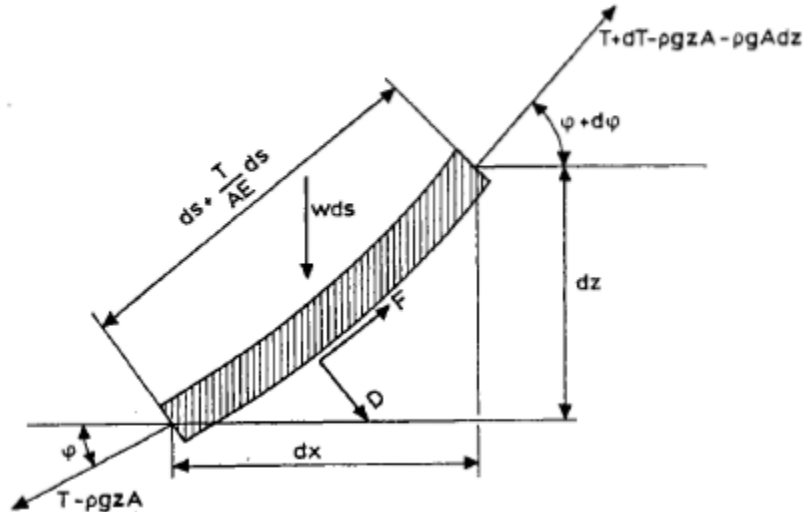


Figure 3.2-1 force acting on a cable element

The following equations are derived from force equilibrium of an infinitesimal cable element illustrated in the figure above:

$$dT - \rho g A dz = \left[w \sin \phi - F \left(1 + \frac{T}{AE} \right) \right] ds \quad (3.2.1)$$

$$T d\phi - \rho g A z d\phi = \left[w \cos \phi - D \left(1 + \frac{T}{AE} \right) \right] ds \quad (3.2.2)$$

Two types of risers will be performed comparison in this section, namely steel catenary (SCR) and lazy wave configuration (LWR). It is assumed that, location of both ends is known and length of each segment is also given.

Integration starts from touchdown point and stops when vertical position is equal to upper end. First, initial tension force at touchdown shall be found. Different approaches to determine the initial value of tension force on sea bed and length of suspended cable are adopted respectively for SCR and LWR. Eq. 3.2.3[12] is used for the former while Eq. 3.1.1 – 3.1.5 are for the latter.

$$X = l - h \sqrt{\left(1 + 2 \frac{a}{h} \right)} + a \cosh^{-1} \left(1 + \frac{h}{a} \right) \quad (3.2.3)$$

However, the initial value will be checked again on completion of integration. If the initial value is not in agreement with the final result, integration will restart with a modified initial value. Iteration will go on until initial value's deviation from final is less than 0.01%.

In general, coding in MATLAB includes two steps: approximation of initial value and integration iteration. The programs see appendix A.

Section 3.3 Comparison of SCR

3.3.1 Parameters

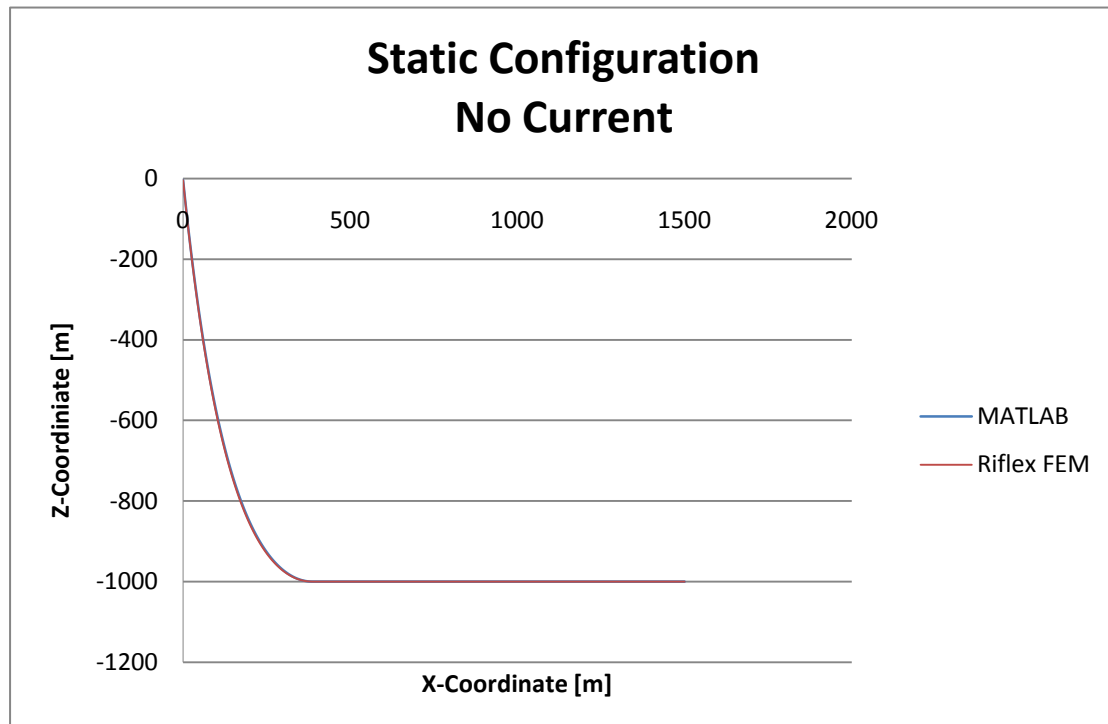
SCR Specification

Parameter	Value
Outer Diameter [mm]	273
Wall Thickness [mm]	12.7
Bare pipe weight [kg/m]	125
Internal fluid density [kg/m^3]	700
Length	2240m
Hang off point	(0 m,0 m,-4.469621658 m)
Lower end	(1500 m,0 m,-1000 m)

Riflex specification

Element Type	Beam element
Analysis method	FEM
Segments Length(from top to bottom)	Element Length
268.88 m	10m
717.02m	5m
358.5m	1m
80.0m	10m

3.3.2 Comparison of results



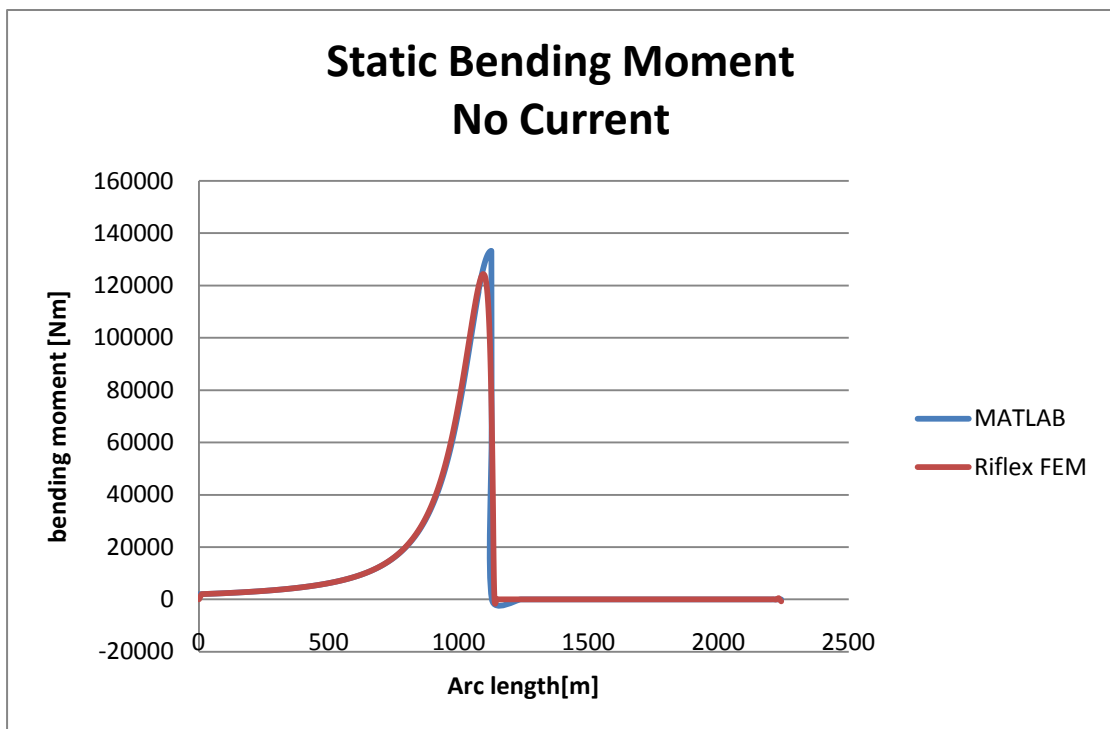
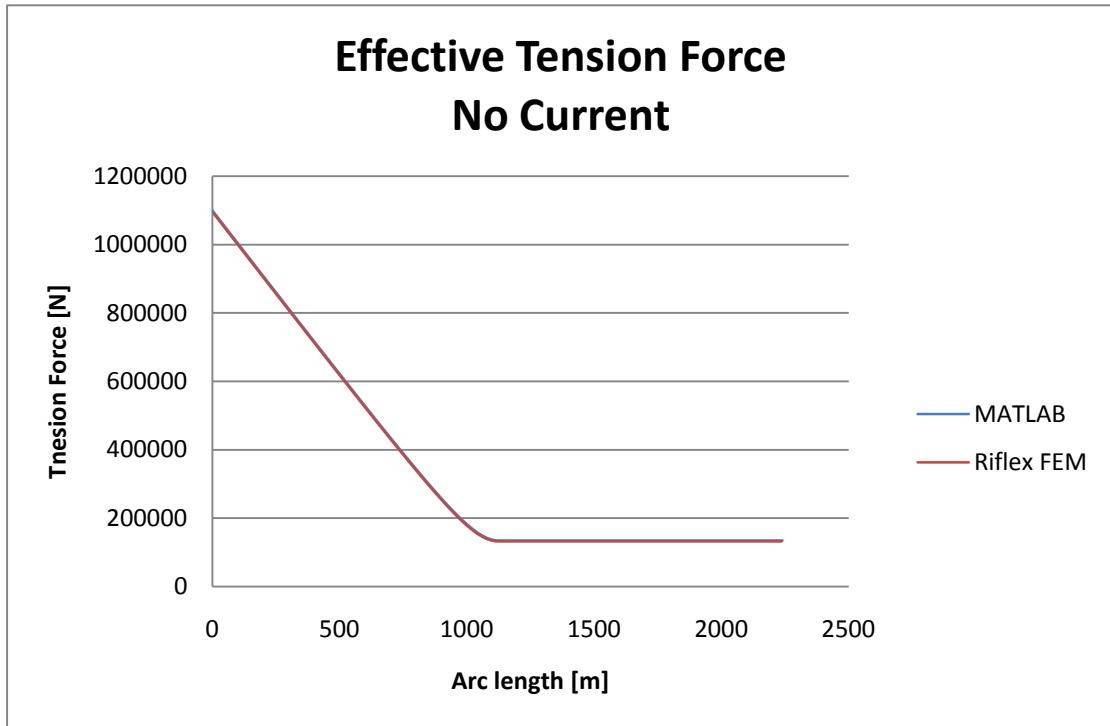


Table 4.2-1 Comparison of Maximum force

Approach	Top tension force [KN]	Maximum bending moment [KNm]
MATLAB	1099.575	133.2
Riflex FEM	1090.478	124.4
Difference	0.83%	7.1%



Next, a current condition is given as shown in the following profile

Current	
Return period	100 years
Depth [m]	Speed [cm/s]
0	126
-30	110
-75	110
-147	85
-200	60
-400	50
-600	45
-800	40
-900	30
-1000	10

Change of force by Riflex computation is listed below:

Approach	Top tension force [KN]	Top angle °	Horizontal component [KN]	Horizontal tension force [KN]
Riflex, No Current	1090.478	83.05	131.9	131.8
Riflex, Current	1088.385	82.7	138.3	129.7

MATLAB is used to calculate overall current force components based on no current geometry.

Current force component	Horizontal [KN]	Vertical [KN]
MATLAB	- 8.1	1.5
Top Tension Force component	Horizontal [KN]	Vertical [KN]
Riflex, no current	131.9	1082.5
Riflex, current included	138.3	1079.6
Riflex force difference	-6.4	2.9
Riflex , current includes horizontal force balance	-8.6	/
Approximate top tension force	1090.0	

Good agreement with global force balance is achieved; even current force is integrated based on no current geometry.

Section 3.4 Comparison of LWR

3.4.1 LWR Specification

Length	2100m
Segments Length(from top to bottom)	Riflex Element Length
900m	5m
800m(Buoyancy Attachment)	10m
400m	5m
Buoyancy Can attachment Diameter	0.55m
Buoyancy Can attachment weight	20Kg/m
Bare pipe weight	125kg/m
Hang off point	(0 m,0 m,-4.469621658 m)
Lower end	(1500 m,0 m,-1000 m)

3.4.2 MATLAB Approaches

Two approaches are used for determining initial value of tension force and suspended cable length.

1. Approach I [14]

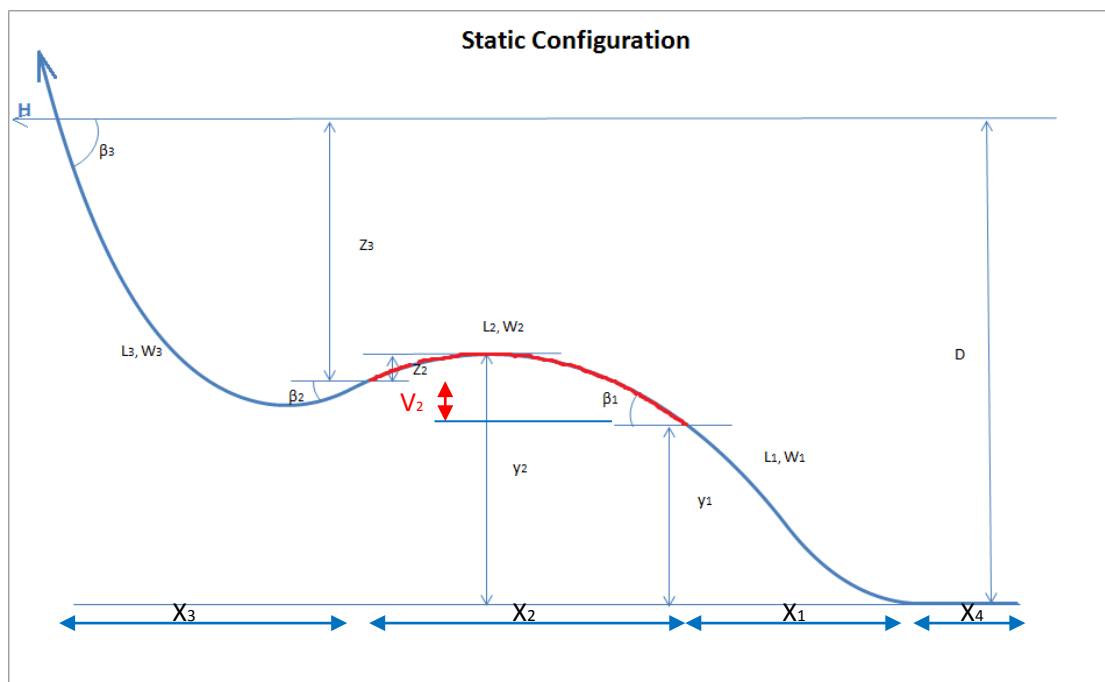


Figure 3.4-1 definition of terms used for static calculation

The figure above shows all necessary parameters for calculation, where H is horizontal tension force, L is segment length, and W is unit weight.

Compatibility of suspended cable establishes the following equations:



$L_1 = \sqrt{\left(\frac{w_2 y_2}{w_1 - w_2}\right)^2 - \frac{2Hw_2 y_2}{w_1(w_1 - w_2)}}$	(3.4.1)
$z_3 = \frac{H}{w_3} \left(\sqrt{1 + \beta_3^2} - \sqrt{1 + \beta_2^2} \right)$	(3.4.2.1)
$z_2 = \frac{H}{w_2} \left(\sqrt{1 + \beta_2^2} - 1 \right)$	(3.4.2.2)
$\beta_1 = \frac{w_1 L_1}{H}$	(3.4.3.1)
$\beta_2 = \beta_1 + \frac{w_2 L_2}{H}$	(3.4.3.1)
$\beta_3 = \beta_2 + \frac{w_3 L_3}{H}$	(3.4.3.3)
$y_2 = D - z_2 - z_3$	(3.4.4)

Then iteration is carried out in the following procedure with two loops:

- 1) Assume H
- 2) Assume y_2^0
- 3) Calculate L_1 from Eq. (3.4.1)
- 4) Calculate angle β at intersections from Eq.(3.4.3)
- 5) Calculate Z by Eq.(3.4.2)
- 6) Calculate y_2^* by Eq.(3.4.4)
- 7) Compare y_2^* with y_2^0
 If the difference is less than tolerance, result is accepted as final, and go to step 8);
 Otherwise, make a new assumption $y_2^i = y_2^{i-1} + f(y_2^* - y_2^{i-1})$ where $f=0.5$, go back to step 3).
- 8) Calculate X_1, X_2, X_3 by Eq.(4.3), and further get X_4 .
- 9) Compare $X_1 + X_2 + X_3 + X_4$ with 1500m
 If the difference is less than 0.1%, data is accepted as final result and iteration stops.
 Otherwise, increase H by an adjustable step, which is smaller while the difference is smaller. Go back to step 2).

2. Approach II

Define vertical distance Z_3, V_2, y_1 between each segment end. Two equations are established based on boundary condition:

$Z_3 + V_2 + y_1 = 1000\text{m}$	(3.4.5)
$X_1 + X_2 + X_3 + X_4 = 1500\text{m}$	(3.4.6)

There are in fact only two unknown variables horizontal force H and segment length L_1 . Substitute Eq. 3.1.3 and 3.1.4 into equations 3.4.5 and 3.4.6, and then utilize MATLAB nonlinear equation solver "fsovl" to compute the results of H and L_1 . The solution is unique.

A comparison of initial value is performed in the following table. Good agreement is achieved.

Table 3.4-1 Initial value comparison between two approaches

Approach	Horizontal tension force [KN]	L_1 [m]
I	166.10	259.189
II	166.01	259.151

Next, the final geometrical configuration and tension force are illustrated in comparison with that gained by Riflex.

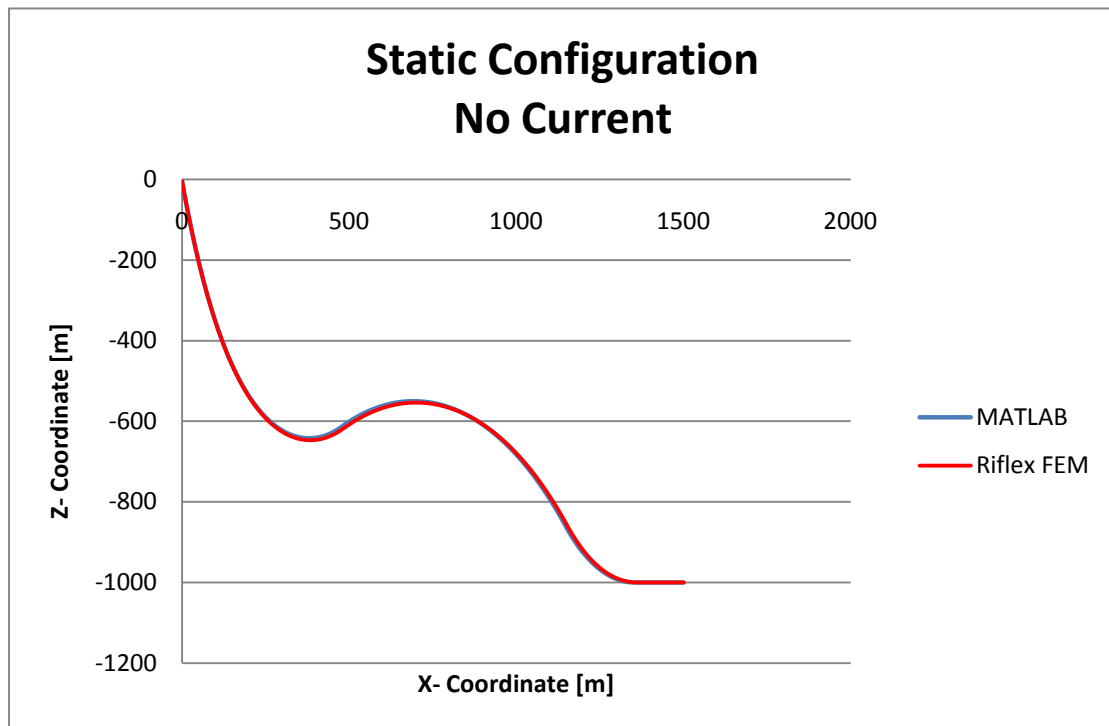


Figure 3.4-2-1 comparison between catenary method and FEM: static geometry

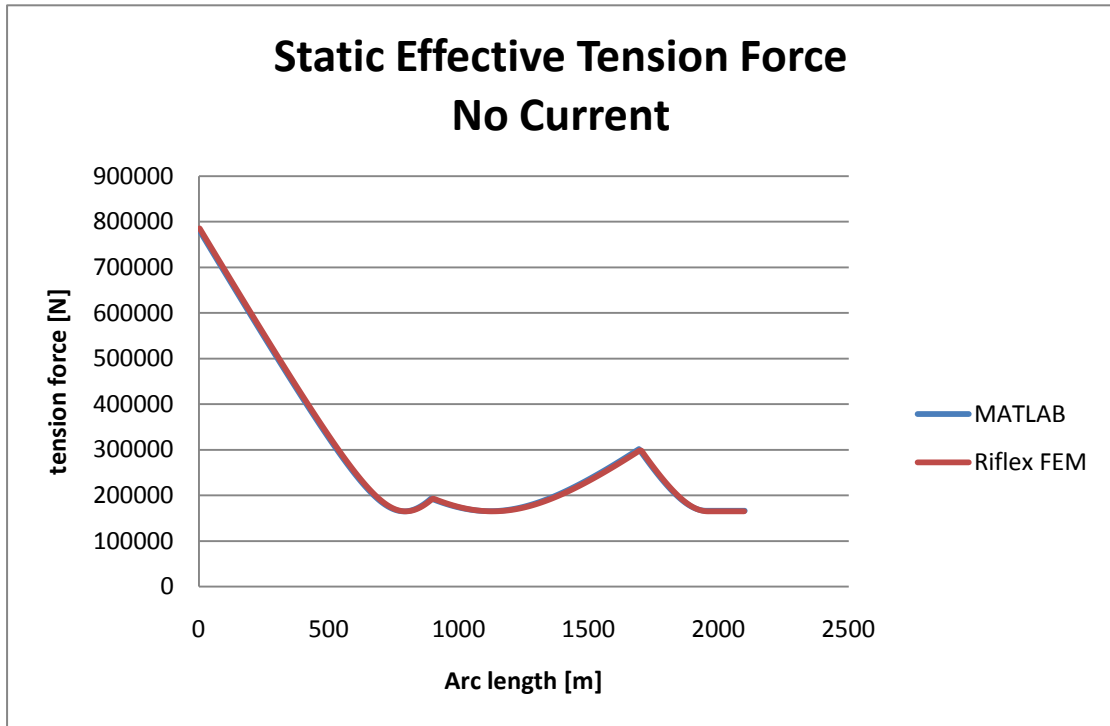


Figure 3.4-2-2 comparison between catenary method and FEM: static effective tension force

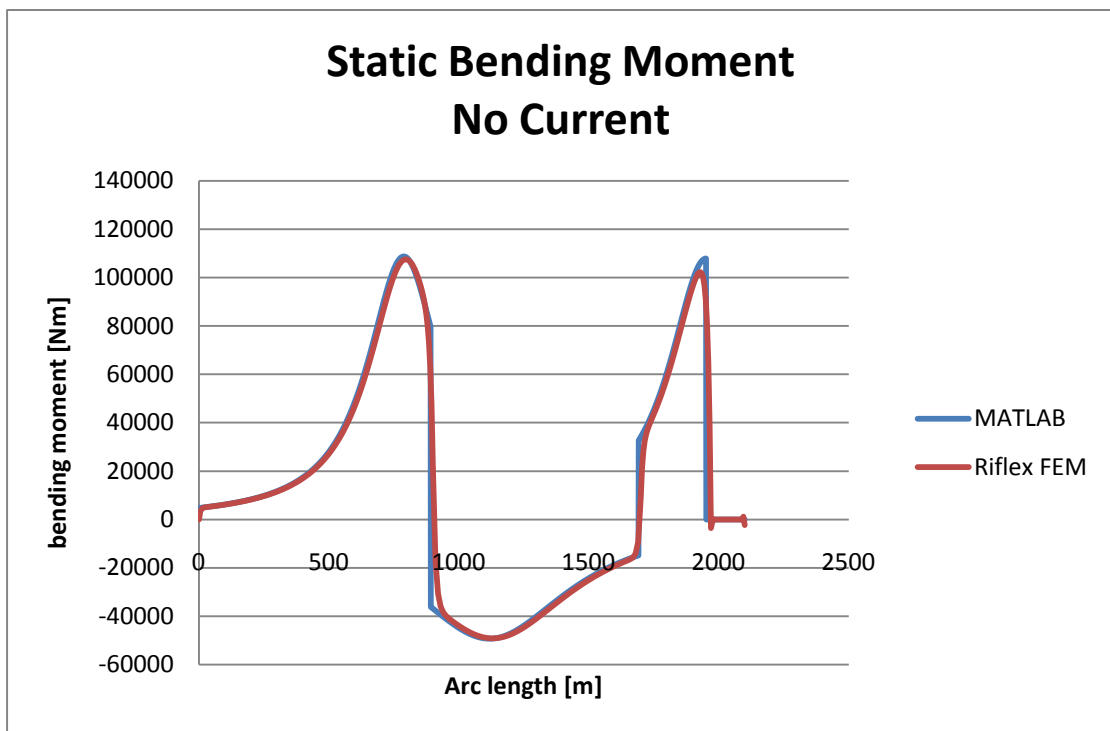


Figure 3.4-2-3 comparison between catenary method and FEM: static bending moment

Table 4.3-1 Comparison of Maximum force

Approach	Top tension force [KN]	Maximum bending moment [KNm]
MATLAB	782.553	108.79
Riflex FEM	785.332	107.6
Difference	0.35%	1.1%



The comparison above is only performed for the case without current included.

Next, a light current condition is given as shown in the following profile

Current	
Return period	100 years
Depth [m]	Speed [cm/s]
0	63
-30	55
-75	55
-147	42.5
-200	30
-400	25
-600	22.5
-800	20
-900	15
-1000	5

The results gained from Riflex are presented below for with and without current.

Approach	Top tension force [KN]	Top angle °	Te Horizontal component [KN]	Horizontal tension force [KN]
Riflex, No Current	785.332	77.85	165.3	165.336
Riflex, Current	782.5	76.6	181.343	162.279

If it is assumed the geometrical configuration of riser is not changed by current, then MATLAB calculates overall current force components as below

Current force component	Horizontal [KN]	Vertical [KN]
MATLAB	-19.45	7.49
Top Tension Force component	Horizontal [KN]	Vertical [KN]
Riflex, no current	165.3	767.7
Riflex, current included	181.3	761.2
Riflex force difference	-16.0	6.5
Riflex, current included Horizontal force balance	-19.06	/
Approximate top tension force	779.6	

MATLAB gives good estimation of the overall current to achieve global balance. However, top tension force with current is not equal to the approximate result obtained by assuming horizontal tension force unchanged and superposing global current force to no current top tension force.

Section 3.5 Conclusion

1. Bending stiffness is negligible in force equilibrium except in large curvature area. Therefore, bar element is proficient to compute static problem of risers. Bending moment can be directly interpreted from geometrical curvature.
2. It is proven that, current indeed does not have large effect on static results. An approximation of overall current computed based on no current geometry is enough to achieve global force balance. However, it is also concluded that, horizontal tension force is influenced by current. Current toward “near” direction reduces horizontal effective tension force. Therefore, in order to approximate top tension force with current effect included, one has to find new initial value of horizontal tension force first and then superpose the estimated overall current force.

Chapter 4 Validation of Dynamic bending moment

Section 4.1 Introduction of boundary layer value method

An analytical approximation for dynamic bending moment at the touchdown point of a catenary riser is cited which is introduced by the paper [15] published in International journal of Offshore and Polar Engineering. A quasi-linear frequency domain solution of a cable (bending stiffness $EI=0$) is used to develop an approximation, of a boundary layer type. It is derived that the bending moment in vicinity of TDP depends on only two quasi-linear dynamic variables: the displacement $x_0(t)$ of touch down point and dynamic tension $\tau(t)$.

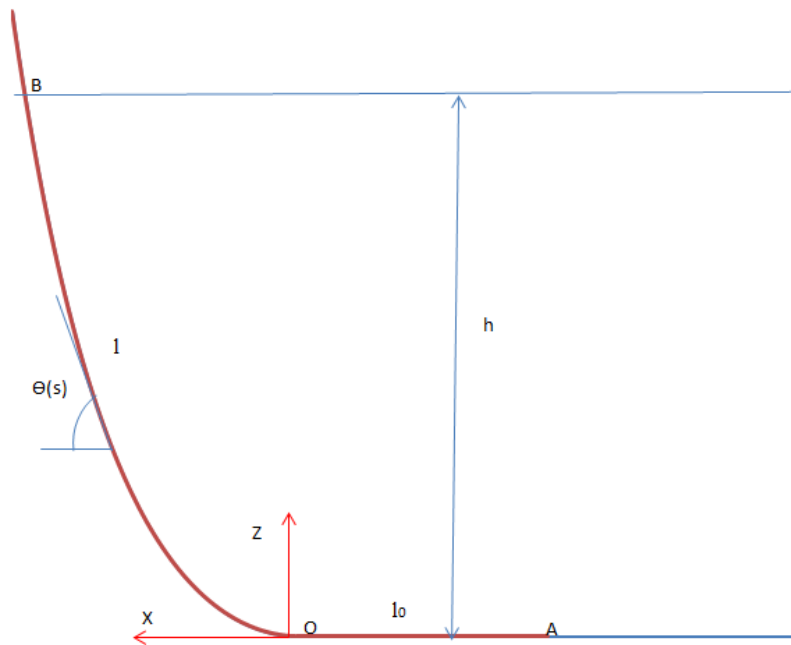


Figure 4.1-1 Static configuration and Coordinate definition

Two basic assumptions are made as premise for formula derivation listed below:

- 1) No bending stiffness, $EI=0$
- 2) No impact phenomenon (the riser does not strike the soil).

First, a linear dynamic solution for $x_0(t)$ is given by Eq.7b)

$$x_0(t) = -\frac{T_0}{q} \frac{\partial Z}{\partial x}(0, t) = -\frac{T_0}{q} \alpha(0, t) \quad 7b)$$

Where T_0 is static tension force at TDP; q is the cable weight per unit.

Once the angle $\alpha(0, t)$ is determined from linear frequency domain solution, and then the displacement $x_0(t)$ is available.

One may estimate the amplitude of $x_0(t)$ by Eq. 8a)



$$X_0 \approx \frac{6A_B}{\theta_B^2} \quad 8a)$$

Where A_B is oscillation amplitude of the hang off point.

Second, if the elastic axial modes are not excited by wave, the dynamic tension is essentially constant along the suspended length, as discussed in Triantafyllou et al.(1985). Therefore, in a large vicinity of TDP, dynamic tension force is given by

$$\tau(t) = \tau_1 \cos \omega t \quad (4.1)$$

Where τ_1 is amplitude of dynamic tension force can also be determined from a linear frequency domain model.

Last, the approximate formula of dynamic bending moment is expressed below

$$M_f(s, t) = \frac{1}{2} (1 + \text{sign} \beta(s, t)) [1 - e^{-\beta(s, t)}] \frac{M_0}{1 + \tau(t)/T_0} \quad 12b)$$

$$\beta(s, t) = \frac{\sqrt{1 + \tau(t)/T_0}}{\lambda} \left[s - x_0(t) + \frac{\lambda}{\sqrt{1 + \tau(t)/T_0}} \right] \quad 12a)$$

$$M_0 = EI \frac{q}{T_0} \quad 1b)$$

where flexural length $\lambda = \sqrt{\frac{EI}{T_0}}$.

In addition, a rough approximation of maximum bending moment range for fatigue analysis is given in Eq. 13c):

$\Delta M_{\max} = (1 - e^{-2X_0/\lambda}) M_0$	13c)
---	------

Where X_0 is amplitude of $x_0(t)$.

The following chart simply illustrates the comparison procedure employed in this chapter sections to validate Riflex results.

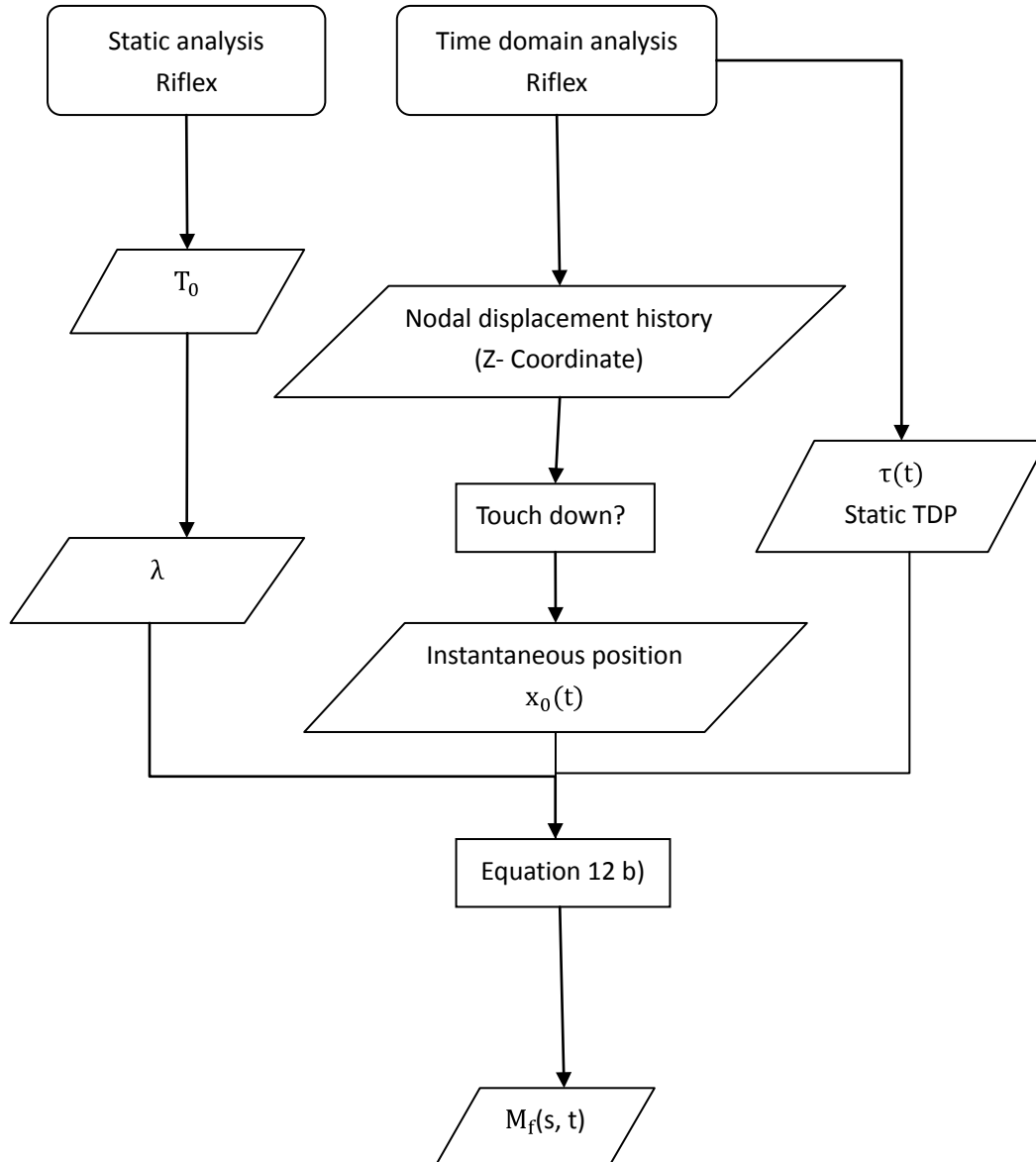


Figure 4.1-2 validation procedure of dynamic bending moment at touchdown area



Section 4.2 Case Study I: Regular wave sea state

4.2.1 Input data [16]

Riser

Parameter	Value
Outer Diameter [mm]	273
Wall Thickness [mm]	12.7
Bare pipe weight [kg/m]	125
Internal fluid density [kg/m^3]	700
Elasticity [Mpa]	2.1E5
Length	2240m
Segments Length(from top to bottom)	Element Length
268 m	10m
717m	5m
359m	1m
896m	10m

Location

Parameter	Value
Hang off point based on Vessel's Coordinate	(0 m,0 m,-4.469621658 m)
Lower end based on Global Coordinate	(1500 m,0 m,-1000 m)

Hydrodynamic Coefficient

Parameter	Value
Cd-axial	0
Cd-normal	0.7
Cm-axial	0
Cm-normal	2
Damping ratio	N/A

Sea state

Parameter	Value
Wave Kinematics	Stokes' 5 th order
Wave height	14m
Wave period	8s

4.2.2 Results

Table 4.2-1 Basic data of results

EI [MNm^2]	q [kg/m]	T_0 [KN]	λ [m]	M_0 [KNm]	ΔM_{\max} [KNm]	X_0 [m]	Location of Origin
18.52	968.3	114.7	12.7	156.346	108.33	7.5	Node no 258



Table 4-2-2 asymptotic value of dynamic bending moment variation along arc length

s [m]	M _f [KNm]		
	Mean	Peak to Peak	Maximum
-20	0.965	14.484	14.484
-19	3.158	26.198	26.198
-18	6.118	37.085	37.085
-17	9.482	47.202	47.202
-16	13.346	56.604	56.604
-15	17.599	65.341	65.341
-14	21.909	73.461	73.461
-13	26.877	81.007	81.007
-12	31.787	88.324	88.324
-11	36.853	95.495	95.495
-10	42.092	102.176	102.176
-9	47.435	108.854	108.854
-8	52.668	115.221	115.221
-7	58.233	121.164	121.164
-6	64.035	126.712	126.712
-5	70.206	131.901	131.901
-4	77.185	131.298	137.185
-3	83.743	125.541	142.123
-2	89.811	120.317	146.740
-1	95.425	115.577	151.055
0	100.620	111.279	155.089
1	105.428	107.384	158.860
2	109.877	103.854	162.385
3	113.995	100.658	165.681
4	117.806	97.765	168.761
5	121.333	95.148	171.640
6	124.598	92.783	174.332
7	127.621	90.913	176.848
8	130.419	89.459	179.225
9	133.009	88.326	181.608
10	135.407	87.654	183.836
11	137.628	87.086	185.921
12	139.684	86.603	187.870
13	141.588	86.197	189.693
14	143.351	85.859	191.398
15	144.983	85.581	192.993
16	146.495	85.355	194.484
17	147.896	85.176	195.879
18	149.193	85.037	197.184

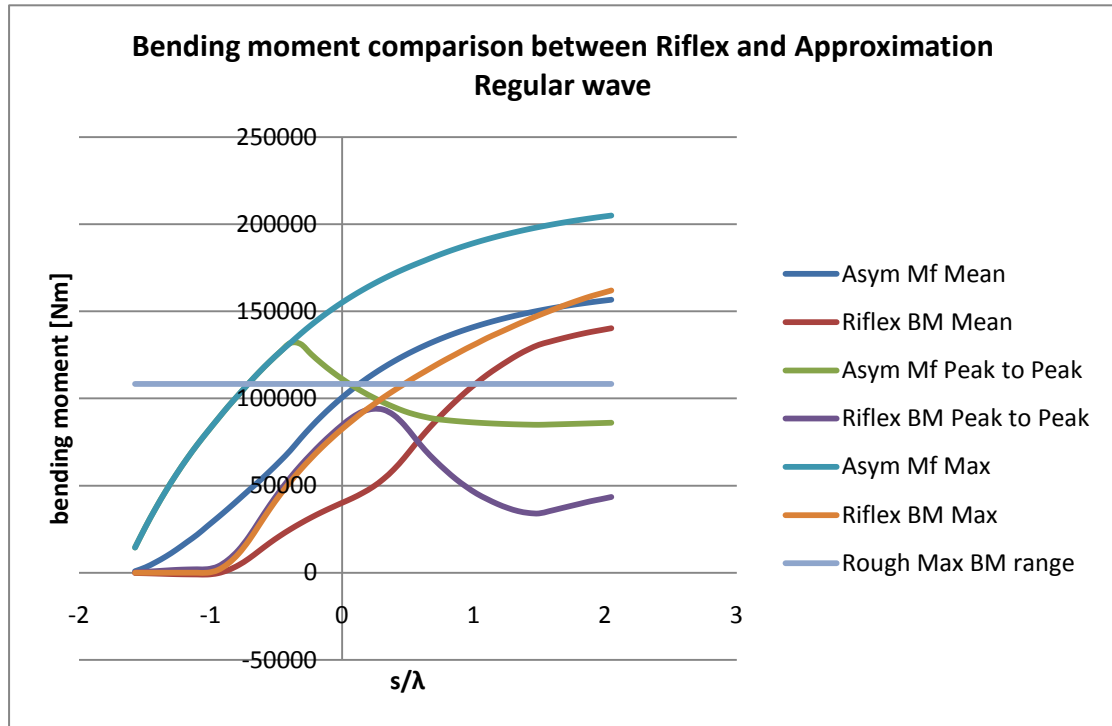


Figure 4.2-1 dynamic bending moment: Asymptotic method v.s. Riflex

Section 4.3 Case Study II: Irregular wave sea state

4.3.1 Input data

Sea state

Parameter	Value
Spectrum type	JONSAWP
Significant height	8m
Peak period	7s

The other data see **Case I**

4.3.2 Results

Based on Z- displacement time history generated from RILFEX OUTMOD, it is observed TDP is oscillating around 6 adjacent elements and hence oscillation amplitude $X_0 = 3\text{m}$.

With RIFLEX results: $A_B \approx 1.15\text{m}$, $\theta_B \approx 82.3^\circ$, Eq. 8 a) estimates X_0 is around 3.3 m. The relation established in Equation 8 a) seems to match the time dependent displacement of TDP in RIFLEX.

In Figure 4-3-1, dynamic tension force shows constant increase after TDP and a flat bottom around 80 m at length before TDP. However, in vicinity of TDP, this increase is so slight (whens = λ , difference from origin is less than 3%) that the assumption of constant tension amplitude could be valid.



SCR - Tension Force Range - Irregular Wave Condition

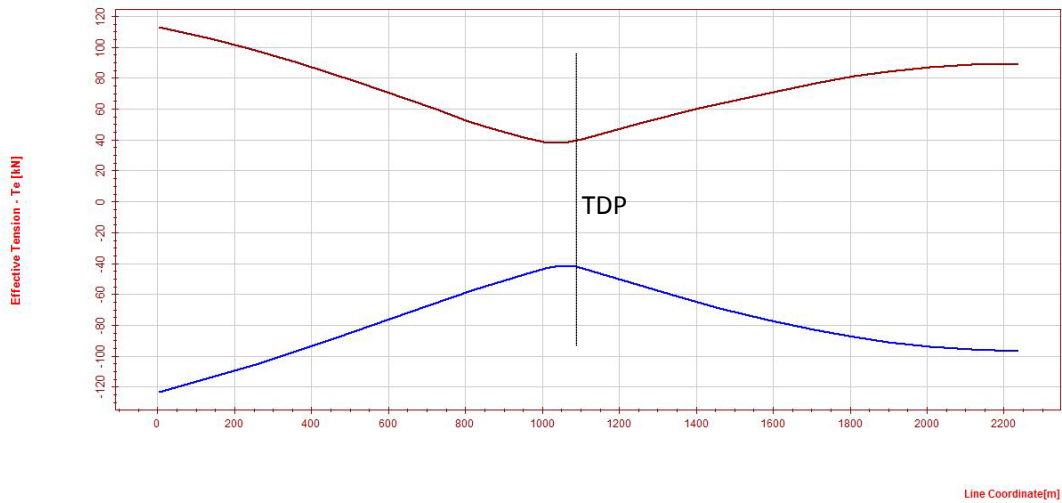


Figure 4.3-1 Maximum and Minimum Dynamic tension force along arc length

Table 4.3-1 Basic data of results

El [MNm ²]	q [kg/m]	T ₀ [kN]	λ [m]	M ₀ [kNm]	ΔM _{max} [kNm]	Location of Origin
18.52	968.2	114.7	12.7	156.346	58.843	Node no 132

Table 4.3-2 asymptotic value of dynamic bending moment variation along arc length

s [m]	M _f [kNm]		
	Mean	Standard deviation	Peak to Peak
-17	0	0	0
-16	0.02466	0.376102	7.578703
-15	0.39994	1.982702	20.68903
-14	1.869013	4.999309	32.92848
-13	5.707045	8.887483	44.41356
-12	12.46965	12.41529	55.97784
-11	21.36325	14.41801	66.81178
-10	31.08038	14.84156	76.96152
-9	40.59747	14.40616	86.18663
-8	49.48423	13.84941	83.94528
-7	57.70134	13.38132	82.03108
-6	65.29938	12.99499	80.40856
-5	72.32508	12.68342	79.04566
-4	78.82167	12.43958	77.91345
-3	84.82907	12.25645	76.98582
-2	90.38421	12.12716	76.48617
-1	95.52121	12.04506	76.56399
0	100.2716	12.00386	76.74786
1	104.6646	11.99766	77.04033
2	108.7271	12.02104	77.79451



3	112.484	12.06911	78.5917
4	115.9584	12.13748	79.42176
5	119.1716	12.22226	80.2758
6	122.1432	12.32008	81.14606
7	124.8915	12.42799	82.02576
8	127.4332	12.54348	82.94751
9	129.784	12.66438	84.06787
10	131.9582	12.78889	85.1647
11	133.9691	12.91547	86.23559
12	135.829	13.04284	87.2786
13	137.5493	13.16995	88.29221
14	139.1404	13.29592	89.27527
15	140.6122	13.42005	90.22694
16	141.9735	13.54178	91.14669
17	143.2327	13.66064	92.0342
18	144.3974	13.7763	92.88938
19	145.4748	13.88848	93.71232
20	146.4714	13.997	94.57995
21	147.3933	14.10171	95.46884

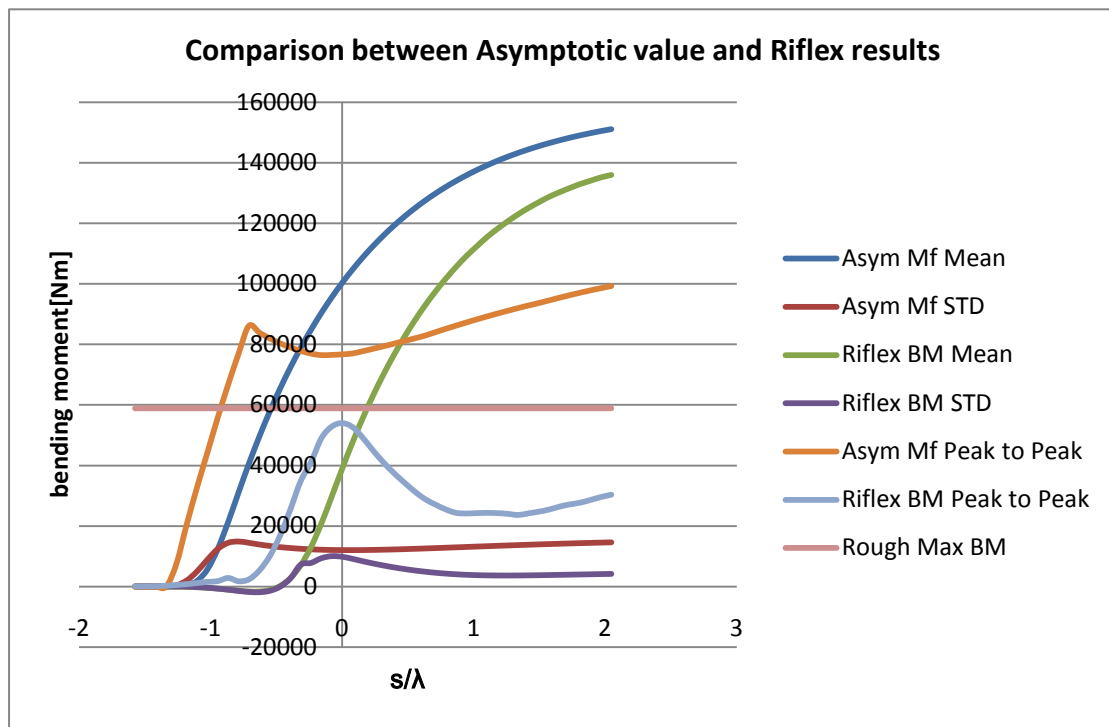


Figure 4-3-2 dynamic bending moment: Asymptotic method v.s. Reflex results

Section 4.4 Summary

1. The curves “Rough Max BM” in the figure 4-2-1 and 4-3-2 indicates, maximum bending moment range ΔM_{\max} gives good agreement with Riflex results.
2. Asymptotic method first makes approximation for TDP static bending moment $M_0 \approx 156\text{KNm}$ when maximum static bending moment calculated by Riflex is 139KNm . Due to restriction of M_0 , magnitude of M_f is generally in line with that in Riflex. However, asymptotic curves obviously shift by left if curves for both methods are supposed to coincide. This could be caused by an ambiguous definition of “location of origin O”. Referring to the paper, the origin is taken from “static touchdown point”, which in this case is Node no 128. But Riflex Z-displacement history shows the mean TDP is located at Node no 132. Therefore, the assumption that TDP oscillates linearly centered by “static touchdown point” is not valid any more. Besides, Riflex illustrates the point with maximum static bending moment, start point of constant tension force, and the static touchdown point is actually not at the same location along cable length coordinate.
3. Approximation results for both regular wave and irregular wave condition have the same error of prediction of “location of origin O”.
4. Although good agreement was shown in the example given by the author in his paper, the verification work in this section generally does not lead to a comparable result. The boundary layer value method involving numeric integration of ODE still requires more effort to prove its value rather than being an illuminating academic exercise. [17]

Chapter 5 Parametric study

Section 5.1 Mesh density

This section makes convergence study of static/dynamic results with respect to variation of mesh size. Effect of element type, e.g. beam element and bar element, is studied also. Based on the findings, an optimized discretization model is tested to prove its good combination of high accuracy and low computation demand.

5.1.1 Input data

Riser specification sees section 4.2

Sea state

Parameter	Value
Spectrum type	JONSAWP
Significant height	8m
Peak period	7s

Dynamic analysis setting

Parameter	Value
Time Step	0.1s
Simulation length	1800s
Wave force included(Y/N)	No

Mesh density Setting

In order to simplify study, each test is only modeled by one element length, namely no mesh variation along arc length. A group of 8 different mesh sizes is selected, varying from 4 m to 60m.

5.1.2 Results

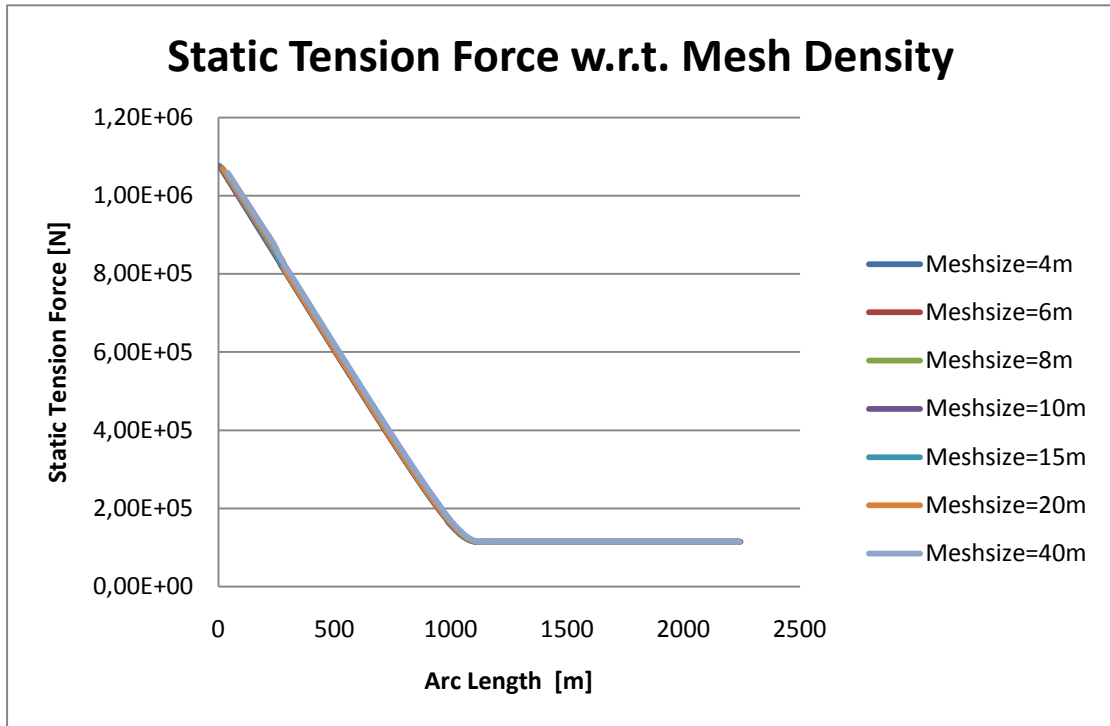


Figure 5.1-1 Static tension force distribution with respect to mesh density

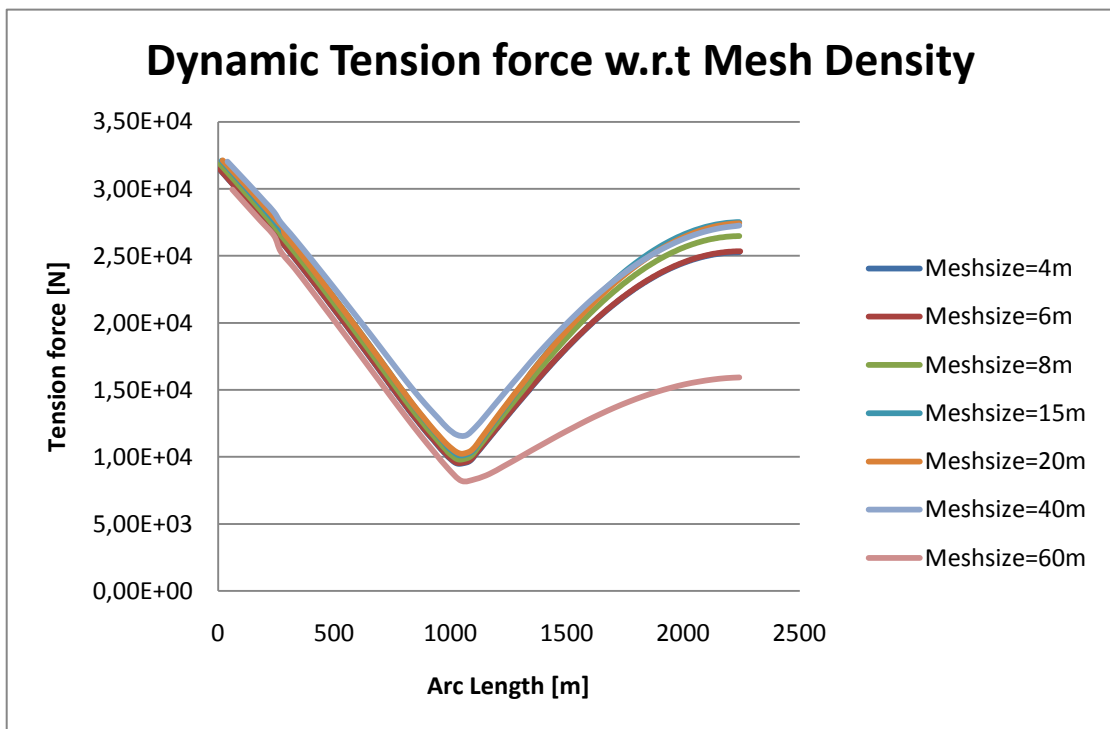


Figure 5.1-2 Dynamic Tension Force standard deviation with respect to mesh density

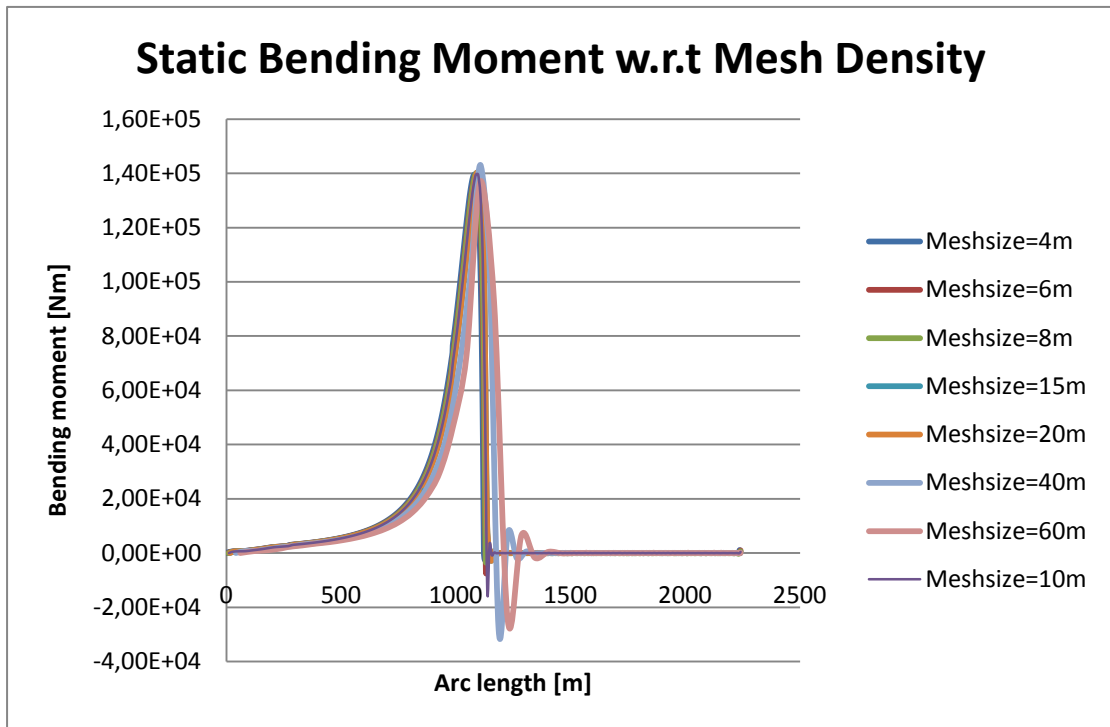


Figure 5.1-3 Static bending moment distribution with respect to mesh density

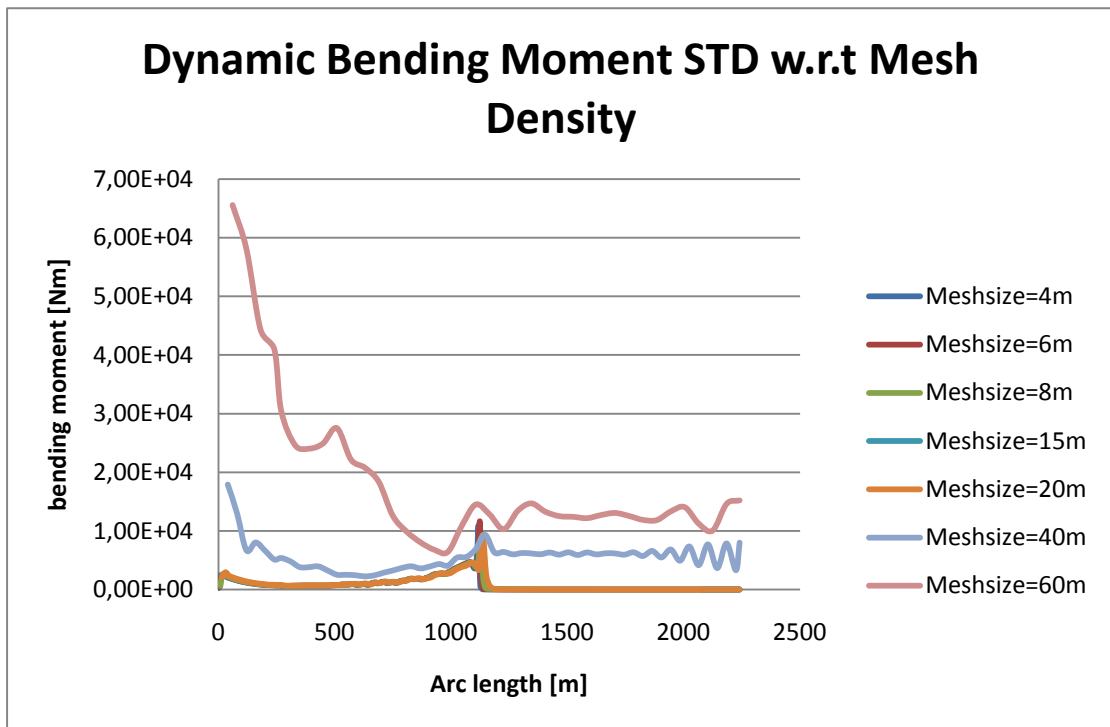


Figure 5.1-4 Dynamic bending moment standard deviation with respect to mesh density



Table 5.1-1 convergence by mesh density

Mesh Type	Mesh density	Element Number	Maximum Static TF [KN]	Max BM Static [KNm]	Max TF STD Dynamic	Max BM STD [KNm]	CPU time
Beam	4	562	1076	139.6	31.49	10.93	1068.6
Beam	6	375	1075	139.7	31.48	11.54	707.8
Beam	8	281	1074	140.1	31.83	8.577	489.5
Beam	10	225	1073	139.6	233.6	89.94	1827.0
Beam	15	150	1071	140.3	32.09	9.268	231.3
Beam	20	113	1069	143.7	32.12	6.6	300.0
Beam	40	57	1059	143.1	32.03	17.94	128.6
Beam	60	38	1050	137.1	29.95	65.59	105.8
Bar	8	281	1075	-	error	-	
Bar	15	150	1071	-	error	-	
API 2RD Suggested Mesh Upper limit: $C = \sqrt{\frac{EI}{T}}$							
Location		Stiffness EI [MNm ²]	Tension force T [KN]		C [m]		
Hang off		18.5	1070		4		
TDA		18.5	115		12		

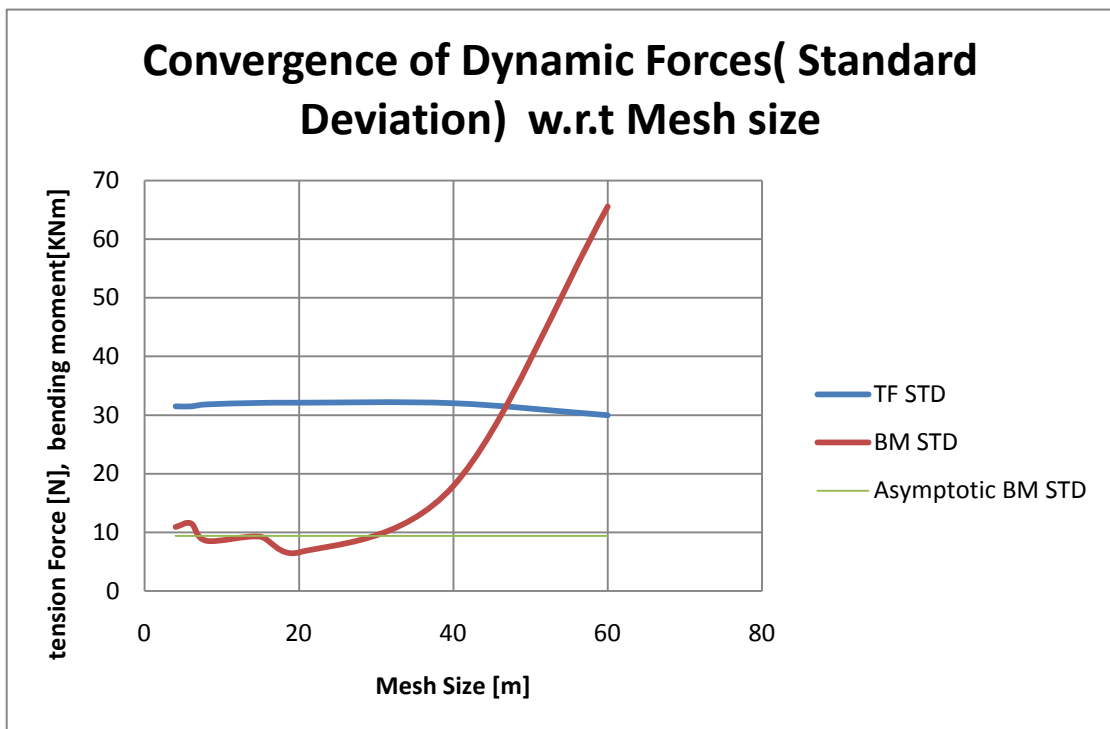


Figure 5.1-5 convergence of dynamic force with respect to mesh density

5.1.3 Conclusion

1. Beam element length 20m is good to acquire a relatively accurate result with economical CPU consumption. The guidance “mesh size should not exceed $C = \sqrt{\frac{EI}{T}}$ ” as recommended by API 2RD is conservative. Tension force converges quickly when increasing mesh density, and even bar element is enough to calculate static tension force. However, bending moment distribution seems more sensitive to mesh size. The reason could be, bending moment is more non-linear in vicinity of TDP as indicated by rapid change of curvature in a short range.
2. The governing rule to optimize mesh density along arc length for SCR is giving special care to the area where bending moment shows nonlinear change. Generally, TDP element should be divided smaller. One suggests a mesh model with mesh size 15m from around 1000m (985.9m) to 1200m (start from hang off point) and the rest 20m. The global analysis result compared with that for the finest model illustrates the optimized model gives good agreement with true value, although static bending moment at TDP indicates visible deviation. One may increase mesh density in the vicinity of TDP (from 1110m to 1160m) to obtain a better solution.

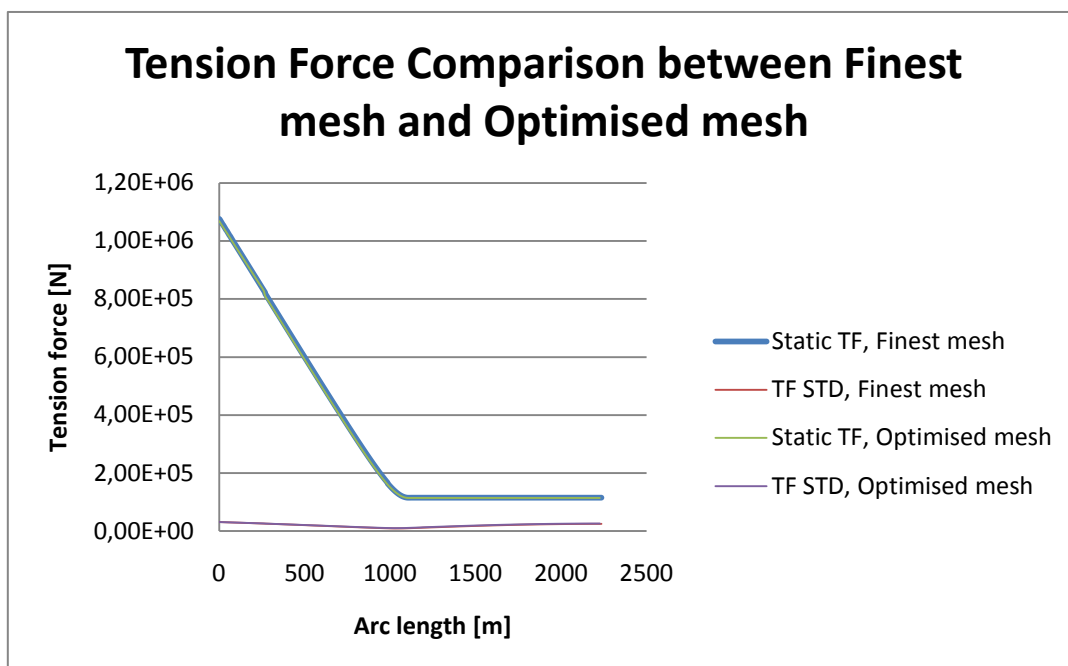


Figure 5.1-6 Effective Tension force for the optimized mesh model

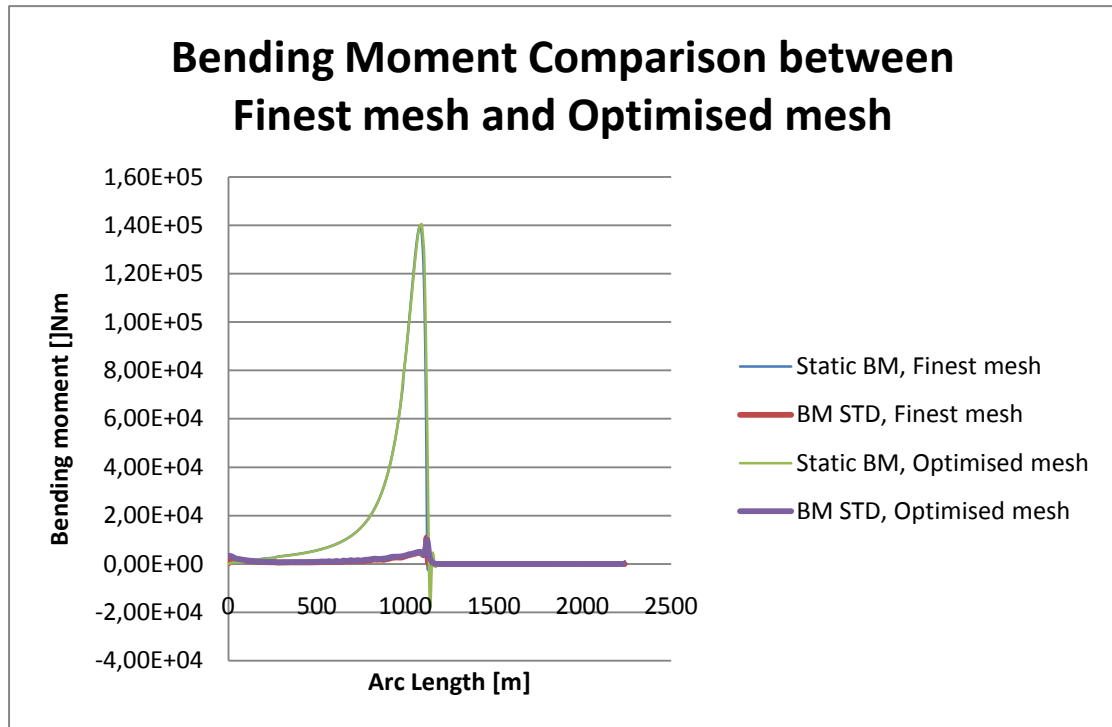


Figure 5.3-7 Bending moments for the optimal mesh model

3. Bar element model is able to get an accurate static tension force. This also validates Faltisen's catenary equation assumption that bending stiffness can be omitted.
4. A finer mesh will not definitely lead to a better result or more CPU time. Mesh size 10m actually consumes much more computation due to more steps of nonlinear iteration both in static and in dynamic analysis. Moreover, dynamic bending moment and tension force surely distort from true value. Special care should be given to selection of mesh size in conjunction with time step. Different discretisation model results in different element Eigen period. This will be investigated in the next section.



Section 5.2 Time Step

In most of global analysis, time step for numerical integration shall be smaller than the shortest system natural period, which is strongly dependent on riser length, mechanical parameters, and also mesh mode. This section is going to study the effect of mesh model and excitation force period on stability of time integration and further find out a optimal time step with good accuracy but not so small. In order to simply interpretation, only regular wave condition is applied.

5.2.1 Input data

Riser specifications see section 4.2

Study case:

Case 1 Regular wave H=14m, T=10s; mesh size = 20m

Case 2 Regular wave H=14m, T=10s; mesh size = 10m

Case 3 Regular wave H=14m, T=10s; mesh size = 5m

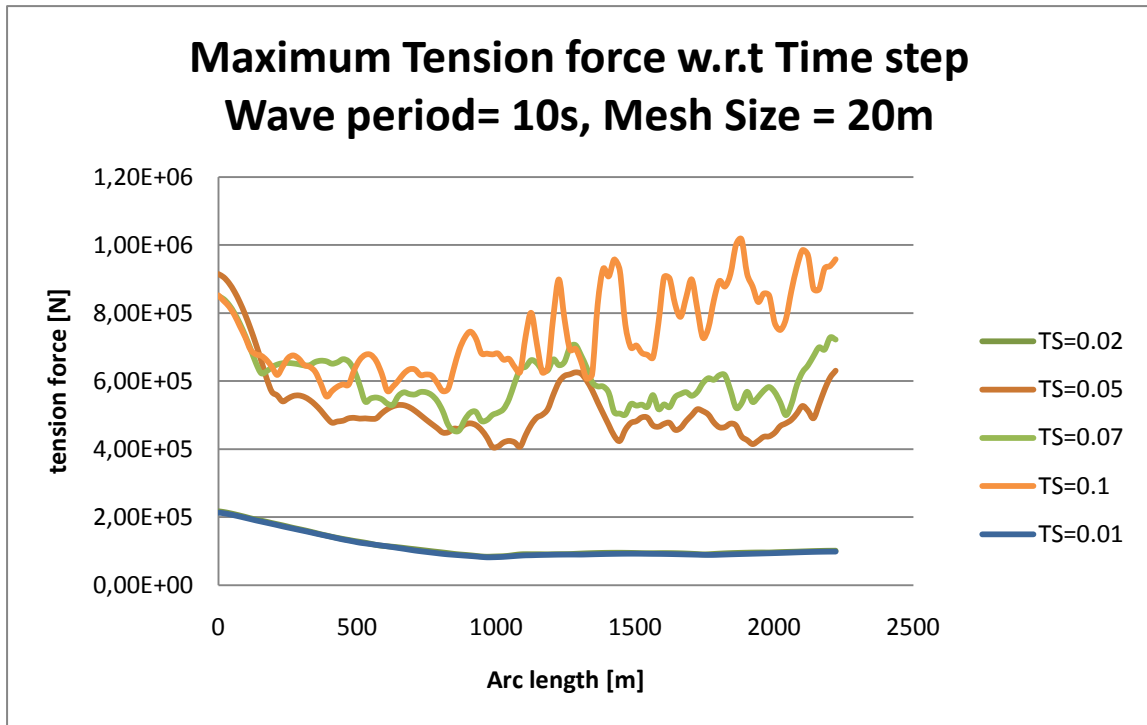
Case 4 Regular wave H=14m, T=5s; mesh size=20m

Case 5 Regular wave H=14m, T=20s; mesh size=20m

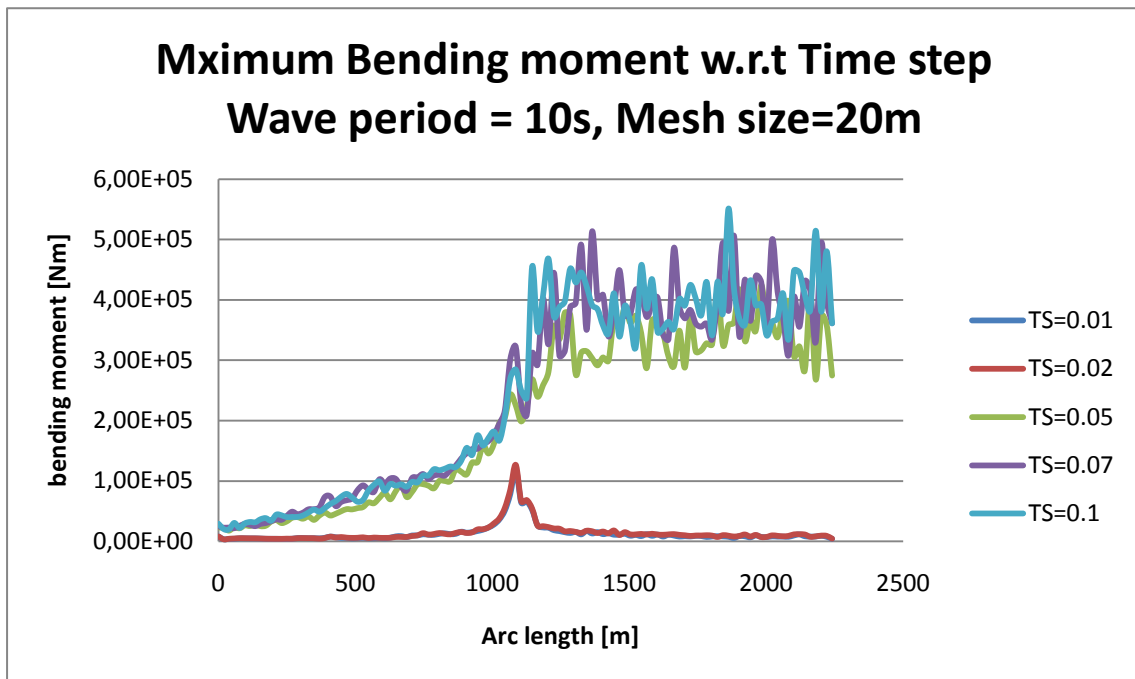
5.2.2 Results

Table 5.4- 1 Convergence by time step size

Case no	Mesh Size [m]	T [s]	Time step [s]	Max BM [KNm]	Max TF [KN]
1	20	10	t=0.01	119.6	213.1
			t=0.02	126.7	217.6
			t=0.05	The results distort	
			t=0.2	The algorithm is diverging	
2	10	10	t=0.01	98.7	208.5
			t=0.02	98.71	208.1
			t=0.05	98.72	209.7
			t=0.1	The results distort	
			t=0.2	The algorithm is diverging	
3	5	10	t=0.1	86.28	207.9
			t=0.2	85.34	208.2
			t=0.4	88.6	210.6
			t=1.0	The results distort	
4	20	5	t=0.02	82.69	100.8
			t=0.05	84.17	105.4
			t=0.1	83.66	120.5
			t=0.2	The results distort	
5	20	20	t=0.005	69.8	648.0
			t=0.01	70.19	649.2
			t=0.02	71.86	651.5
			t=0.05	The results distort	



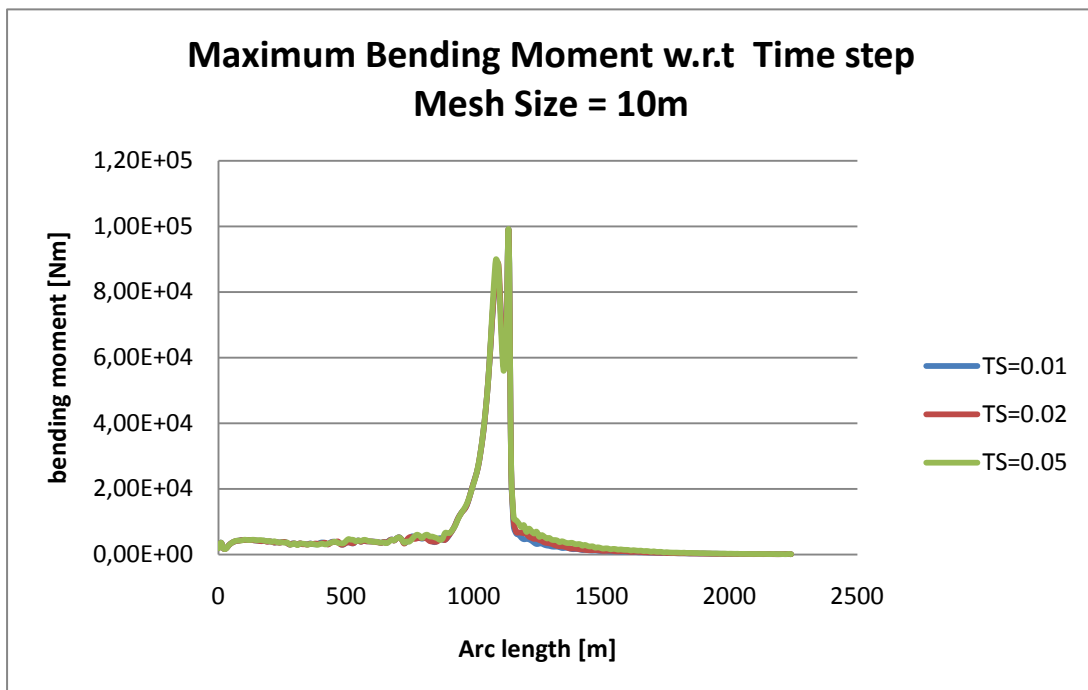
Case 1 Maximum dynamic Tension force with respect to Time step



Case 1 Maximum dynamic Bending moment with respect to Time step



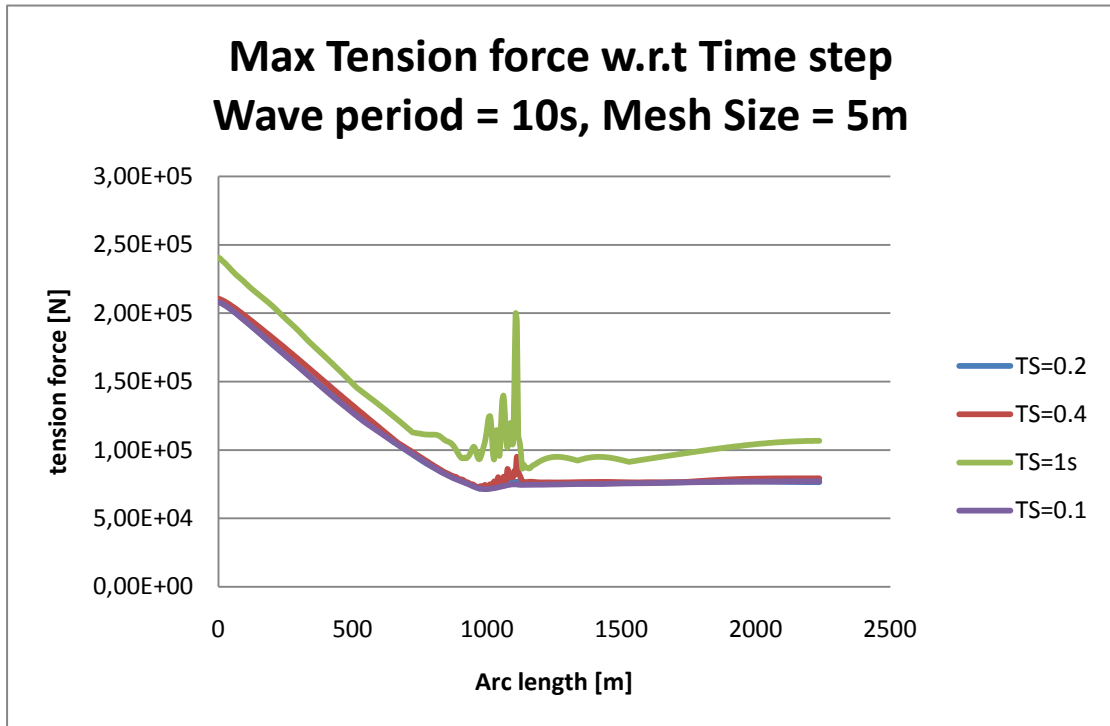
Case 2 Maximum dynamic Tension force with respect to Time step



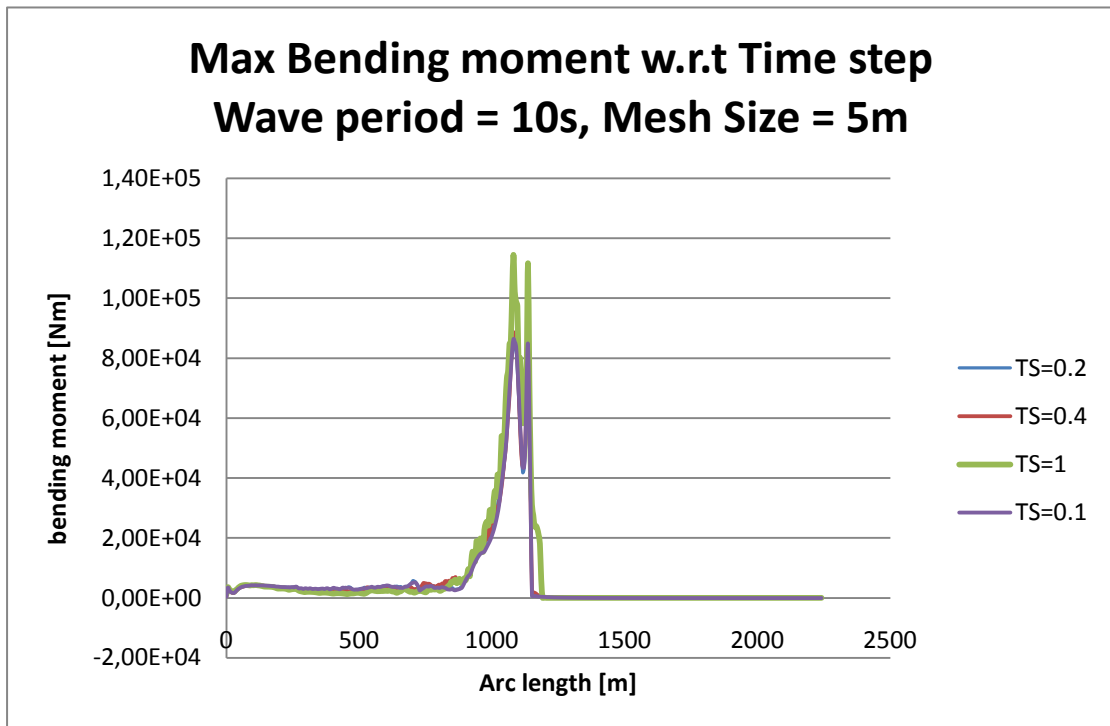
Case 2 Maximum dynamic Bending moment with respect to Time step



Case 3 Maximum dynamic Tension force with respect to Time step

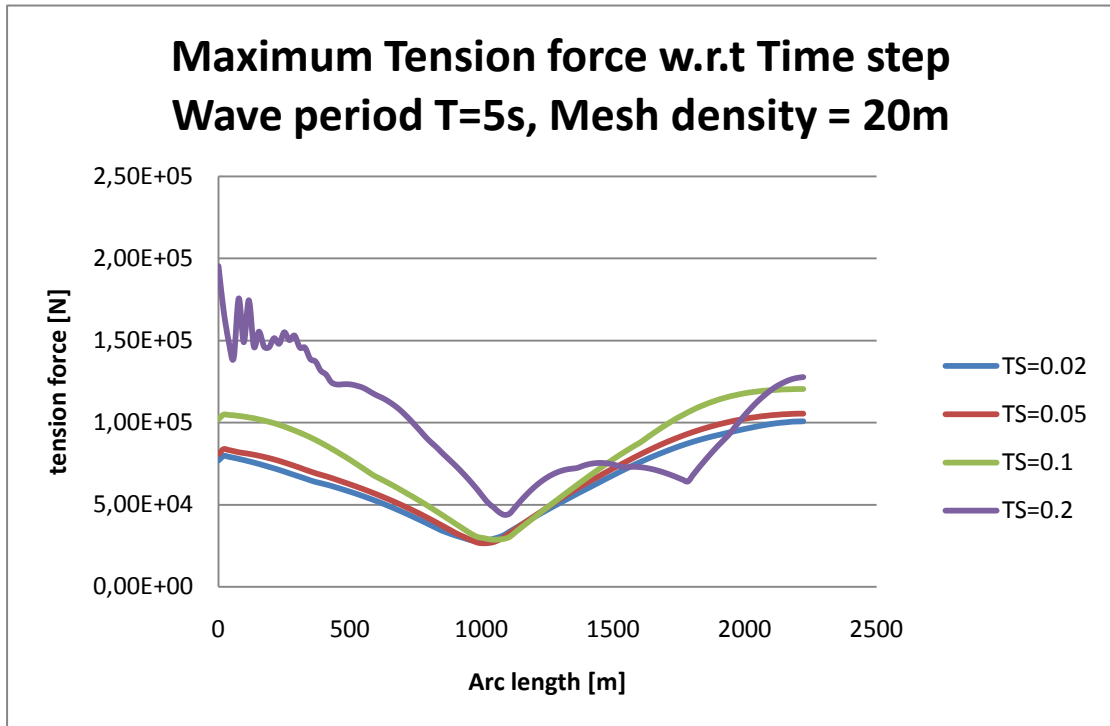


Case 3 Maximum dynamic Bending moment with respect to Time step

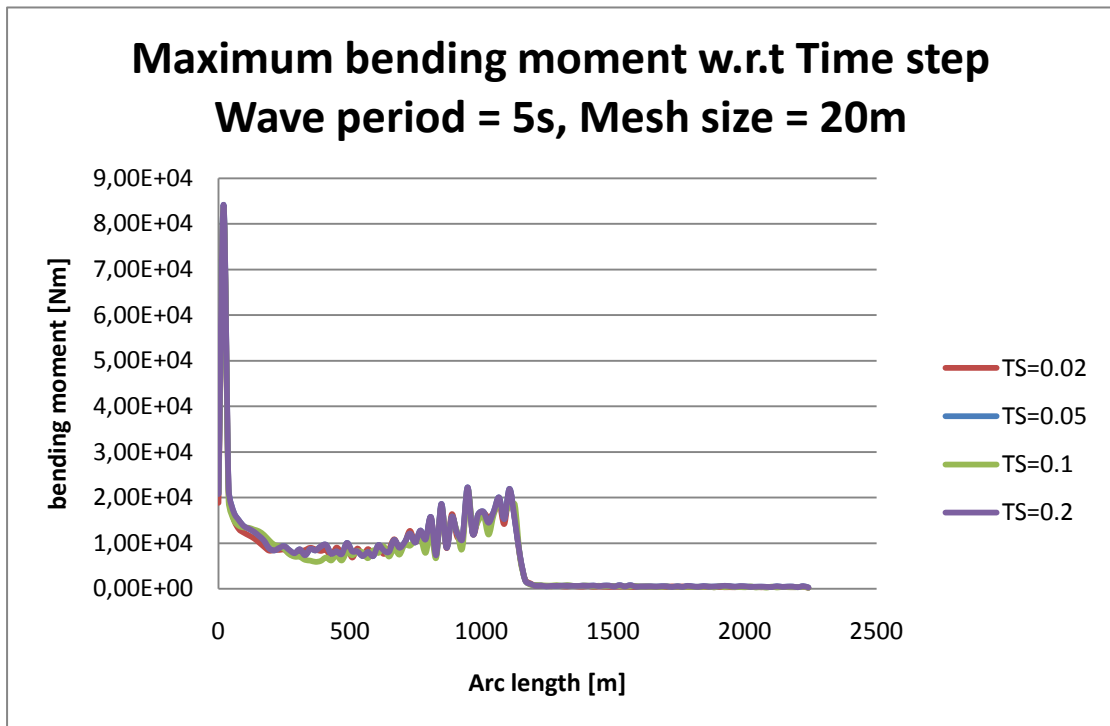




Case 4 Maximum dynamic Tension force with respect to Time step

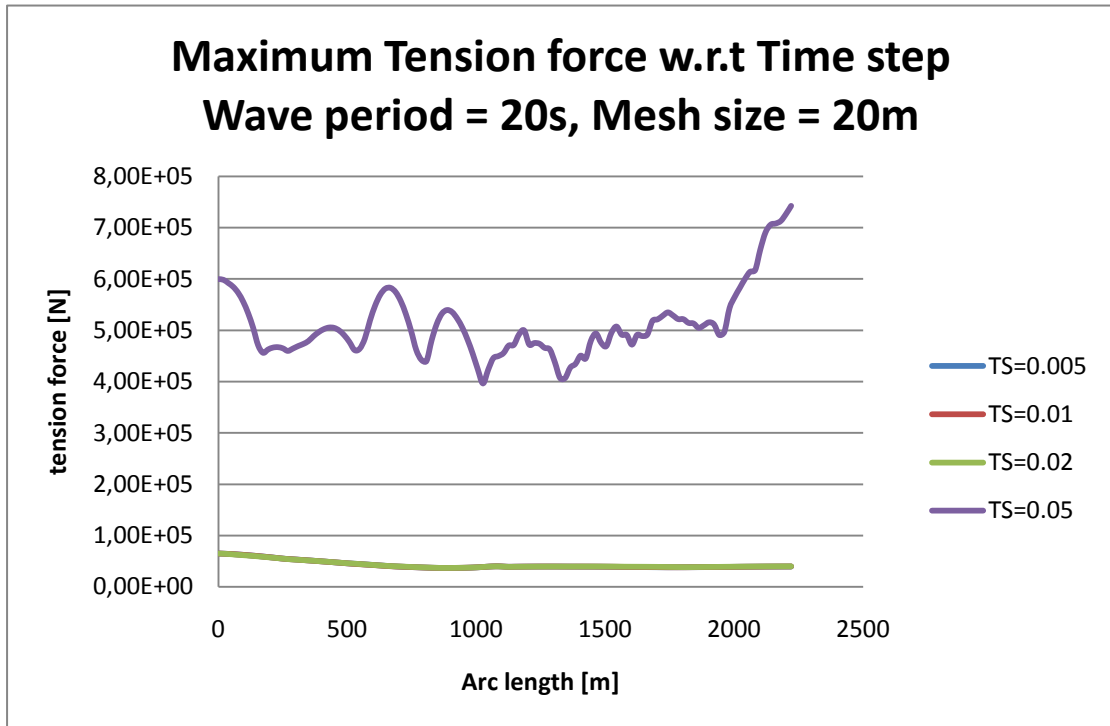


Case 4 Maximum dynamic Bending moment with respect to Time step





Case 5 Maximum dynamic Tension force with respect to Time step



Case 5 Maximum dynamic Bending moment with respect to Time step

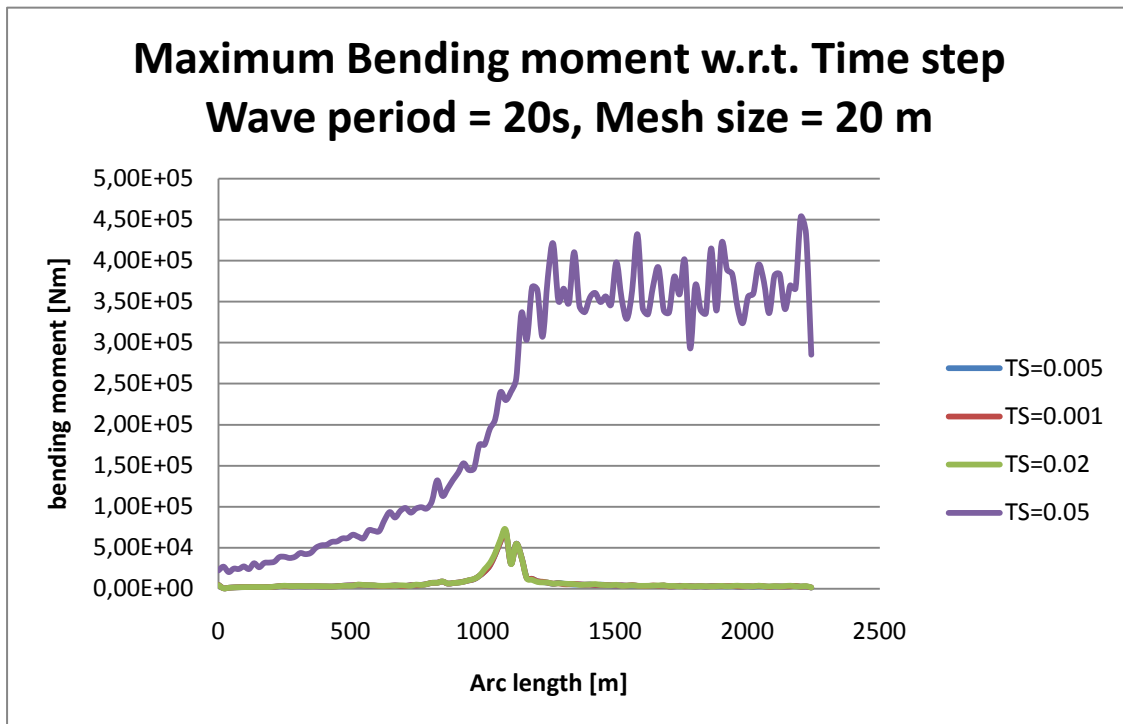
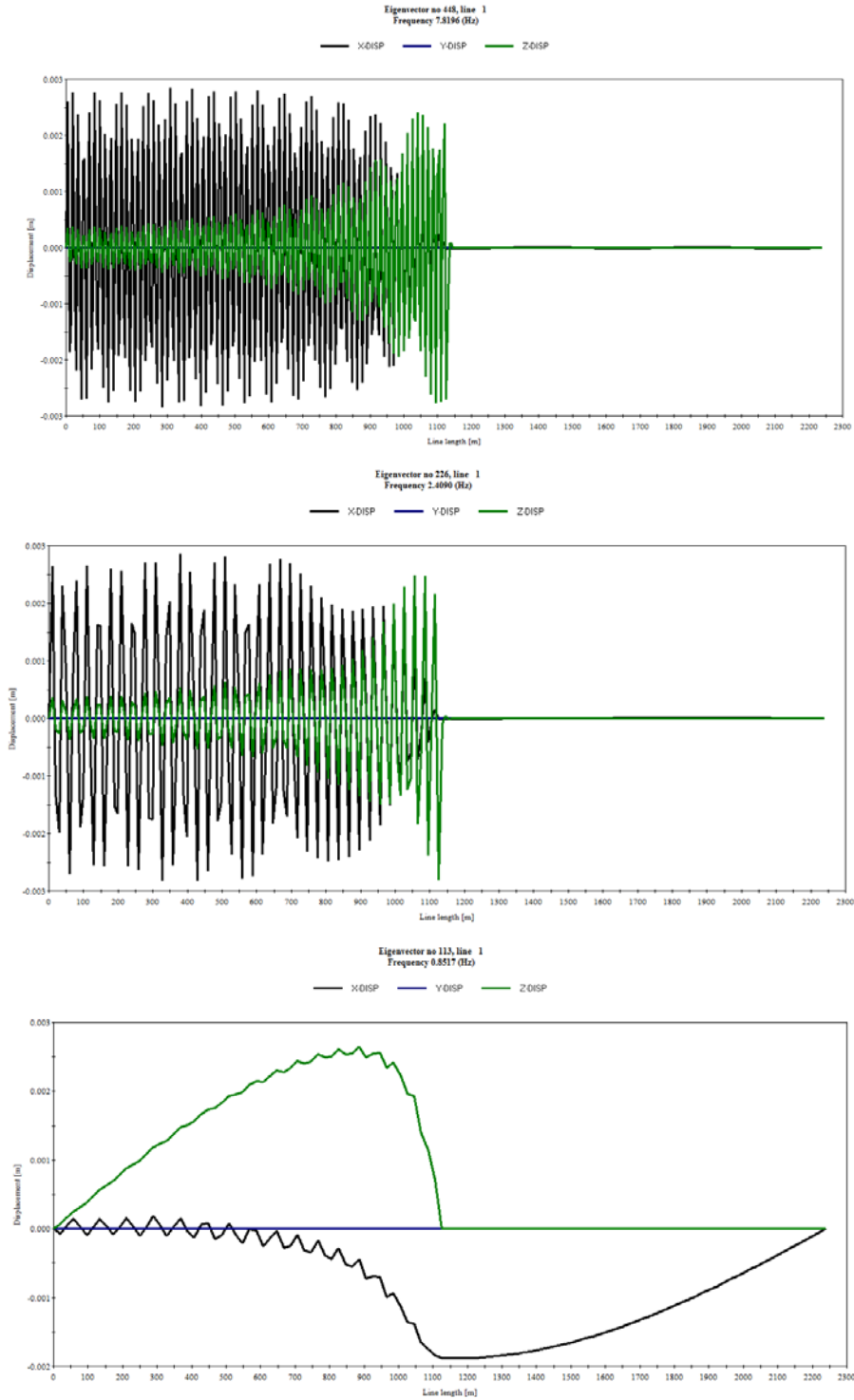


Table 5.2-2 The Largest natural period variation with mesh size

Mesh Size [m]	Node number	Largest mode XZ Plane	Largest Eigen frequency [Hz]	Shortest natural period [s]
5	451	448	7.8196	0.128
10	226	226	2.4090	0.415
20	114	113	0.8517	1.170

Figure 5.2-1 Eigen Mode corresponding to the shortest natural period for Mesh=5m, 10m, 20m





5.2.3 Conclusion

1. In general, time step for numerical integration is preferred to be small enough in order to give an adequate representation of the external loading and to give stable integration of all Eigen periods of the discretized system model.
2. The time step size required to obtain a stable numerical solution is strongly system- and dependent. In this case study, convergence speed correlates to mesh size. Larger mesh size needs smaller time step. This finding seems not aligned with practice recommended by OrcaFlex. OrcaFlex user manual advises time step to be 1/10 of the shortest nodal natural period. This implies, a fine mesh demands a small time step.
3. Stability of numerical integration is excitation dependent. Comparison among case 1, 4 and 5 reveals that, large wave period requests smaller time step to converge. Dynamic response of riser mainly is excited by motion of suspended end as concluded in the previous project thesis. Transfer function of semi submersible determines larger motion amplitude for wave period 20s. Amplitude of top motion is larger; riser response is more nonlinear so that time step should be divided smaller. Therefore, when evaluate design wave load effect, one has to define much smaller times step, rather than 70~200 steps per period.
4. Large time step will not definitely lead to non-convergence. For instance, in case 5, when time step is set as 0.05s, the analysis still converges. Whereas, it is observed that there is high frequency response. This is obviously unexpected for regular wave sea states. It is also indicated unreasonable oscillation of force results along arc length replaces smooth variation. This phenomenon could be a good indicator to judge whether time step is bad.

Section 5.3 Water depth influence on riser design

5.3.1 Model 1: Amplify length and depth only

Comparison is made at three different water depths with the same floater under the same environment condition: Regular wave height 14m, period 10 s. Specifications see in the following table.

Table 5.1-1 variation of water depth

Depth [m]	Length [m]	Wellhead location [m]	Segment length / Mesh size [m]		
200	400	300	280/2	60/1	60/2
600	1200	900	840/6	180/3	180/6
1000	2000	1500	1400/10	300/5	300/10

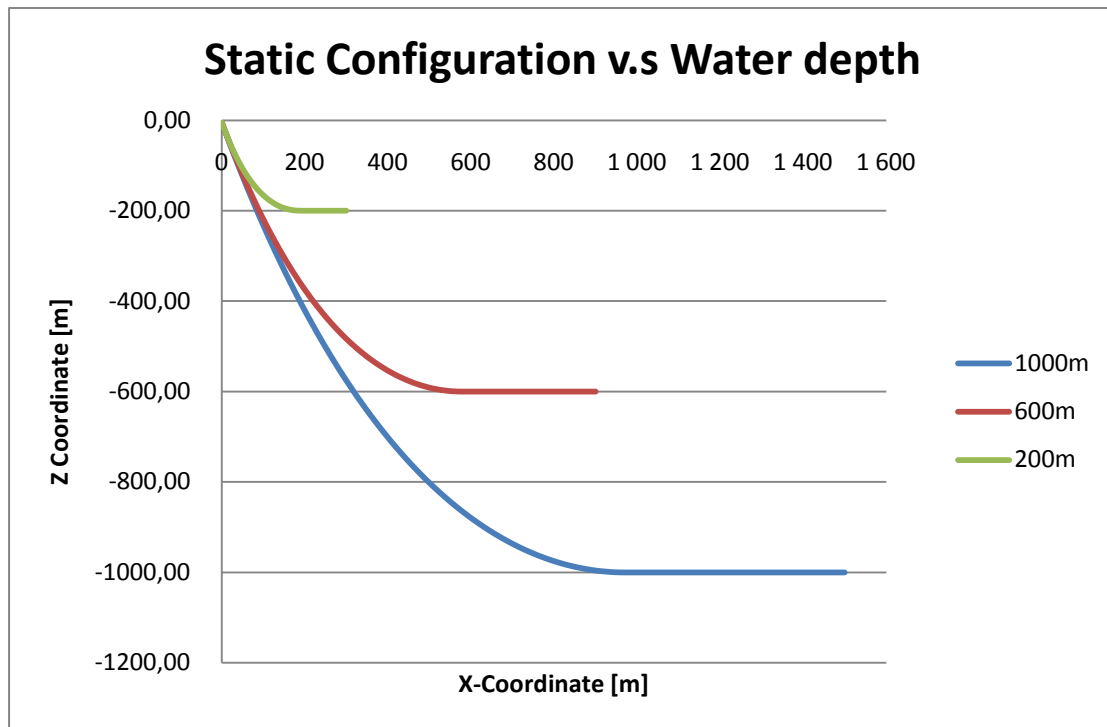


Figure 5.3-1 Variations of Static configuration with respect to Water depth

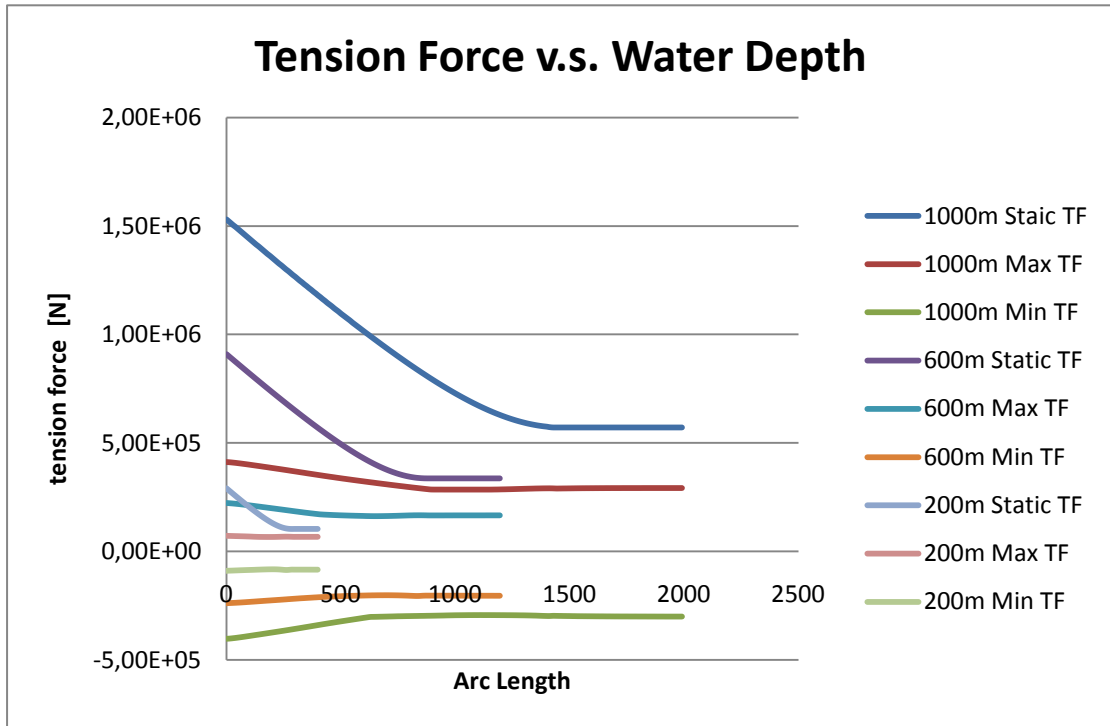


Figure 5.3-2 Variations of Tension force with respect to Water depth

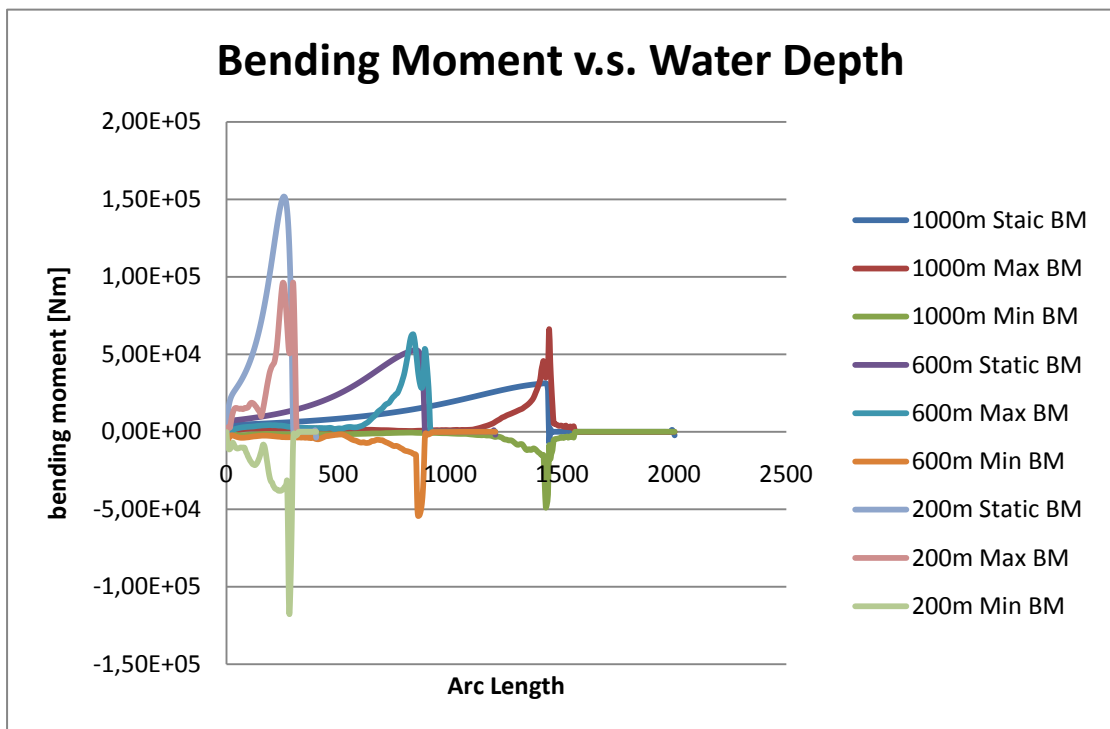


Figure 5.3-3 Bending moment variations with respect to Water depth

5.3.2 Conclusion:

1. The ratio of static tension force to water depth seems constant. Deeper water requires higher top tension force. Oppositely, bending moment increases as riser moves to shallow water. Top angle is equal but the arc length from top to TDP is shorter, so that the slope gradient (curvature) becomes larger. The ratio of static bending moment maxima for 1000m, 600m and 200m is almost equal to $\frac{1}{5}:\frac{1}{3}:1$. This implies the maximum static bending moment is proportional to H^{-1} , where H is water depth, if one simply scales the configuration of riser to apply in different water depths without changing riser section. As suggested by previous report, combined load factor is governed by bending stress. Therefore in shallow water, the top angle¹ should be increased, or in other words the length of riser shall be prolonged in order to reduce bending stress and further lower resistance utilization factor. Alternatively, increasing wall thickness or adding ballast weight could be solution to raise tension force and overcome over bending problem. This proposal will be studied in section “wall thickness”.
2. Shape of dynamic bending moment envelope does not vary so much with respect to water depth. However, it is observed that maximum/minimum dynamic tension force almost remains unchanged along arc length in shallow water.

5.3.3 Model 2: Different depth with the same horizontal force[18]

Effect of water depth was studied in an OMAE paper. A group of risers with depth varying from 300m up to 1800m have the same cross-section and horizontal force for the different water depth. A static analysis indicates, the length of the TDA also increases with increasing water depth as more of the riser is lifted off the seabed.

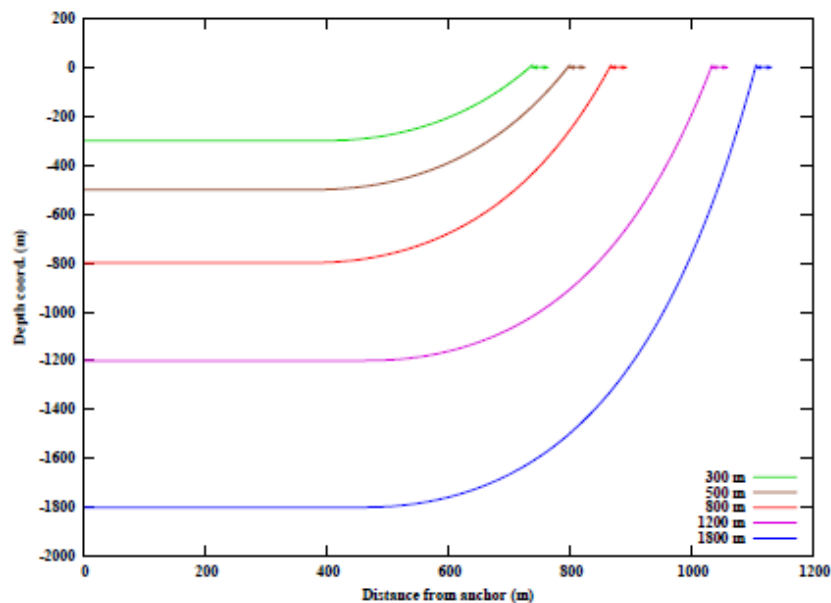


Figure 5.3-4 Static configurations for 300, 500, 800, 1200 and 1800 m water depths

¹ Top angle: the angle between vertical coordinate and top segment of the cable

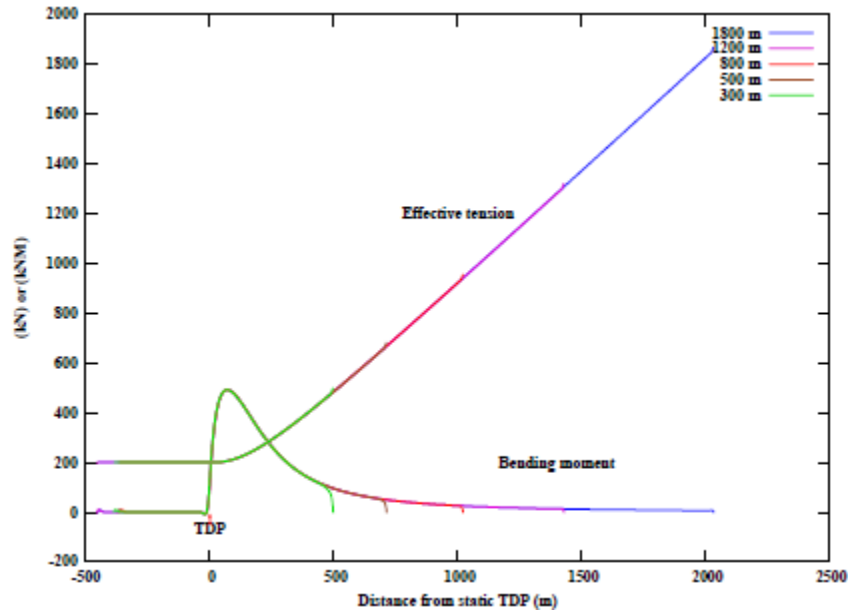


Figure 5.3-5 Static forces

The five models have different lengths of riser between the anchor at the lower end and the static touchdown points. With the TDPs aligned, the five models have the same tension at the lower end and the same bending moment in the TDA.

Further, dynamic analysis under a regular wave condition: height 12m, period 12s leads to the following conclusions:

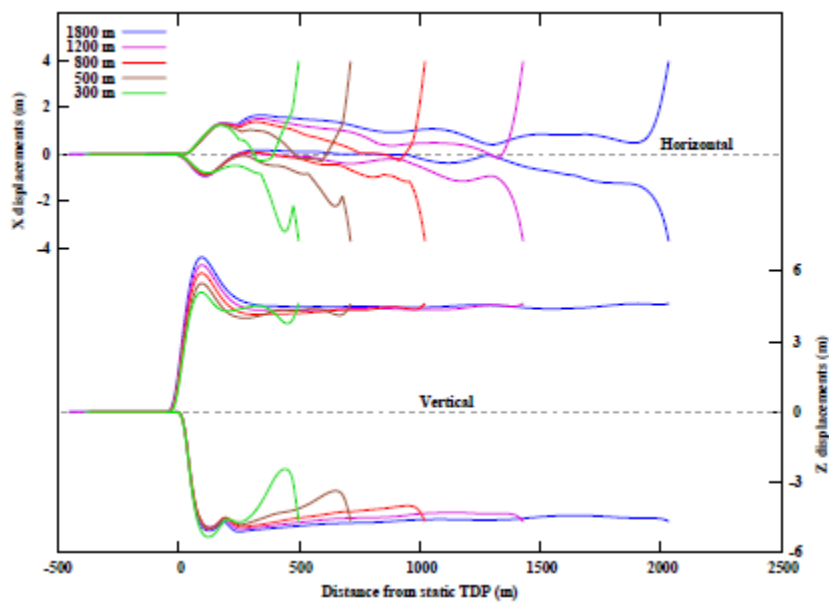


Figure 5.3-6 Displacement envelope curves

1. The identical motions at the upper end follow different curves along the riser towards the TDA. The horizontal motions immediately over the TDA are similar for all five water depths and increase approximately 20 cm while the depth increases to 1800 m. The maximum vertical displacements in the TDA increase by approximately 2 m as the water depth increases to 1800 m.

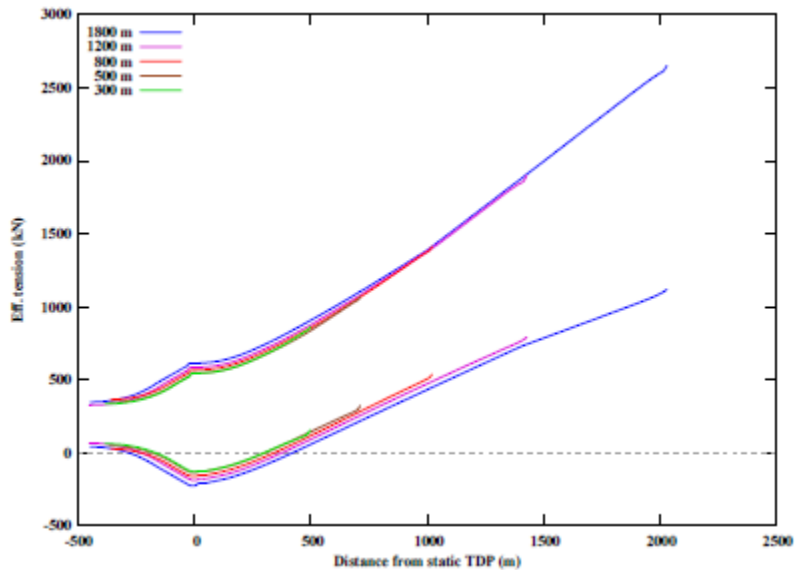


Figure 5.3-7 Tension force envelope curves

2. The minimum effective tension decreases with increasing water depth and the length of line in compression increases.

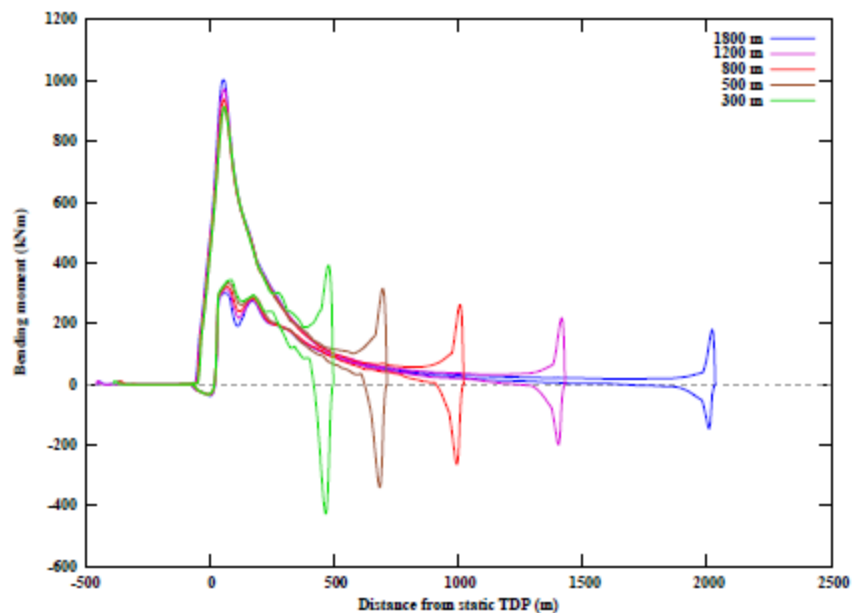


Figure 5.3-8 Bending moment envelope curves

3. The maximum bending moment is found immediately above the TDA for all five water depths. Except for a slight decrease from 300 to 500 m, the maximum bending moment increases with increasing water depth, see Figure 5 and Table 2. The bending moments in the wave zone, however, decreases with increasing water depth.

Section 5.4 Variation of Wall thickness V.S Arc Length

In this section, the riser for 1000m depth in last section is used. In order to compare the effect of wall thickness and arc length, in one case it is investigated by only increasing outer diameter, when in the other case, only arc length is extended with the same weight increase. The results could help to optimize the design of riser aimed for lower global stress.

5.4.1 Wall thickness Increase

Table 5.4-1 Force and stress variation with respect to wall thickness

Outer diameter [mm]	Weight increase	Max Static tension force [KN]	Max Static bending moment [KNm]	Max Dynamic tension force [KN]	Max dynamic bending moment [KNm]	Max von-mises stress [MPa]
273	-	1530	31.22	413.2	48.62	190.55
276	12.455%	1751	35.54	441.5	50.95	191.09
278	20.835%	1900	38.50	460.7	53.94	191.35

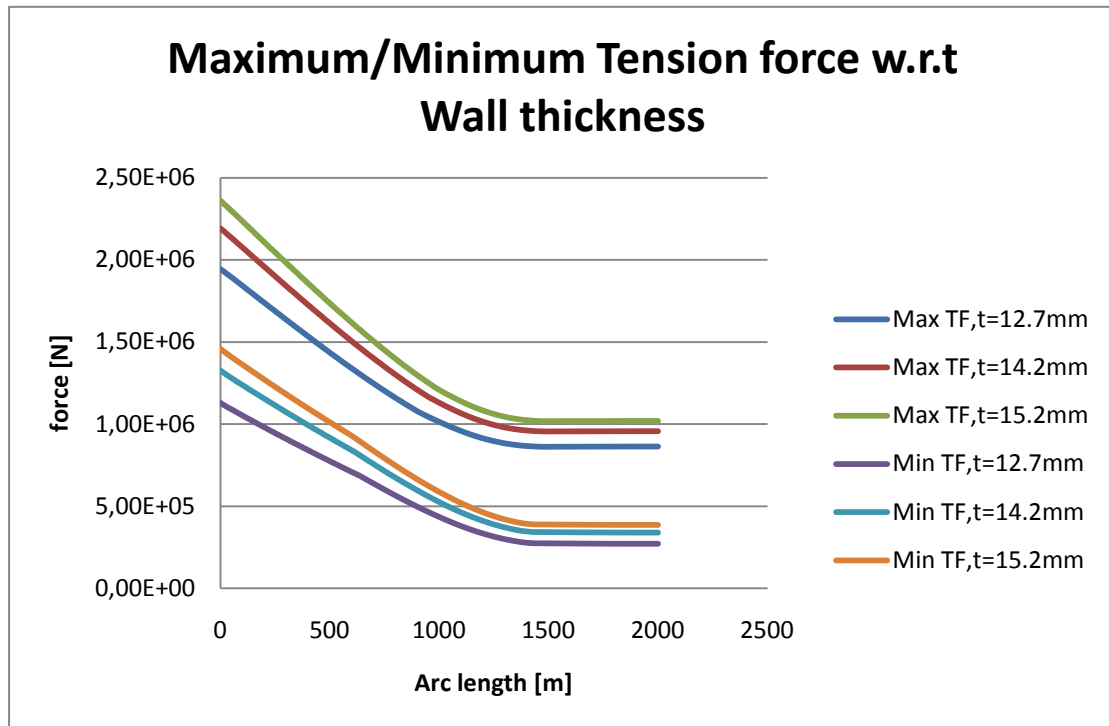


Figure 5.4-1 tension force along riser length with respect to wall thickness

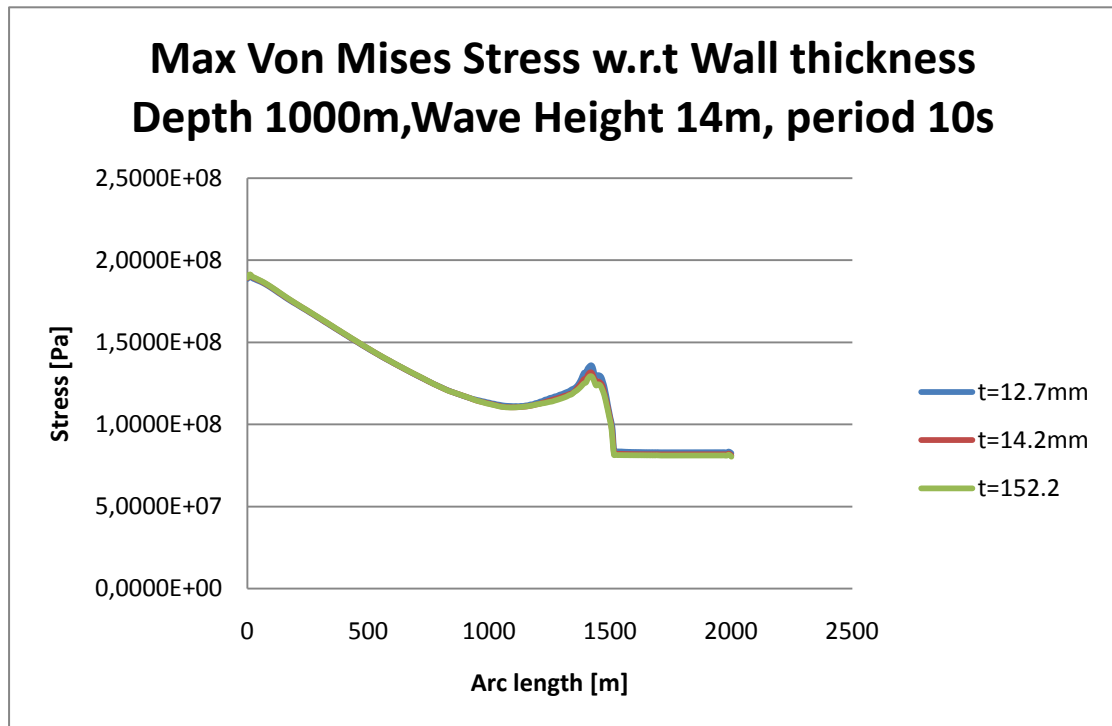


Figure 5.4-2 maximum stress along riser length with respect to wall thickness

5.4.2 Arc length increase

Table 5.4-2 Force and stress variation with respect to arc length

Arc length [m]	Weight increase	Max Static tension force [KN]	Max Static bending moment [KNm]	Max Dynamic tension force [KN]	Max dynamic bending moment [KNm]	Max von-mises stress [MPa]
2000	-	1530	31.22	413.2	48.62	190.55
2249.11	12.455%	1082	131.2	212.6	99.49	183.19
2416.69	20.835%	978.1	361.8	183.9	130.5	349.75

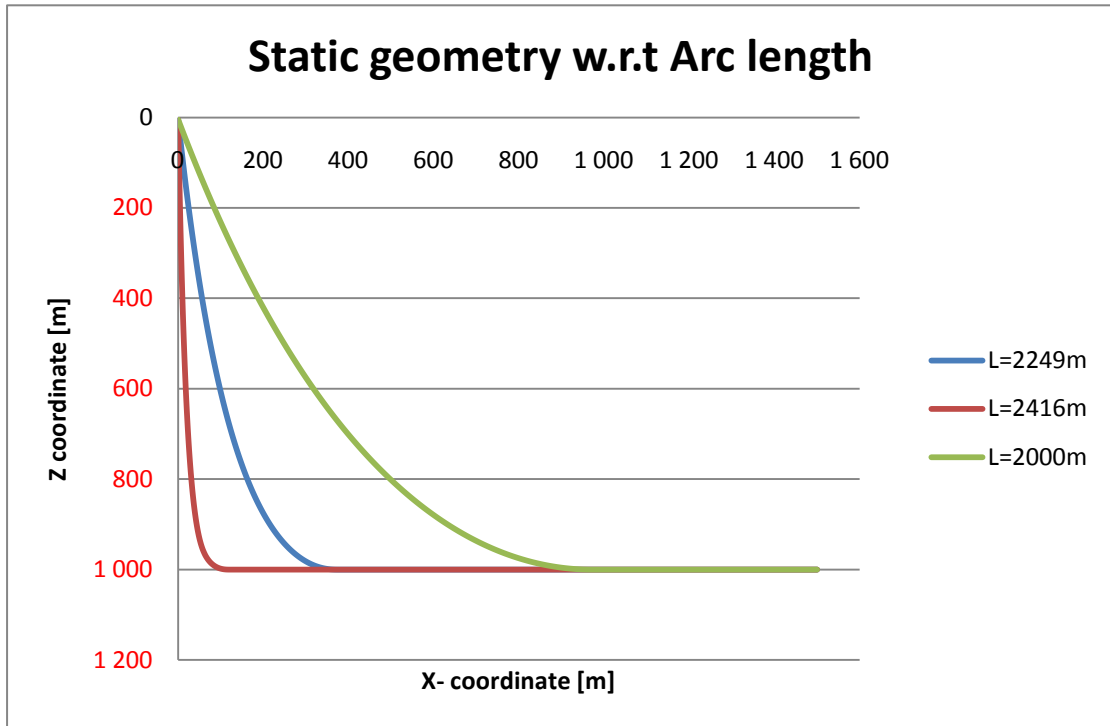


Figure 5.4-3 static configuration variation with respect to arc length

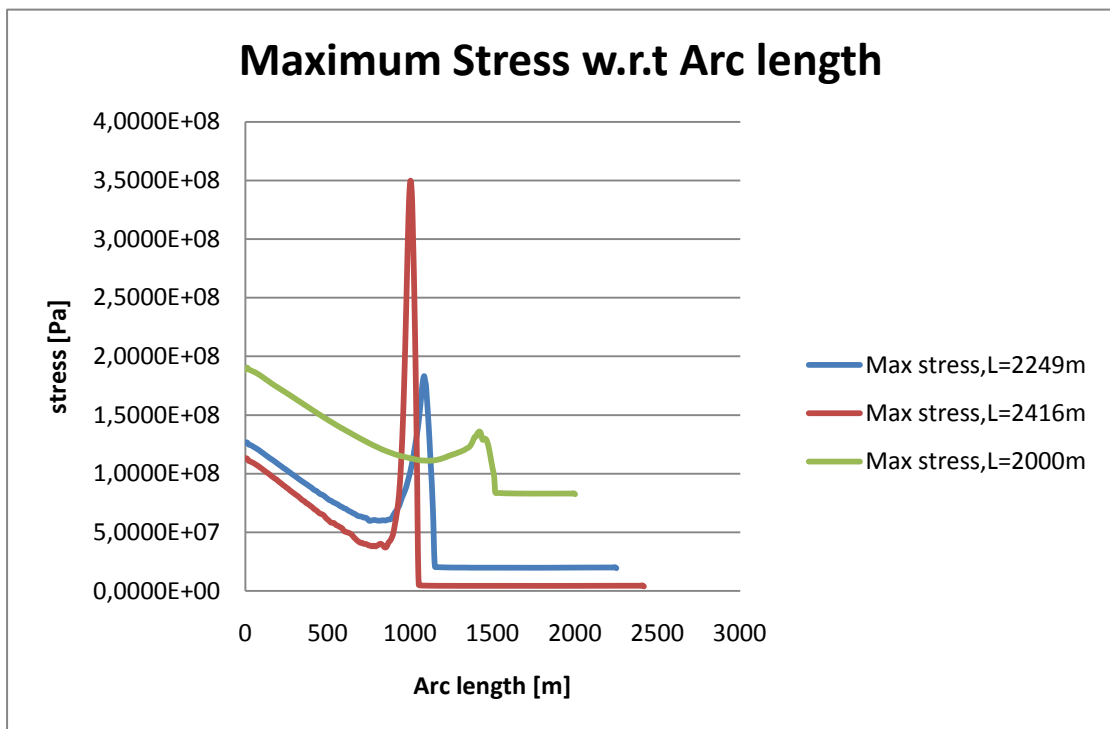


Figure 5.2-4 Maximum stress variation with respect to arc length

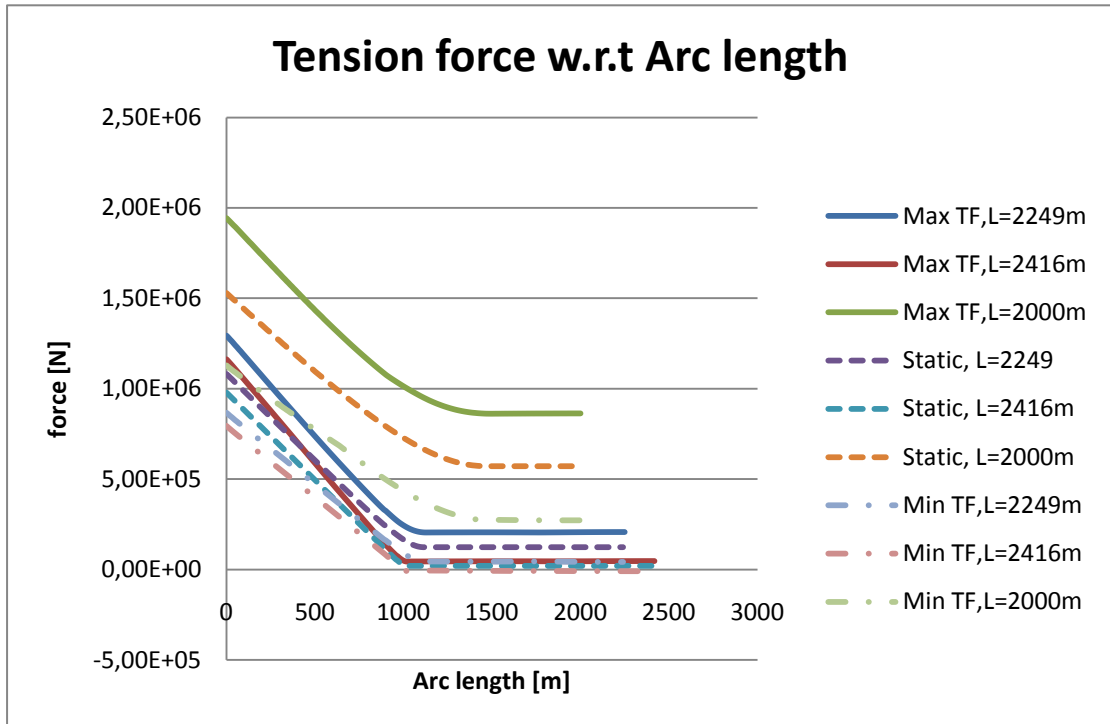


Figure 5.4-5 Tension force variation with respect to arc length

5.4.3 Conclusion:

1. As indicated in figure 5.4-2, thicker wall indeed increases minimum tension force, which has positive influence on buckling prevention. But maximum von-mises stress is not effectively improved. Hence, if only not for the sake of buckling control, global wall thickness increase is not recommended. Whereas, increasing local wall thickness at critical bending area could be feasible to reduce maximum bending stress.
2. Reduction of arc length shows remarkable improvement of maximum stress due to dramatic decrease of bending moment at TDA.
3. Compared with modification of section parameter like thickness, increase of top angle is a more effective approach to improve global behavior of response, both static and dynamic.

Chapter 6 Summary

This paper gives a brief description of the most popular commercial programs for riser analysis. A summary of their features reveals the basic methodology employed by these computation packages. It is indicated that all these programs perform static/dynamic analyze by similar methods. For instance, static solution is catenary analysis and FEM, when dynamic solution is frequency domain method for linear problem, and time domain approach for all problems. Time domain solution generally is accomplished by numerical integration combined with stepwise iteration. Typical iteration approach is full or modified Newton-Raphson method.

Although these programs have been validated by tests or experiments, and proven to be proficient in plenty of industrial applications, limitations of use due to weakness of internal mechanism or imperfection of design, deserve special care. Therefore, a careful review of theory manuals and published papers, along with personal experience of Riflex leads to a list of limitations or uncertainties of programs with explanation to the reasons. Moreover, a few useful examples are presented to interpret when and how to handle the limitations or uncertainties.

Further, independent verification of Riflex is performed in Chapter 3 and 4 for static analysis and dynamic analysis respectively. This paper focuses on global response analysis of catenary risers. Based on Faltisen's catenary equations, static analysis is verified by simple programs compiled in the environment of MATLAB. Codes are programmed separately for SCR and LWR. Static results show very good agreement with those results from Riflex by FEM.

Due to shortage of analytical solutions, this paper only verifies dynamic bending moment at TDA, where is the critical part of catenary riser. The boundary layer value method proposed by J.A.P Aranha is used for verification. Instead of calculating dynamic tension force and instantaneous TDP position by frequency domain method, this paper copies the tension force and displacement results from Riflex and then substitutes them into the proposed approximation formulas to calculate dynamic bending moment. Good agreement with ANSYS is shown in Aranha's journal. However, not all formulas agree with the results from Riflex, even though the asymptotic formulas show comparable value to predict maximum bending moment range and trend of bending moment variation along arc length.

Proper use of analysis software strongly relies on good command of program features. The author carries out parametric study to investigate effects of time step and mesh density. Some conclusions are made in the following:

1. The most critical part of catenary risers requiring finer mesh is TDA. API 2RD provides a conservative upper limit for discretisation. If only tension force is interested, coarse mesh and bar element is even enough for mesh model.
2. The required time step depends not only on system and excitation force, but also discretisation model. Recommended time step given by Orcaflex seems too small and over conservative in the studied case. Therefore it is suggested specifying time step



manually for standard configuration. Besides, one has to beware that time step should be smaller than normal, if wave period excites large floater motion which can be implied from vessel's RAO function. When time step is large, divergence is not definitely the only result. The indicator of a bad time step which still achieves convergence is unexpected oscillation of force results along length instead of smooth variation.

Good understanding of structural behavior of risers is essential for the analyst to perform more effective analysis and design. To supplement behavior study in the project thesis last semester, effects of water depth, wall thickness and arc length are studied hereby. A few conclusions are listed below:

1. Shallow water installation results in larger bending moment compared with deep water installation, if the riser is scaled without modifying cross section. Even though tension force is much smaller, bending moment is the governing factor for structural design. A better design shall increase top angle considering over bending.
2. Wall thickness is not as influential as arc length on global response. Reducing arc length or increasing top angle is a better solution to control global stress compared to increasing wall thickness.



Reference

- [1] Orcina, "OrcaFlex Theory manual", version 9.3c, 2009
- [2] Principia, "Deeplines Theory manual", version 4.4, October 2009
- [3] MCS Kenny (2010). Flexcom. *Software: Analysis Software news*. Retrieved May 18th,2010, from <http://www.mcs.com/site.php?page=15>
- [4] Sintef (May, 2010). RIFLEX. *MARINTEK: Software developed at MARINTEK*. Retrieved May 24th, 2010, from <http://www.sintef.no/Home/Marine/MARINTEK/Software-developed-at-MARINTEK/RIFLEX>
- [5] Michael Lane, "Advanced Frequency Domain Analysis Techniques for Steel Catenary Risers", OTC 13017, 2001, Houston, Texas
- [6] D. McCann, "Guidelines for Compression Modeling in Flexible Risers for Deepwater Applications", OTC 15168, 2003, Houston, Texas
- [7] Luca Du Amicis, "Advanced Design Methodology for SCRs", ISOPE 2008, Canada
- [8] J.You, "Seafloor interaction with SCRs", ISOPE 2008, Canada
- [9] Marintek, "Riflex Theory Manual", version 3.6.3 , 2009
- [10] API, "Recommended Practice 2RD", 2009
- [11] M.H.Patel, "Review of flexible riser modeling and analysis techniques", *Engineering Structures*, Vol. 17, No. 4, pp. 293-304, 1995, U.K.
- [12] O.M. Faltisen, "Sea Loads", Chapter 8 pp 259-265, Cambridge University press, 1990
- [13] Peyrot A.H., Goulois A.M., "Analysis of cable structures", *Computers and structures*, Vol.10 pp.805-813, 1979
- [14] C.M.Larsen, "Static analysis of non-vertical marine risers by simplified methods", NTNU, 1996
- [15] J.A.P. Aranha, "Analytical approximation for the dynamic bending moment at the touchdown point of a catenary riser", *ISOPE Vol.7, No.4*, 1997
- [16] Jinping, Zhan, "Deep ocean riser: concept design and analysis", NTNU, 2009
- [17] Orcina, "Comparison of OrcaFlex with numerical method developed at University of São Paulo for Touchdown modeling", *OMAE 99-103*, 2007
- [18] Elezabeth Passano, "Efficient analysis of a catenary riser", *OMAE 92308*,2006, Hamburg



Appendix A Static Validation: MATLAB Code

SCR

```
function []=staticSCR()
clear all;
%riser specification
OD=0.273;
WT=0.0127;
g=9.81;
L=2240;
xL=1500;
rhoW=1.025*1000;
m=125;
rhoI=700;
E=2.1e11;
A=pi*OD^2/4;
AI=pi*(OD-WT*2)^2/4;
w=(m+rhoI*AI-rhoW*A)*g;
EA=E*A;
EI=E*pi*((OD)^4-(OD-WT*2)^4)/64;
%-----attached buoy-----
%range from 985m to 1881m, counted from well head
s2=985;
blength=896;
BOD=0.55;
mB=20;
wB=(m+mB+rhoI*AI-rhoW*pi*BOD^2/4)*g;
%-----hydrodynamic coefficient
Cd1=0.7;
Cd2=0.7;
Cd3=2;
%-----Current profile-----
Curfile=load('CurrentLWR.txt');
CurZ=Curfile(:,1);
Current=Curfile(:,2);
%-----
% location of hangoff point
x1=1500;y1=0; z1=-4.4696;
z0=-1000;
%assume T0, and iterate
%use Faltisen classic catenary equation for the first approximation.
```



```
a=1;%!!!!!!case a<1
h=z1-z0;
X=0;
while(X<=x1)

    X=L-h*(1+2*a/h)^0.5+a*acosh(1+h/a);
    a=a+1;
end
tempu=a;
templ=a-1;
%X=L-h*(1+2*a/h)^0.5+a*acosh(1+h/a);
while((X-x1)/x1>0.001)
    a=(templ+tempu)/2;
    X=L-h*(1+2*a/h)^0.5+a*acosh(1+h/a);
    if (X>x1)
        tempu=a;
    elseif (X<x1)
        templ=a;
    end
end

end
lengthxs=a*acosh(1+h/a);
ls=h*(1+2*a/h)^0.5;
TH=a*w;
%-----iteration-----
%increment length
dx1=1;dx2=0.2;
xs=[0:dx1:50,(50+dx2):dx2:1000];
nlength=length(xs);
%suspended line x coordinate
fi=zeros(1,nlength);
s=zeros(1,nlength);
%vertical plane tangential angle
T=zeros(1,nlength);
z=zeros(1,nlength);
z(1)=z0;
Te(1)=TH;
T(1)=TH+rhoW*g*A*z(1);
etaX=1;
etaZ=1;
THC=0;
TVC=0;
while(abs(etaX)>0.001 || abs(etaZ)>0.001)
for i=2:length(xs)
```



```
%if(s(i)>=s2&& s(i)<=(s2+blength))
% tempw=wB;
%else
tempw=w;
tempCd=Cd1;
tempOD=OD;
%end
%----no current included
dfi=(tempw*(xs(i)-xs(i-1)))/(T(i-1)-rhoW*g*A*z(i-1));
%-----Current included-----
for j=1:(length(CurZ)-1)
    if(z(i-1)>=CurZ(j+1)&&z(i-1)<CurZ(j))

D1(i-1)=(sin(fi(i-1))*((Current(j+1)-Current(j))/(CurZ(j+1)-CurZ(j))*
(z(i-1)-CurZ(j))+Current(j)))^2;
        D2(i-1)=tempCd*rhoW/2*tempOD*(s(i)-s(i-1));

D(i-1)=tempCd*rhoW/2*tempOD*(xs(i)-xs(i-1))/cos(fi(i-1))*(sin(fi(i-1)
)*((Current(j+1)-Current(j))/(CurZ(j+1)-CurZ(j))*(z(i-1)-CurZ(j))+Cur
rent(j)))^2;
        %Accumulative current force- horizontal component,
        THC=D(i-1)*sin(fi(i-1))+THC;
        TVC=-D(i-1)*cos(fi(i-1))+TVC;
    end
end

%-----

dT=rhoW*g*A*tan(fi(i-1))*(xs(i)-xs(i-1))+tempw*tan(fi(i-1))*(xs(i)-xs
(i-1));
    fi(i)=fi(i-1)+dfi;
    T(i)=T(i-1)+dT;
    z(i)=z(i-1)+(xs(i)-xs(i-1))*tan(fi(i-1));
    s(i)=s(i-1)+(xs(i)-xs(i-1))/cos(fi(i-1));
    Te(i)=T(i)-rhoW*g*A*z(i);
    %xs(i)=xs(i-1)+ds*cos(fi(i-1));
    if(z(i)>=z1)
        break;
    end

end
%rememeber the final fi, xs, s, T
endi=i;
```



```
etaX=(xs(endi)+L-s(endi)-x1)/L;  
etaZ=(z(endi)-z1)/L;  
if(abs(etaX)<=0.001&&abs(etaZ)<=0.001)  
    break;  
end  
T(1)=T(1)*(1+(etaZ)*0.5);  
end  
% illustrate tension force, bending moment, displacement, curvature  
nl=endi+10;  
X=zeros(nl,1);  
Z=zeros(nl,1);  
TE=zeros(nl,1);  
S=zeros(nl,1);  
BM=zeros(nl,1);  
for i=1:nl  
    if(i<=endi)  
        X(i)=xs(endi)-xs(endi-i+1);  
        Z(i)=z(endi-i+1);  
        S(i)=s(endi)-s(endi-i+1);  
        TE(i)=Te(endi-i+1);  
    else  
        X(i)=xs(endi)+(xL-xs(endi))/10*(i-endi);  
        Z(i)=z0;  
        S(i)=s(endi)+(L-s(endi))/10*(i-endi);  
        TE(i)=Te(1);  
    end  
end  
for i=1:nl  
    if(i~=nl)  
        d1(i)=(Z(i)-Z(i+1))/(X(i)-X(i+1));  
    else  
        d1(i)=0;  
    end  
end  
for i=1:nl  
    if(i~=nl)  
        d2(i)=(d1(i)-d1(i+1))/(X(i)-X(i+1));  
    else  
        d2(i)=0;  
    end  
end  
for i=1:nl  
    if((i~=1)&&(i~=nl))  
        TT=X(i+1)+X(i-1)-2*X(i);  
    end  
end
```



```
    if(TT~=0)
        QQ=i-1;
d1(QQ)=d1(QQ-1)+(d1(QQ+1)-d1(QQ-1))/(S(QQ+1)-S(QQ-1))*(S(QQ)-S(QQ-1));
d2(QQ)=d2(QQ-1)+(d2(QQ+1)-d2(QQ-1))/(S(QQ+1)-S(QQ-1))*(S(QQ)-S(QQ-1))
;
        end
    end
end
for i=1:nl
    BM(i)=EI*d2(i)/(1+d1(i)^2)^1.5;
end
%-----
figure(1);
plot(X,Z,'-');
%plot(xs(1,1:endi),z(1,1:endi),'.-');
%hold on;
grid;
title('vertical profile');
xlabel('X, m');
ylabel('Z,m');
figure(2);
plot(S,TE,'-');
%plot(s(1,1:endi),Te(1,1:endi),'.-');
%hold on;
grid;
title('Tension force');
xlabel('s, m');
ylabel('T,N');
figure(3);
plot(S,BM,'-');
grid;
title('Bending moment');
xlabel('S, m');
ylabel('BM,Nm');
```



LWR Approach I

```
function []=staticLWR1()
clear all;
%global EA w wB L3 L2 L;
%riser specification
OD=0.273;
WT=0.0127;
g=9.81;
L=2100;
xL=1500;
rhoW=1.025*1000;
m=125;
rhoI=700;
E=2.1e11;
A=pi*OD^2/4;
AI=pi*(OD-WT*2)^2/4;
w=(m+rhoI*AI-rhoW*A)*g;
EA=E*A;
EI=E*pi*((OD)^4-(OD-WT*2)^4)/64;
%-----attached buoy-----
%range from 985m to 1881m, counted from well head
L3=900;
blength=800;
L2=blength;
BOD=0.55;
mB=40;
wB=(m+mB+rhoI*AI-rhoW*pi*BOD^2/4)*g;
w1=w;
w2=wB;
w3=w;
%-----hydrodynamic coefficient
Cd1=0.7;
Cd2=0.7;
Cd3=2;
%-----Current profile-----
Curfile=load('CurrentLWR.txt');
CurZ=Curfile(:,1);
Current=Curfile(:,2);
%-----
% location of hangoff point
x1=1500;y1=0; z1=-4.4696;z0=-1000;
z1=z1-z0;
%TH=zeros(1,1000);
```



```
%-----  
%-- assume tension force  
itel=1000;  
y2=zeros(1,200);  
lstep=1000;  
for j=1:itel  
    if (j==1)  
        TH(j)=j*lstep;  
    else  
        TH(j)=TH(j-1)+lstep;  
    end  
%-----iteration---  
%---intial y2=50%depth--  
%iteration steps <=200  
    y2(1)=z1/2;  
    f=0.5;  
%eq(19)  
    for i=2:length(y2)  
        xxx=(w2*y2(i-1)/(w1-w2))^2-2*TH(j)*w2*y2(i-1)/(w1*(w1-w2));  
        L1=sqrt(xxx);  
%eq(22)  
        beta1=w1*L1/TH(j);  
        beta2=beta1+w2*L2/TH(j);  
        beta3=beta2+w3*L3/TH(j);  
%eq(20)  
        z3=TH(j)/w3*(sqrt(1+beta3^2)-sqrt(1+beta2^2));  
%eq(21)  
        z2=TH(j)/w2*(sqrt(1+beta2^2)-1);  
%Eq(23)  
        y2temp=z1-z2-z3;  
        if (abs(y2temp-y2(i-1))<0.01)  
            break;  
        else  
            y2(i)=y2(i-1)+f*(y2temp-y2(i-1));  
        end  
    end  
end  
  
%-----grs  
Tv3=w1*L1+w3*L3+w2*L2;  
Tv2=w1*L1+w2*L2;  
Tv1=w1*L1;  
T1=sqrt(Tv1^2+TH(j)^2);  
T2=sqrt(Tv2^2+TH(j)^2);  
T3=sqrt(Tv3^2+TH(j)^2);
```



```
H1=TH(j)*(L1/EA+log((Tv1+T1)/TH(j))/w1);
H2=TH(j)*(L2/EA+log((Tv2+T2)/(T1+Tv1))/w2);
H3=TH(j)*(L3/EA+log((Tv3+T3)/(T2+Tv2))/w3);

tole=H2+H1+H3+(L-L1-L2-L3)-xL;
if(abs(tole/xL)<0.01)
    lstep=100;
end
if(tole>0)
    break;
end
end

%-----plot-----
%dx1=1;dx2=0.2;
%xs=[0:dx1:1000,(1000+dx2):dx2:1500];
%s=[0:1:2500];
nlength=2500;
%suspended line x coordinate
xs=zeros(1,nlength);
fi=zeros(1,nlength);
%vertical plane tangetial angle
T=zeros(1,nlength);
Te=zeros(1,nlength);
z=zeros(1,nlength);
%Integration start from TDP
z(1)=z0;
%define intial value for integration
Te(1)=TH(j);
iniT=TH(j)+rhoW*g*A*z(1);%TH(j)+rhoW*g*A*z(1);
T(1)=iniT;
%-----
etaX=100;
etaZ=100;
%assume length laying on seabed
lx=L-L1-L2-L3;%L-s2-blength-58;
temps=0;
%while(abs(etaX)>0.0001 || abs(etaZ)>0.0001)
Ls1=L1;
s(1)=0;
step=1;
Diff=1;
THC=0;
TVC=0;
%while(Diff>0.0001)
```




```
for i=2:nlength
    s(i)=s(i-1)+step;
    temps=s(i-1);
    if (temps>=Ls1&&temps<=(Ls1+L2))
        tempw=w2;
        tempOD=BOD;
        tempCd=Cd2;
    elseif (temps>(Ls1+L2))
        tempw=w3;
        tempOD=OD;
        tempCd=Cd3;
    else
        tempw=w1;
        tempOD=OD;
        tempCd=Cd1;
    end
    %-----No current included
    dfi=(tempw*(s(i)-s(i-1))*cos(fi(i-1)))/(T(i-1)-rhoW*g*A*z(i-1));
    %-----Current included-----
    for j=1:(length(CurZ)-1)
        if (z(i-1)>=CurZ(j+1)&&z(i-1)<CurZ(j))
            D(i-1)=tempCd*rhoW/2*tempOD*(s(i)-s(i-1))*(sin(fi(i-1))*((Current(j+1)
            )-Current(j))/(CurZ(j+1)-CurZ(j))*(z(i-1)-CurZ(j))+Current(j))^2;
        end
    end
    %Accumulative current force- horizontal component,
    THC=D(i-1)*sin(fi(i-1))+THC;
    TVC=-D(i-1)*cos(fi(i-1))+TVC;
    %dfi=(tempw*cos(fi(i-1))+D(i-1))*(s(i)-s(i-1))/(T(i-1)-rhoW*g*A*z
    (i-1));
    %-----
    dT=rhoW*g*A*sin(fi(i-1))*(s(i)-s(i-1))+tempw*sin(fi(i-1))*(s(i)-s(i-1)
    ));
    fi(i)=fi(i-1)+dfi;
    T(i)=T(i-1)+dT;
    z(i)=z(i-1)+(s(i)-s(i-1))*sin(fi(i-1));
    xs(i)=xs(i-1)+(s(i)-s(i-1))*cos(fi(i-1));
    Te(i)=T(i)-rhoW*g*A*z(i);
    %integrate up to suspended end z=z1
    etaZ=(z(i)-z1)/z1;
    if (abs(etaZ)<0.01)
        step=0.1;
    end
    if (z(i)>=z1)
```



```
        break;
    end
end
endi=i;
Ls=L-s(endi)+xs(endi);
etaX=(xs(endi)+L-s(endi)-x1)/L;
Diff=abs((T(1)-rhoW*g*z(1)*A-T(endi)*cos(fi(endi)))/(T(1)-rhoW*g*z(1)
*A));
%if(Diff>0.0001)
% T(1)=T(1)-(T(1)-rhoW*g*z(1)*A-T(endi)*cos(fi(endi)))*0.7;
%end
%end
% illustrate tension force, bending moment, displacement, curvature
% Incorporate the part laying on seafloor with the suspended part
nl=endi+10;
X=zeros(nl,1);
Z=zeros(nl,1);
TE=zeros(nl,1);
S=zeros(nl,1);
BM=zeros(nl,1);
for i=1:nl
    if(i<=endi)
        X(i)=xs(endi)-xs(endi-i+1);
        Z(i)=z(endi-i+1);
        S(i)=s(endi)-s(endi-i+1);
        TE(i)=Te(endi-i+1);
    else
        X(i)=xs(endi)+(xL-xs(endi))/10*(i-endi);
        Z(i)=z0;
        S(i)=s(endi)+(L-s(endi))/10*(i-endi);
        TE(i)=Te(1);
    end
end
for i=1:nl
    if(i~=nl)
        d1(i)=(Z(i)-Z(i+1))/(X(i)-X(i+1));
    else
        d1(i)=0;
    end
end
for i=1:nl
    if(i~=nl)
        d2(i)=(d1(i)-d1(i+1))/(X(i)-X(i+1));
    else
```



```
d2(i)=0;
end
end
for i=1:nl

    if((i~=1)&&(i~=nl))
        TT=S(i+1)+S(i-1)-2*S(i);
        if(TT~=0)
            QQ=i-1;
d1(QQ)=d1(QQ-1)+(d1(QQ+1)-d1(QQ-1))/(S(QQ+1)-S(QQ-1))*(S(QQ)-S(QQ-1))
;
d2(QQ)=d2(QQ-1)+(d2(QQ+1)-d2(QQ-1))/(S(QQ+1)-S(QQ-1))*(S(QQ)-S(QQ-1))
;
            end
        end
end
for i=1:nl
    BM(i)=EI*d2(i)/(1+d1(i)^2)^1.5;
end
%-----Plot-----
figure(1);
plot(X,Z,'-');
grid;
title('vertical profile');
xlabel('X, m');
ylabel('Z,m');
figure(2);
plot(S,TE,'-');
grid;
title('Tension force');
xlabel('s, m');
ylabel('T,N');
figure(3);
plot(S,BM,'-');
grid;
title('Bending moment');
xlabel('S, m');
ylabel('BM,Nm');
```



LWR Approach II

```
function []=LWR2()
clear all;
global EA xl z1 w wB ls1 ls2 L;
%riser specification
OD=0.273;
WT=0.0127;
g=9.81;
L=2100;
rhoW=1.025*1000;
m=125;
rhoI=700;
E=2.1e11;
A=pi*OD^2/4;
AI=pi*(OD-WT*2)^2/4;
w=(m+rhoI*AI-rhoW*A)*g;
EA=E*A;
EI=E*pi*((OD)^4-(OD-WT*2)^4)/64;
%-----attached buoy-----
%range from 985m to 1881m, counted from well head
ls1=900;
blength=800;
ls2=blength;
BOD=0.55;
mB=40;
wB=(m+mB+rhoI*AI-rhoW*pi*BOD^2/4)*g;
%-----
% location of hangoff point
xl=1500;y1=0; z1=-4.4696;z0=-1000;
xl=xl;z1=z1-z0;

%assume T0, and iterate
%----use Peyrot classic catenary equation for the first approximation.
ap0=[10;10];
ap=fsolve(@fun,ap0);
%ap(1)=TH;
apTH=ap(1);
ls3=ap(2);
%----iteration-----
%increment length
dx1=1;dx2=0.2;
xs=[0:dx1:1000,(1000+dx2):dx2:1500];
nlength=length(xs);
```



```
%suspended line x coordinate
fi=zeros(1,nlength);
s=zeros(1,nlength);
%vertical plane tangetial angle
T=zeros(1,nlength);
z=zeros(1,nlength);
%Integration start from TDP
z(1)=z0;
%define intial value for integration
iniT=apTH+rhoW*g*A*z(1);
T(1)=iniT;
%---used for test only---
%iniT=177000+rhoW*g*A*z(1);
%T(1)=iniT;
%ls3=258;
%-----
etaX=100;
etaZ=100;
%assume length laying on seabed
lx=L-ls1-ls2-ls3;%L-s2-blength-58;
temps=0;
%-----inhibited, linked to line 100-105-----
%while(abs(etaX)>0.001||abs(etaZ)>0.001)
%-----
for i=2:length(xs)
    temps=s(i-1);
    if(temps>=ls3&&temps<=(ls3+ls2))
        tempw=wB;
    else
        tempw=w;
    end
    dfi=(tempw*(xs(i)-xs(i-1)))/(T(i-1)-rhoW*g*A*z(i-1));
    %ds=(T(i-1)-rhoW*g*A*z(i-1))*dfi/(w*cos(fi(i-1)));

dT=rhoW*g*A*tan(fi(i-1))*(xs(i)-xs(i-1))+tempw*tan(fi(i-1))*(xs(i)-xs
(i-1));
    %if(i==2)
    %dfi=(w*cot(fi(2))*(z(i)-z(i-1)))/(T(i-1)-rhoW*g*z(i-1));
    %else
    %dfi=(w*cot(fi(i-1))*(z(i)-z(i-1)))/(T(i-1)-rhoW*g*z(i-1));
    %end
    fi(i)=fi(i-1)+dfi;
    T(i)=T(i-1)+dT;
    z(i)=z(i-1)+(xs(i)-xs(i-1))*tan(fi(i-1));
```



```
s(i)=s(i-1)+(xs(i)-xs(i-1))/cos(fi(i-1));
%integrate up to suspended end z=z1
if(z(i)>=z1)
    break;
end
end
%record the final fi, xs, s, T
endi=i;
etaX=(xs(endi)+L-s(endi)-x1)/L;
etaZ=((z(endi)-z1)/L);
%-----Inhibited-----
%if(abs(etaX)<=0.001&&abs(etaZ)>=0.001)
%    break;
%end
%T(1)=T(1)+(etaX+etaZ)*abs(iniT)*L/x1;
%lx=lx*(1-(etaX+etaZ)/2);
%end
%-----
% illustrate tension force, bending moment, displacement, curvature
figure(1);
plot(xs(1,1:endi),z(1,1:endi),'.-');
grid;
title('vertical profile')
xlabel('Xs, m');
ylabel('Z,m');
function f=fun(x)
global EA xl z1 w wB ls1 ls2 L;
TH=x(1);
l3=x(2);
Tv1=w*(ls1+l3)+wB*ls2;
Tv2=Tv1-w*ls1;
Tv3=Tv1-w*ls1-wB*ls2;
T1=sqrt(Tv1^2+TH^2);
T2=sqrt((Tv1-w*ls1)^2+TH^2);
T3=sqrt((Tv1-w*ls1-wB*ls2)^2+TH^2);
H1=TH*(ls1/EA+log((Tv1+T1)/(T2+Tv2))/w);
H2=TH*(ls2/EA+log((Tv2+T2)/(T3+Tv3))/wB);
H3=TH*(l3/EA+log((Tv3+T3)/TH)/w);
V1=(T1^2-T2^2)/(2*EA*w)+(T1-T2)/w;
V2=(T2^2-T3^2)/(2*EA*wB)+(T2-T3)/wB;
V3=(T3^2-TH^2)/(2*EA*w)+(T3-TH)/w;
f=[H1+H2+H3+(L-ls1-ls2-l3)-x1;V1+V2+V3-z1];
```



File of Current Profile

“CurrentLWR.txt”

-0	0.63
-30	0.55
-75	0.55
-147	0.43
-200	0.3
-400	0.25
-600	0.22
-800	0.2
-900	0.15
-1000	5.e-002

Appendix B Validation of dynamic bending moment at TDA

Regular wave sea state

Time Step	X0 [m]	Total tension force [N]	$\tau(t)$ [N]	β	Mf [Nm]
50	3.5	1.43E+05	28380	1.3955319	94289.28
51	5.5	1.40E+05	25370	1.2174163	90132.659
52	6.5	1.35E+05	20420	1.128124	89765.469
53	7.5	1.28E+05	13550	1.0416081	90484.427
54	7.5	1.20E+05	5430	1.0402694	96530.012
55	7.5	1.11E+05	-3340	1.0387716	104046.8
56	6.5	1.03E+05	-11280	1.1120916	116373.15
57	5.5	9.71E+04	-17601	1.1810201	127994.43
58	4.5	9.26E+04	-22101	1.247486	138037.31
59	2.5	8.90E+04	-25729	1.3812119	150912.58
60	0.5	8.60E+04	-28684	1.5111288	162479.37
61	-1.5	8.39E+04	-30802	1.6394093	172259.56
62	-2.5	8.34E+04	-31267	1.7047543	175858.55
63	-4.5	8.46E+04	-30072	1.8449803	178416.19
64	-5.5	8.78E+04	-26932	1.9293544	174645.71
65	-6.5	9.28E+04	-21908	2.0263672	167785.11
66	-6.5	9.97E+04	-14962	2.0640887	156977.49
67	-6.5	1.08E+05	-7050	2.1054893	146297.6
68	-6.5	1.16E+05	1180	2.1469692	136673.06
69	-5.5	1.23E+05	8580	2.1014368	127677.39
70	-4.5	1.30E+05	14840	2.0454216	120532.11
71	-2.5	1.35E+05	19850	1.8949745	113245.64
72	-2.5	1.39E+05	24180	1.9092612	109990.21
73	-2.5	1.42E+05	27530	1.9201623	107602.14
74	-2.5	1.44E+05	29300	1.9258701	106383.43
75	3.5	1.43E+05	28430	1.395601	94258.486
76	5.5	1.40E+05	25160	1.2172532	90261.805
77	6.5	1.35E+05	20020	1.1279342	90023.817
78	6.5	1.28E+05	13290	1.1246978	94610.445
79	7.5	1.20E+05	5070	1.040209	96816.963
80	7.5	1.11E+05	-3650	1.0387176	104334.17
81	6.5	1.03E+05	-11650	1.1118909	116779.5
82	5.5	9.66E+04	-18074	1.1805787	128595.82
83	3.5	9.20E+04	-22717	1.3171362	142729.22



84	2.5	8.86E+04	-26141	1.3803282	151569.68
85	0.5	8.58E+04	-28855	1.5106205	162779.58
86	-1.5	8.38E+04	-30885	1.6390929	172417.01
87	-3.5	8.30E+04	-31686	1.7699332	179224.52
88	-4.5	8.42E+04	-30474	1.842971	179200.07
89	-5.5	8.76E+04	-27061	1.9286712	174882.47
90	-6.5	9.28E+04	-21883	2.0265055	167743.43
91	-7.5	9.95E+04	-15200	2.1361162	158942.83
92	-7.5	1.07E+05	-7380	2.1799172	148207.08
93	-6.5	1.16E+05	850	2.1453349	137033.73
94	-5.5	1.23E+05	8260	2.1000064	127984.13
95	-4.5	1.29E+05	14380	2.0435638	120928.24
96	-3.5	1.34E+05	19310	1.9782412	115309.11
97	-1.5	1.38E+05	23610	1.8209749	108670.04
98	0.5	1.42E+05	27110	1.6562876	102323.45
99	1.5	1.44E+05	29070	1.5726998	98853.155
100	3.5	1.43E+05	28490	1.3956839	94221.562
101	4.5	1.40E+05	25380	1.3043937	93282.783
102	6.5	1.35E+05	19940	1.1278963	90075.669
103	6.5	1.28E+05	13000	1.1245564	94818.854
104	7.5	1.20E+05	5000	1.0401973	96872.959
105	7.5	1.11E+05	-3450	1.0387525	104148.59
106	6.5	1.03E+05	-11550	1.1119452	116669.39
107	5.5	9.66E+04	-18080	1.1805731	128603.49
108	3.5	9.20E+04	-22711	1.3171465	142720.46
109	2.5	8.87E+04	-25979	1.3806759	151310.6
110	0.5	8.61E+04	-28615	1.5113338	162358.56
111	-1.5	8.41E+04	-30631	1.6400605	171936.13
112	-2.5	8.32E+04	-31461	1.7039345	176236.28
113	-4.5	8.44E+04	-30260	1.8440412	178781.89
114	-5.5	8.77E+04	-27003	1.9289785	174775.94
115	-6.5	9.29E+04	-21775	2.0271025	167563.66
116	-7.5	9.98E+04	-14944	2.1375768	158565.93
117	-7.5	1.08E+05	-7160	2.181126	147926.66
118	-6.5	1.16E+05	850	2.1453349	137033.73
119	-5.5	1.23E+05	8320	2.1002747	127926.5
120	-4.5	1.29E+05	14570	2.0443315	120764.3
121	-3.5	1.34E+05	19570	1.9791897	115103.34
122	-1.5	1.38E+05	23700	1.821242	108604.97
123	0.5	1.42E+05	27070	1.656195	102350.08
124	1.5	1.44E+05	29020	1.5726002	98884.967



Irregular sea state

NB! Only example, not full list

Time Step	X0 [m]	Total tension force [N]	$\tau(t)$ [N]	β	Mf [Nm]
999	132	1.28E+05	13770	1	88236.67
1004	134	1.03E+05	-12000	1.148934	119266.2
1009	133	1.34E+05	18890	1.084931	88875.92
1014	133	9.24E+04	-22278	1.070643	127520.8
1019	133	1.15E+05	740	1.078951	102534.5
1024	130	1.08E+05	-6520	0.847144	94714.33
1029	130	1.03E+05	-11220	0.850501	99265.18
1034	131	1.36E+05	21080	0.914376	79142.72
1039	132	1.11E+05	-3320	1	101775.6
1044	134	1.22E+05	7110	1.1622	101170.3
1049	133	1.19E+05	4020	1.080065	99758.86
1054	134	9.84E+04	-16335	1.145757	124338.5
1059	132	1.19E+05	3870	1	95603.99
1064	131	1.09E+05	-5940	0.923367	99396.21
1069	131	1.10E+05	-4610	0.9229	98165.17
1074	131	1.22E+05	7130	0.918893	88470.77
1079	131	1.11E+05	-3710	0.922586	97348.97
1084	132	1.14E+05	-790	1	99515.1
1089	132	1.25E+05	10680	1	90411.27
1094	133	9.95E+04	-15235	1.073285	118654.3
1099	133	1.28E+05	13310	1.083138	92665.11
1104	133	1.10E+05	-4800	1.077033	107596.8
1109	133	1.10E+05	-4910	1.076995	107702.4
1114	132	1.19E+05	4210	1	95330.63
1119	132	1.04E+05	-11010	1	109323.6
1124	131	1.14E+05	-1200	0.921715	95141.45
1129	131	1.22E+05	7580	0.918744	88136.44
1134	132	1.07E+05	-7500	1	105744.1
1139	132	1.34E+05	19360	1	84557.4
1144	133	1.09E+05	-5940	1.076633	108702.1
1149	134	1.12E+05	-2260	1.155837	109282.7
1154	132	1.10E+05	-4950	1	103287.2
1159	131	1.00E+05	-14700	0.926518	108327.4
1164	131	1.22E+05	6800	0.919003	88717.54
1169	130	1.16E+05	1440	0.84162	87856.2
1174	132	1.18E+05	3610	1	95814.09



1179	133	1.26E+05	11420	1.082522	94024.1
1184	133	1.01E+05	-13310	1.073991	116444.1
1189	133	1.18E+05	3080	1.079747	100538.6
1194	132	1.12E+05	-2790	1	101293.6
1199	132	1.02E+05	-12850	1	111298.6
1204	131	1.34E+05	19500	0.914875	80101.26
1209	131	9.48E+04	-19938	0.928469	114461.2
1214	132	1.25E+05	10290	1	90693.37
1219	131	1.20E+05	5610	0.919401	89618.69
1224	133	1.03E+05	-12160	1.074409	115163.2
1229	133	1.33E+05	18670	1.084861	89019.34
1234	133	9.82E+04	-16463	1.072831	120109.2
1239	133	1.11E+05	-3370	1.077533	106242.1
1244	131	1.22E+05	7530	0.91876	88173.46
1249	131	1.01E+05	-13920	0.926232	107468.8
1254	132	1.29E+05	14660	1	87629.6
1259	132	1.15E+05	220	1	98640.49
1264	134	1.09E+05	-5840	1.153336	112746.7
1269	133	1.23E+05	8340	1.081508	96327.68
1274	132	9.95E+04	-15176	1	113899.8
1279	131	1.18E+05	3100	0.920246	91579.51
1284	131	1.18E+05	3210	0.920209	91491.81
1289	132	1.10E+05	-4480	1	102846.7
1294	132	1.26E+05	10970	1	90202.63
1299	133	1.09E+05	-5570	1.076763	108340.8
1304	133	1.14E+05	-440	1.078546	103571.8
1309	132	1.15E+05	-40	1	98864.16
1314	132	1.08E+05	-6830	1	105087.3
1319	132	1.22E+05	7080	1	93083.96
1324	132	1.07E+05	-7870	1	106110.3
1329	132	1.18E+05	3500	1	95903.26
1334	131	1.19E+05	4280	0.919848	90647.32
1339	133	1.07E+05	-7600	1.076046	110353.4
1344	133	1.30E+05	15760	1.08393	90961.72
1349	133	1.02E+05	-12990	1.074107	116084.8
1354	133	1.13E+05	-1570	1.078157	104585.4
1359	131	1.23E+05	8730	0.918362	87293.16
1364	132	9.54E+04	-19314	1	118841
1369	132	1.37E+05	21900	1	82985.1
1374	132	1.03E+05	-11980	1	110356
1379	133	1.13E+05	-1610	1.078143	104621.6
1384	132	1.29E+05	14060	1	88037.94
1389	132	8.88E+04	-25892	1	127643.5



NTNU
Norwegian University of Science and Technology
Department of Marine Technology



Appendix C Parametric Study

Example files for Riflex Input

Mesh size =5m, Time step=0.01s

“M5TS01_inpmod.inp”

```

=====
'          DATA SECTION A
=====
INPMOD IDENTIFICATION TEXT   3.4
-----
File generated by :DeepC V4.0-02
  Exported from analysis : M5TS_01
  DATE : April 30, 2010 - 17:54:39
-----
          UNIT NAME SPECIFICATION
-----
'      ut ul um uf grav      gcons
      s  m  Kg N  9.80665 1
-----
          DATA SECTION C
=====
-----
          NEW SINGLE RISER
-----
'      AR   SLEND1
-----
          ARBITRARY SYSTEM AR
-----
'      nsnod nlin nsnfix nves nricon nspr nakc
      2      1      2      1      0      0      0
-----
'      ibtang zbot  ibot3d
      1      -1000 0
-----
'      stfbot  stfaxi stflat friaxi frilat
      1000000 0      0      0.3      0.2
-----
'      Line types
'riser1
'      ilinty isnod1 isnod2

```



```

1      1      2
~~~~~
'      Boundary conditions fixed nodes
~~~~~
'      isnod vessel_no ix      iy      iz      irx      iry      irz      chcoo
'      chupro
2      0      1      1      1      1      1      1      GLOBAL      &
YES
'      x0      y0      z0      x1      y1      z1
'      rot      dir
2.007372342e+003 0      -1000      1500      0      -1000      &
2.637851817e+001 180
1      1      1      1      1      0      0      0      VESSEL      &
NO
0      0      -4.469621658e+000 0      0      &
-4.469621658e+000 0      0
~~~~~

```

```

'      Boundary conditions free nodes
~~~~~

```

```

'      Support vessels reference
~~~~~

```

```

'      ives      idwftr      xg      yg      zg      dirx
1      SEMI      0      0      0      0
~~~~~

```

```

'      Linear springs to global fixed system
~~~~~

```

```

'      Line and segment specification
-----

```

NEW LINE DATA

```

'      ilinty nseg icn1ty ifluty
1      4      0      3
'      icmpty icn1ty iexwty nelseg slgth
2      0      0      54      268.881
1      0      0      144      717.016
1      0      0      72      358.508
1      0      0      180      896.27

```

```

=====
'      DATA SECTION D
=====

```

```

-----
NEW COMPONENT CRS1

```



 ' Section: axiRiser10inch
 '-----

' icmpty temp
 ' 1 20
 '-----

' ams ae ai rgyr ast wst
 ' 125 5.853493972e-002 4.814943131e-002 0.13
 ' ieaj igt ipress imf
 ' 1 1 1 0 0
 ' ea
 ' 2.180957e+009
 ' ejy
 ' 18515600
 ' gt+ gt-
 ' 14243000
 '-----

' Hydrodynamic force coefficients
 ' cqx cqy cax cay clx cly icode d_hydro
 ' 0 0.70 1 0 0 2 0.273
 '-----

' Capacity parameters (dummy)
 ' tb ycurmx
 ' 0 0
 '-----

NEW COMPONENT CRS1

 ' Section: axiRiser10inch
 '-----

' icmpty temp
 ' 2 20
 '-----

' ams ae ai rgyr ast wst
 ' 125 5.853493972e-002 4.814943131e-002 0.13
 ' ieaj igt ipress imf
 ' 1 1 1 0 0
 ' ea
 ' 2.180957e+009
 ' ejy
 ' 18515600
 ' gt+ gt-
 ' 14243000
 '-----

' Hydrodynamic force coefficients



```
' cqx cqy cax cay clx cly icode d_hydro
  0  2  0  1.5 0  0  2  0.273
```

```
' Capacity parameters (dummy)
' tb ycurmx
  0  0
```

```
' Components Internal Fluid
```

```
-----
NEW COMPONENT FLUID
```

```
' Internal fluid: Oil
```

```
' icmpty
  3
' rhoi vveli pressi dpress idir
  700 0  0  0  1
```

```
=====
DATA SECTION E
```

```
-----
ENVIRONMENT IDENTIFICATION
```

```
Environment Condition: RegCond_14x10_D0
```

```
' idenv
VIBHEZ
```

```
-----
WATERDEPTH AND WAVETYPE
```

```
' wdepth noirw norw ncusta
  1000  0  1  1
```

```
-----
ENVIRONMENT CONSTANTS
```

```
' airden warden wakivi
  1.025  1025  1.19e-006
```

```
-----
REGULAR WAVE DATA
```

```
' nrwc amplit period wavedir
  1  7  10  0
```




NEW CURRENT STATE

```
' Current name: CurProf1
' icustanculev
'   1      10
' curlev   curdir   curvel
'   0       0       0.63
'  -30     0       0.55
'  -75     0       0.55
' -147     0       0.43
' -200     0       0.3
' -400     0       0.25
' -600     0       0.22
' -800     0       0.2
' -900     0       0.15
' -1000    0       5.e-002
```

=====

' DATA SECTION F

'Vessel transfer functions

TRANSFER FUNCTION FILE

```
' chftra
' semi_RAO.tra
```

END



"M5TS01_stamod.inp"

```

=====
'
DATA SECTION A
=====
'

```

```

'
STAMOD CONTROL INFORMATION 3.4
=====
'

```

File generated by :DeepC V4.0-02

Export from: M5TS_01, DATE : April 30, 2010 - 17:54:40

Irreg_8x7static analysis

```

=====
'
irunco idris ianal iprdat iprcat iprfem ipform iprnod ifilm
1 SLEND1 2 5 1 5 2 1 2
=====
'

```

```

'
RUN IDENTIFICATION
=====
'

```

STA1

```

'
ENVIRONMENT REFERENCE IDENTIFIER
=====
'

```

idenv
 VIBHEZ

```

=====
'
DATA SECTION B
=====
'

```

```

'
STATIC CONDITION INPUT
=====
'

```

nlcomp icurin curfac lcons isolvr
 0 1 1 1 2

```

'
COMPUTATIONAL PROCEDURE
=====
'

```

ameth
 FEM

```

'
FEM ANALYSIS PARAMETERS
=====
'

```

```

'
LOAD GROUP DATA
=====
'

```

nstep maxit racu
 200 200 1.e-006



' lotype

VOLU

SFOR

'-----

LOAD GROUP DATA

'-----

' nstep maxit racu

200 200 1.e-006

' lotype

DISP

'-----

LOAD GROUP DATA

'-----

' nstep maxit racu

20 200 1.e-006

' lotype

FLOA

'-----

LOAD GROUP DATA

'-----

' nstep maxit racu

5 200 1.e-006

' lotype

CURR

FRIC

'-----

PARAMETER VARIATION DEFINITION

'-----

' nstvar iofpos icuvar ifovar maxipv racupv

1 1 0 0 / /

'-----

STATIC OFFSET INCREMENTS

'-----

' iref dxoff dyoff dzoff irot

-1 0 0 0 0

'-----

STAMOD PRINT CONTROL

'-----

' istep

/

'=====

END

'=====



"M5TS01_dynmod.inp"

```

=====
'
  DATA SECTION A
=====
'
  DYNMOD CONTROL INFORMATION  3.4
=====
File generated by :DeepC V4.0-02
  Export from: M5TS_01, DATE : April 30, 2010 - 17:54:59
M5TS_01 dynamic analysis
'
'   irunco  ianal  idris  idenv  idstat idirr idres
  ANAL  REGU  SLEND1  VIBHEZ  STA1  IRR1  DYN1
=====
'
  DATA SECTION C
=====
'
  REGULAR WAVE ANALYSIS
=====
'
  nper nstppr irwcn imotd
  10  1000  1  1
=====
'
  REGULAR WAVE LOADING
=====
'
  iwtyp isurf iuppos
  2  4  1
=====
'
  REGWAVE PRINT OPTION
=====
'
  nprenc nprenf nprenc
  1  1  1
=====
'
  DATA SECTION E
=====
'
  TIME DOMAIN PROCEDURE
=====
'
  itdmet inewil idisst iforst icurst istrst
  2  1  1  1  1  0
'
  betin gamma theta a1 a2  a1t a1to a2t a2to a2b
  4  0.5  1.5  0  1.e-003 0  0  0  0  0
'
  indint indhyd maxhit epshyd  tramp indrel iconre istepr ldamp
  1  1  5  1.e-002 10  0  0  0  0

```



 NONLINEAR INTEGRATION PROCEDURE

itfreq	isolit	maxit	daccu	icocod	ivarst	istat	
1	1	10	1.e-006	1	0	1	

 DISPLACEMENT RESPONSE STORAGE

idisp	nodisp	idisfm		cfndis
2	4			
ilin	iseg	inod		
1	1	1		
1	2	145		
1	3	1		
1	4	181		

 FORCE RESPONSE STORAGE

ifor	noforc	iforfm		cnfor
2	4			
ilin	iseg	inod		
1	1	1		
1	2	144		
1	3	1		
1	4	180		

 CURVATURE RESPONSE STORAGE

icurv	nocurv	icurfm		cfncur
2	4			
ilin	iseg	inod		
1	1	1		
1	2	144		
1	3	1		
1	4	180		

 ENVELOPE CURVE SPECIFICATION

ienvd	ienvf	ienvc	tensv	tene	nprend	nprenv	nprenc	ifilmp	ifilas	
1	1	1	10	43200	1	1	1	4	0	

=====
 END
 =====



“semi_RAO.tra”

 SUPPORT VESSEL IDENTIFICATION

1st order wave motion transfer functions for vessel: semi
 SEMI

~~~~~  
 HFTRAN REFERENCE POSITION  
 ~~~~~

0

~~~~~  
 HFTRANSFER CONTROL DATA  
 ~~~~~

' ndhftr nwhftr isymhf itypin
 1 17 0 1

~~~~~  
 WAVE DIRECTIONS  
 ~~~~~

' ihead head (deg)
 1 0.000

~~~~~  
 WAVE FREQUENCIES  
 ~~~~~

' ifreq whftr (rad/T)
 1 0.39270
 2 0.41888
 3 0.44880
 4 0.48332
 5 0.52360
 6 0.57120
 7 0.62832
 8 0.69813
 9 0.73920
 10 0.78540
 11 0.83776
 12 0.89760
 13 0.96664
 14 1.04720
 15 1.14240
 16 1.25664
 17 1.57080

~~~~~  
 HFTRANSFER FUNCTION SURGE  
 ~~~~~



~~~~~  
'idir ifreq a b  
1 1 1.8839e-003 -7.4702e-001  
1 2 2.6103e-003 -7.0387e-001  
1 3 3.6725e-003 -6.5157e-001  
1 4 5.1915e-003 -5.8741e-001  
1 5 7.2595e-003 -5.0801e-001  
1 6 9.7445e-003 -4.0945e-001  
1 7 1.1655e-002 -2.8766e-001  
1 8 9.6084e-003 -1.3894e-001  
1 9 5.4146e-003 -5.2904e-002  
1 10 2.7082e-004 4.2477e-002  
1 11 1.4337e-003 1.4535e-001  
1 12 2.1656e-002 2.4001e-001  
1 13 6.3040e-002 2.8606e-001  
1 14 8.3907e-002 2.4582e-001  
1 15 5.5235e-002 1.4976e-001  
1 16 2.6267e-003 2.3752e-002  
1 17 -2.0865e-002 -3.5724e-002  
~~~~~

HFTRANSFER FUNCTION SWAY
~~~~~

'idir ifreq a b  
1 1 -1.7517e-013 -8.7807e-012  
1 2 8.1096e-014 2.2249e-012  
1 3 1.2219e-013 2.1423e-012  
1 4 -2.7228e-011 -9.0218e-012  
1 5 9.6474e-012 -1.0185e-011  
1 6 3.4538e-013 1.5898e-012  
1 7 3.6455e-013 1.1941e-012  
1 8 2.6191e-012 3.9461e-012  
1 9 -3.6486e-013 5.9726e-012  
1 10 2.4304e-012 -7.4566e-012  
1 11 2.7252e-012 2.2355e-012  
1 12 5.0038e-012 -1.5867e-012  
1 13 3.7750e-012 9.6745e-013  
1 14 3.4148e-012 2.1545e-012  
1 15 -5.6267e-012 2.4118e-012  
1 16 2.8201e-014 2.6884e-012  
1 17 4.8860e-013 5.3695e-013  
~~~~~

HFTRANSFER FUNCTION HEAVE
~~~~~

'idir ifreq a b



|   |    |              |              |
|---|----|--------------|--------------|
| 1 | 1  | 5.7911e-001  | -8.9035e-004 |
| 1 | 2  | 5.9085e-001  | -1.6655e-003 |
| 1 | 3  | 5.8650e-001  | -3.9117e-003 |
| 1 | 4  | 5.6902e-001  | -8.9317e-003 |
| 1 | 5  | 5.3803e-001  | -1.9266e-002 |
| 1 | 6  | 4.8850e-001  | -3.8562e-002 |
| 1 | 7  | 4.0746e-001  | -6.6216e-002 |
| 1 | 8  | 2.8512e-001  | -8.1218e-002 |
| 1 | 9  | 2.1728e-001  | -7.4863e-002 |
| 1 | 10 | 1.5461e-001  | -6.0967e-002 |
| 1 | 11 | 1.0234e-001  | -4.4856e-002 |
| 1 | 12 | 6.3211e-002  | -3.2464e-002 |
| 1 | 13 | 3.5885e-002  | -2.8790e-002 |
| 1 | 14 | 1.1704e-002  | -2.9847e-002 |
| 1 | 15 | -2.9935e-003 | -1.5193e-002 |
| 1 | 16 | 4.2888e-003  | -8.6324e-004 |
| 1 | 17 | -2.2637e-004 | 2.8973e-003  |

~~~~~  
HFTRANSFER FUNCTION ROLL
~~~~~

| 'idir | ifreq | a            | b            |
|-------|-------|--------------|--------------|
| 1     | 1     | -2.2826e-013 | 6.7123e-011  |
| 1     | 2     | 1.3411e-014  | -1.4773e-011 |
| 1     | 3     | 3.5031e-014  | -1.2240e-011 |
| 1     | 4     | 1.2760e-010  | 5.6345e-011  |
| 1     | 5     | -4.5860e-011 | 3.5575e-011  |
| 1     | 6     | 1.4679e-013  | -5.8180e-012 |
| 1     | 7     | 2.3179e-013  | -4.1259e-012 |
| 1     | 8     | -3.6922e-012 | -1.7213e-011 |
| 1     | 9     | 5.3422e-012  | -2.4139e-011 |
| 1     | 10    | -2.3894e-012 | 2.6969e-011  |
| 1     | 11    | -7.5847e-012 | -2.3816e-012 |
| 1     | 12    | -6.4321e-012 | 4.7881e-012  |
| 1     | 13    | -4.3257e-012 | -3.3484e-013 |
| 1     | 14    | -2.9855e-012 | -2.2338e-012 |
| 1     | 15    | 5.9798e-012  | -8.3698e-013 |
| 1     | 16    | 6.4610e-014  | -2.7055e-012 |
| 1     | 17    | -2.6789e-013 | -2.8223e-013 |

~~~~~  
HFTRANSFER FUNCTION PITCH
~~~~~

| 'idir | ifreq | a           | b           |
|-------|-------|-------------|-------------|
| 1     | 1     | 2.0692e-003 | 2.0978e-001 |
| 1     | 2     | 1.2817e-003 | 2.3110e-001 |





```
1 3 4.3660e-004 2.4085e-001
1 4 -5.7744e-004 2.3981e-001
1 5 -1.8765e-003 2.2821e-001
1 6 -3.5336e-003 2.0604e-001
1 7 -5.3667e-003 1.7355e-001
1 8 -6.2358e-003 1.3199e-001
1 9 -5.3929e-003 1.0850e-001
1 10 -3.2318e-003 8.3360e-002
1 11 -4.8075e-004 5.6967e-002
1 12 1.3332e-003 3.1626e-002
1 13 1.6686e-003 1.1424e-002
1 14 1.8109e-003 4.1385e-004
1 15 4.5254e-003 -2.3427e-003
1 16 2.2338e-003 -4.1000e-003
1 17 -6.1924e-004 2.5563e-004
```

~~~~~  
HFTRANSFER FUNCTION YAW
~~~~~

```
'idir ifreq a b
1 1 1.5027e-011 6.4976e-012
1 2 1.2202e-011 -1.8284e-010
1 3 9.5577e-012 7.4464e-012
1 4 7.2538e-012 7.4012e-012
1 5 5.2302e-012 7.0245e-012
1 6 3.4835e-012 6.3136e-012
1 7 2.0218e-012 5.2713e-012
1 8 1.2572e-011 3.9763e-012
1 9 1.8727e-011 3.3364e-012
1 10 -2.0812e-011 1.8845e-012
1 11 4.6001e-013 -8.8620e-012
1 12 -7.8439e-012 -1.3431e-013
1 13 4.3622e-013 -2.5264e-012
1 14 6.3398e-013 -2.3098e-012
1 15 -1.5089e-012 5.9309e-012
1 16 2.8753e-012 1.1771e-013
1 17 3.2066e-013 -2.4967e-013
```

=====  
END  
=====